IN THE UNITED STATES PATENT AND TRADEMARK OFFICE

APPLICANT :	Tur, Vicente R.; Van der Sloot, Albert Martinus; Mullally, Margaret M.; Cool, Robbert H.; Szegezdi; Eva E.; Samali; Afshin; Fernandez-Ballester; Gregorio; Serrano; Luis; Quax; Wilhelmus J.		
SERIAL NO :	10/581,856	EXAMINER:	DANIEL C. GAMETT
FILED :	July 13th, 2007	ART UNIT :	1647
FOR :	CYTOKINE DESIGN		

Certificate of Mailing Under 37 CFR 1,.8

I hereby certify that this correspondence is being deposited with the United States Postal Service as first class mail in an envelope addressed to ASSISTANT COMMISSIONER FOR PATENTS, WASHINGTON, D.C. 20231 ON _____.

_____ _____

(Name of Registered Rep.) (Signature and Date)

DECLARATION UNDER 37 C.F.R. §1.132

ASSISTANT COMMISSIONER FOR PATENTS

WASHINGTON, D.C. 20231

Sir:

WILHELMUS J. QUAX hereby declares and states that:

1. I am presently employed at the UNIVERSITY OF GRONINGEN, **University Centre for Pharmacy,** P.O. Box 72, 9700 AB, Groningen, Netherlands where I am the head of the department of Pharmaceutical Biology.

2. My qualifications are as follows:

Prof. Dr. Wim. J. Quax (PhD, Msc Biol, Bsc Biol)

Appointments held

2004-present: Program manager Biopharmaceuticals: Design, Discovery & Delivery GUIDE
1998-present: Full Professor in Pharmaceutical Biology & Biotechnology at the University of Groningen. Head of department Pharmaceutical Biology
2003-2007: Chairman of the Board of Research School GUIDE
2001-2006: Vice-speaker of European Graduate College Ruhr-Universität Bochum/Univerisity of Groningen (RUB/RUG).
1999-2001: Deputy-Director of Research School GUIDE.
1995-1998: Staff Scientist at Genencor International (Palo Alto and Delft).
1995-2000: Appointed to Full Professor (0.2 fte) in Industrial Biochemistry at the University of Leiden.
1995-1998: Visiting Professor at University of Nottingham.
1991-1995: Principal Scientist, primary Scientific Responsible for Molecular Biology
1987-1991: Head of Department Bacterial Genetics, Royal Gist-Brocades
1984-1986 : scientific staff member of the Bacterial Genetics department Royal Gist-brocades
1980-1984: PhD Research fellowship NWO at the University of Nijmegen.

Honors and awards

Graduation "cum laude", University of Nijmegen (1980).
PhD "cum laude" (1985), University of Nijmegen.
"NBV" prize for the best thesis of the year in the field of Biochemistry by the Dutch Society for Biochemistry and Molecular Biology (NVBMB)(1986).
Elected "Principal Scientist" of Gist-brocades (1991)
Awarded Visiting Professor fellowship at the University of Nottingham (1995).
Elected member of Executive Board of European Federation of Biotechnology (1999).
Elected member of BioPartner advisory committee (2003).
Elected member of STW valorization committee (2006).

Participation in External Committees:

1986-1990: member of the Health Council Commission advising on the use of Recombinant Virusses
1986-1992: Member of the Programme Commission Industrial Biotechnology.
1988-1993 Member of the Programme Commission on Agricultural Biotechnology.
1994-1998 Chairman of BACIP (Bacillus Industrial Platform).
1994-2007 Dutch delegate for the "Working Party Applied Genetics" from the European Federation of Biotechnology.
1997-2007 Chairman of the study group "Applied Molecular Genetics" of the "Nederlandse Biotechnologische Vereniging" (NBV).
1999-2002 Chairman of the Applied Genome Research Section of the European Federation of Biotechnology (EFB)
1998-2007 Member of the board of FIGON (Federation of innovative drug research in the Netherlands)
1999- current Member of the editorial board of the Journal of Biotechnology
2001-2003 Member of NWO STIGON "programmacommissie"
2003-2007 Member of BioPartner/STIGON First Stage Grant committee.

2004-2008 Member of ZonMW Veni committee.
2005-2008 Chairman of ZonMW Veni committee.
2006-current Member of STW valorization committee.
2006-current Member of CW Top/Echo committee
2006-current Member of editorial board of Microbiology
2009-current Chairman of NWO Top-Program (Multidisciplinary).

Publications

Author on >160 professional publications in journals and books. Named inventor on >45 patents.

3. I am a co-inventor with Vicente R. Tur, Albert Martinus Van der Sloot, Margaret M Mullally, Robbert H. Cool, Eva E. Szegezdi, Afshin Samali, Gregorio Fernandez-Ballester, and Luis Serrano on US patent application no. 10/581,856. I have reviewed the application and the pending claims, as well as the Office Action issued by the USPTO on September 9th, 2009. It is my understanding that the Examiner currently considers that the invention is only supported in relation to the specific TRAIL mutants D269R-T214R and D269H-E194I-I196S. As explained below, it is my opinion that the application is supported beyond these mutants in view of the disclosures in the application as filed.

4. From my reading of the application as filed, I consider that the application leads the skilled person through the process for developing mutants falling within the scope of the present claims, and includes tests which were performed to illustrate the receptor selectivity of the resulting mutants. These methods and tests are not limited to the specific TRAIL mutants D269R-T214R and D269H-E194I-I196S.

5. I understand that the application as filed does not explicitly demonstrate the receptor selectivity of all TRAIL mutants falling within the scope of the claims. However, the application teaches the skilled person how to produce and test such mutants, and provides experimental support for a representative number of relevant mutants. I consider that the application leads the skilled person through the process for

developing mutants falling within the scope of the present claims, and includes tests which were performed to illustrate the receptor selectivity of the resulting mutants.

6. I understand that the application provides experimental details about the production of both DR4- and DR5- selective TRAIL mutants (pages 39-43). Figures 7 and 8 of the application as filed show the specificity of a large number of different TRAIL mutants falling within the scope of claim 1 for DR5 and DR4, respectively, as determined using surface plasmon resonance. This is the same method which was used in the experiments described in the annex and in the accompanying papers.

7. The methods and tests described in the application as filed are not limited to the specific TRAIL mutants D269R-T214R and D269H-E194I-I196S, and have subsequently been used to verify the activity of other TRAIL mutants.

8. In the Annex to this declaration, I hereby submit additional experimental data obtained according to the invention described in the application, which provide further experimental support for the activity of mutants described in the present application, and extend the range of mutants for which receptor selectivity has been specifically demonstrated. I also include as annexes to this declaration five papers which were published after the filing date of the application and which disclose additional DR4 specific TRAIL mutants produced and characterised according to the methods described in the application.

9. Taking account of the enclosed additional data, and the data provided in the application, we have described a total of 27 receptor specific mutants, which contain mutations at an even larger number of different positions.

10. The annex includes supplemental figures produced by the inventors which relate to TRAIL mutants D218Y and D218H. The activity of D218Y was disclosed in the

application as filed, and this has now been further exemplified. The D218H mutant was originally disclosed and its activity has subsequently been verified as shown in the annex.

11. The figures in the annex illustrate that mutating the amino acid at position 218 of TRAIL results in the production of a DR4-selective mutant.

12. Van der Sloot *et al.* (PNAS, 2006, 103(23) pg. 8634-8639) describes the analysis of mutations at a large number of positions of TRAIL, in order to determine their effect on receptor binding. This paper describes experimental studies relating to the receptor selectivity of a subset of individual TRAIL mutations, 4 of which had not been previously described in the application. This publication also describes the effect on receptor selectivity of a number of newly produced double mutants, and demonstrates the biological activity and receptor selectivity of such mutants.

13. Tur *et al.* (Journal of Biological Chemistry, 2008, 283(29), pg.20560-20568) describes numerous proposed receptor selective TRAIL mutants, several of which are not explicitly described in the application. Further experimental analysis of these variants using surface plasmon resonance and competitive ELISA is also described.

14. Mahalingham *et al.* (Cancer Treatment Reviews, 2009, 35, pg.280-288) is a review of the understanding of the function and characterisation of TRAIL as of the beginning of 2009. Table 2 of Mahalingham *et al.* describes a vast array of receptor selective TRAIL mutants which had been produced by the inventors at this date. Furthermore, pages 282-284 discuss the specific characterisation of certain receptor selective mutants and their advantages.

15. Duiker *et al.* (Clinical Cancer Research, 2009, 15(6), pg.2048-2057) describes the further characterisation of the DR5-specific TRAIL variant D269H/E195R. This document illustrates our ongoing work to further characterise the claimed mutants.

16. Reis *et al.* (Biochemistry, 2009, 48, pg.2180-2191) describes further binding analysis of G131R, which is included in the application, and G131K, which is not explicitly described in the application as filed. This further analysis indicates the importance of position 131 in binding of TRAIL of DR4.

17. Bibliography (appended to this declaration)

18. I hereby further declare that all statements made herein of my own knowledge are true and that all statements made on information and belief are believed to be true and further that the statements are made with the knowledge that wilful false statements and the like so made are punishable by fine or imprisonment or both under §10001 of Title 18 of the United States code and that such wilful false statements may jeopardize the validity of the Application for any patent issuing thereon.

Date: March 2nd 2010 WILHELMUS J. QUAX

REFERENCES

For the declaration:

Van der Sloot *et al.* PNAS, *2006*, 103(23) pg. 8634-8639

Tur *et al.* Journal of Biological Chemistry, *2008*, 283(29), pg.20560-20568

Mahalingham *et al.* Cancer Treatment Reviews, *2009*, 35, pg.280-288

Duiker *et al.*(Clinical Cancer Research, *2009*, 15(6), pg.2048-2057

Reis *et al.* Biochemistry, *2009*, 48, pg.2180-2191

WILHELMUS J. QUAX

Patents and publications

PATENTS (10 most relevant)

1. IMPROVED CYTOKINE DESIGN: WO 2005/056596 (23.06.2005)
2. TRAIL VARIANTS FOR TREATING CANCER: WO/2009/077857 (25.06.2009)
3. IMPROVED CYTOKINE DESIGN: WO 2009/066174 (28.05.2009)
4. NOVEL SECRETION FACTORS FOR GRAM-POSITIVE MICOORGANISMS, GENES ENCODING THEM AND METHODS OF USING IT: US2003077729 20030424
5. GLUTARYL AMIDASES AND THEIR USES: WO2005054452
6. MODULATION OF THE THIOREDOXIN PATHWAY: WO2004056987
7. EXPRESSION SYSTEM FOR ALTERED EXPRESSION LEVELS US6225106
8. MUTATED PENICILLIN G ACYLASE GENES WO9605318
9. PENICILLIN G ACYLASE, A GENE ENCODING THE SAME AND A METHOD FOR THE PRODUCTION OF THIS ENZYME US5695978
10. PRODUCTION OF ENZYMES IN SEEDS AND THEIR USE US5714474

PUBLICATIONS (10 most relevant)

1. Bokhove, M., Jimenez, P. N., Quax, W. J. & Dijkstra, B. W. (2010). The quorum-quenching N-acyl homoserine lactone acylase PvdQ is an Ntn-hydrolase with an unusual substrate-binding pocket. Proc. Natl. Acad. Sci. U. S. A 107, 686-691.
2. Duiker, E. W., de Vries, E. G., Mahalingam, D., Meersma, G. J., Boersma-van, E. W., Hollema, H., Lub-de Hooge, M. N., van Dam, G. M., Cool, R. H., Quax, W. J., Samali, A., van der Zee, A. G. & de, J. S. (2009). Enhanced antitumor efficacy of a DR5-specific TRAIL variant over recombinant human TRAIL in a bioluminescent ovarian cancer xenograft model. Clin. Cancer Res. 15, 2048-2057.
3. Reis, C. R., van der Sloot, A. M., Szegezdi, E., Natoni, A., Tur, V., Cool, R. H., Samali, A., Serrano, L. & Quax, W. J. (2009). Enhancement of antitumor properties of rhTRAIL by affinity increase toward its death receptors. Biochemistry 48, 2180-2191.

4. Tarrus, M., van der Sloot, A. M., Temming, K., Lacombe, M., Opdam, F., Quax, W. J., Molema, G., Poelstra, K. & Kok, R. J. (2008). RGD-avidin-biotin pretargeting to alpha v beta 3 integrin enhances the proapoptotic activity of TNF alpha related apoptosis inducing ligand (TRAIL). Apoptosis 13, 225-235.
5. Tur, V., van der Sloot, A. M., Reis, C. R., Szegezdi, E., Cool, R. H., Samali, A., Serrano, L. & Quax, W. J. (2008). DR4-selective tumor necrosis factor-related apoptosis-inducing ligand (TRAIL) variants obtained by structure-based design. J. Biol. Chem. 283, 20560-20568.
6. van der Sloot, A. M., Mullally, M. M., Fernandez-Ballester, G., Serrano, L. & Quax, W. J. (2004). Stabilization of TRAIL, an all-beta-sheet multimeric protein, using computational redesign. Protein Eng Des Sel 17, 673-680.
7. van der Sloot, A. M., Tur, V., Szegezdi, E., Mullally, M. M., Cool, R. H., Samali, A., Serrano, L. & Quax, W. J. (2006). Designed tumor necrosis factor-related apoptosis-inducing ligand variants initiating apoptosis exclusively via the DR5 receptor. Proc. Natl. Acad. Sci. U. S. A 103, 8634-8639.
8. Vrielink, J., Heins, M. S., Setroikromo, R., Szegezdi, E., Mullally, M. M., Samali, A. & Quax, W. J. (2010). Synthetic constrained peptide selectively binds and antagonizes death receptor 5. FEBS J.
9. Wassenaar, T. A., Quax, W. J. & Mark, A. E. (2008). The conformation of the extracellular binding domain of Death Receptor 5 in the presence and absence of the activating ligand TRAIL: a molecular dynamics study. Proteins 70, 333-343.
10. Westers, L., Dijkstra, D. S., Westers, H., van Dijl, J. M. & Quax, W. J. (2006). Secretion of functional human interleukin-3 from Bacillus subtilis. J. Biotechnol. 123, 211-224.

Designed tumor necrosis factor-related apoptosis-inducing ligand variants initiating apoptosis exclusively via the DR5 receptor

Almer M. van der Sloot*†, Vicente Tur†‡, Eva Szegezdi§, Margaret M. Mullally*¶, Robbert H. Cool*, Afshin Samali§, Luis Serrano*, and Wim J. Quax*||

*Department of Pharmaceutical Biology, University of Groningen, Antonius Deusinglaan 1, 9713 AV, Groningen, The Netherlands; ‡Structural Biology and Biocomputing Program, European Molecular Biology Laboratory, Meyerhofstrasse 1, D-69117 Heidelberg, Germany; and §Cell Stress and Apoptosis Research Group, Department of Biochemistry and National Centre for Biomedical Engineering Science, National University of Ireland, Galway, Ireland

Edited by Stephen L. Mayo, California Institute of Technology, Pasadena, CA, and approved April 12, 2006 (received for review December 1, 2005)

Tumor necrosis factor-related apoptosis-inducing ligand (TRAIL) is a potential anticancer drug that selectively induces apoptosis in a variety of cancer cells by interacting with death receptors DR4 and DR5. TRAIL can also bind to decoy receptors (DcR1, DcR2, and osteoprotegerin receptor) that cannot induce apoptosis. The occurrence of DR5-responsive tumor cells indicates that a DR5 receptor-specific TRAIL variant will permit tumor-selective therapies. By using the automatic design algorithm FOLD-X, we successfully generated DR5-selective TRAIL variants. These variants do not induce apoptosis in DR4-responsive cell lines but show a large increase in biological activity in DR5-responsive cancer cell lines. Even wild-type TRAIL-insensitive ovarian cancer cell lines could be brought into apoptosis. In addition, our results demonstrate that there is no requirement for antibody-mediated cross-linking or membrane-bound TRAIL to induce apoptosis through DR5.

computational protein design | receptor selectivity | biopharmaceutical | death receptor | apoptosis-inducing ligand 2

Tumor necrosis factor (TNF)-related apoptosis-inducing ligand (TRAIL) is currently attracting great interest as a potential anticancer therapeutic. TRAIL, in its soluble form, selectively induces apoptosis in tumor cells *in vitro* and *in vivo* by a death receptor-mediated process. Unlike other apoptosis-inducing TNF family members, soluble TRAIL appears to be inactive against normal healthy tissue (1). Reports in which TRAIL induces apoptosis in normal cells could be attributed to the specific preparations of TRAIL used (2). TRAIL shows a high degree of promiscuity as it binds to five cognate receptors: DR4 (TRAIL-R1) and DR5 (TRAIL-R2) and the decoy receptors DcR1 (TRAIL-R3), DcR2 (TRAIL-R4), and osteoprotegerin (OPG) (3). Upon binding to TRAIL, DR4 and DR5 receptors recruit Fas-associated death domain, which binds and activates the initiator caspase 8, leading to apoptosis (4–6). DcR1 or DcR2 do not contain a death domain or a truncated death domain, respectively, and therefore could prevent apoptosis by sequestering available TRAIL or by interfering in the formation of a TRAIL-DR4 or -DR5 signaling complex (7).

Use of TRAIL receptor-selective variants could permit better tumor-specific therapies through escape from the decoy receptor-mediated antagonism, resulting in a lower administrated dose with possibly fewer side effects and as alternatives to existing agonistic receptor antibodies (8–10). In experimental anticancer treatments, the receptors DR4 and/or DR5 were shown to be up-regulated after treatment with DNA-damaging chemotherapeutic drugs, and the response to TRAIL-induced apoptosis was significantly increased (3, 11). In addition, irradiation appears to specifically up-regulate DR5 receptor expression, and the combination of irradiation and TRAIL treatment has been demonstrated to have an additive or synergistic effect (12). Thus, we chose to develop DR5 receptor-selective TRAIL variants by using a computational design strategy. Computational design methods have been successfully used to redesign several protein–protein interactions (13–16) but have, as yet, hardly been applied to therapeutic proteins. One exception is the design of dominant negative TNF-α variants that prevent formation of active TNF-α trimers (17). By using the automatic design algorithm FOLD-X (18–20), we were able to redesign TRAIL into exclusively DR5-specific agonistic variants. Because the computational method used in our study is based on general applicable principles and has been successfully tested on a variety of proteins (14, 19, 21–23), our method can be further applied to design other protein therapeutics with reduced promiscuity and improved receptor-binding characteristics.

Results

Modeling of TRAIL–Receptor Complexes. Monomeric subunits of TRAIL self-associate in bell-shaped homotrimers, the bioactive form of the ligand, like other members of the TNF ligand family (24, 25). A trimer binds three subunits of a cognate receptor, with each receptor subunit bound in the grooves between two adjacent monomer ligand subunits (26, 27). At present, only crystal structures of TRAIL in complex with the DR5 receptor are known (26–28). The sequence alignment of the different TRAIL receptors shows a large overall sequence identity (except for OPG), practically no insertions or deletions, and conservation of all cysteines involved in the formation of internal disulfide bridges (Fig. 5*A*, which is published as supporting information on the PNAS web site). Consequently, good quality homology models of DR4, DcR1, and DcR2, but not of OPG, could be built. The homology models were built by using the WHAT IF web interface (29). Afterward, these models were refined by using the protein design options of FOLD-X, removing incorrect side-chain torsion angles, eliminating van der Waals clashes, and accommodating TRAIL and receptor residues to their new interface.

The accuracy of the models and the force field was tested by using the data derived from the alanine scanning of wild-type TRAIL as performed by Hymowitz *et al.* (30). The predictions of the energy change in the complex formation correlates with the changes in the dissociation constants measured (Fig. 1). The calculated R^2 factor is 0.6 (R^2 factors calculated for DR4 and DR5 individually also amount to 0.6). However, several factors involved in accuracy should be taken into account. The methodology used focuses on energy changes in ligand–receptor complex formation. Some mutations to alanine might be predicted not to change receptor-

Conflict of interest statement: No conflicts declared.

The paper was submitted directly (Track II) to the PNAS office.

Abbreviations: GPC, osteoprotegerin; SPR, surface plasmon resonance; TNF, tumor necrosis factor; TRAIL, TNF-related apoptosis-inducing ligand.

†A.M.v.d.S. and V.T. contributed equally to this paper.

‡Present address: Bijvoet Center for Molecular Life Sciences, Padualaan 8, 3584 CH, Utrecht, The Netherlands.

¶Present address: Nijmegen Centre for Molecular Life Sciences, Radboud University Nijmegen Medical Centre, 6525 GA, Nijmegen, The Netherlands.

||To whom correspondence should be addressed. E-mail: w.j.quax@rug.nl.

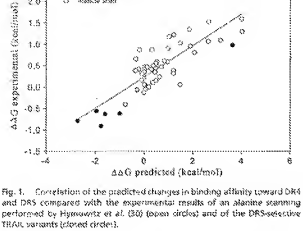

Fig. 1. Correlation of the predicted changes in binding affinity toward DR4 and DR5 compared with the experimental results of an alanine scanning performed by Hymowitz *et al.* (30) (open circles) and of the DR5-selective TRAIL variants (closed circles).

binding affinity but only to produce slight changes in TRAIL stability, thereby affecting the correlation. The prediction error is, on average, within the error of this methodology (0.6–0.7 kcal/mol) (1 kcal ≈ 4.18 kJ). Because many changes in affinity, as measured in the alanine scanning, are within this error, it is not possible to obtain a better correlation. Taken together, these data imply that our method can reliably predict mutations in the receptor-binding interface that will severely affect the complex formation.

Computational Design of the Variants. For the computational screening, all residues from the TRAIL interface were considered. TRAIL residues interacting with a conserved amino acid environment in all four receptors were disregarded. Amino acids finally considered were as follows: Arg-130, Gly-131, Arg-132, Lys-145, Leu-147, Gly-148, Arg-149, Lys-190, Glu-155, Arg-158, Gly-160, His-161, Tyr-189, Arg-191, Phe-192, Gln-193, Glu-195, Asn-199, Thr-200, Lys-201, Asp-203, Gln-205, Val-207, Gln-208, Tyr-209, Thr-214, Asp-218, Asp-234, Glu-236, His-264, Ile-266, Asp-267, and Asp-269. Tyr-216 was included as a positive control because of its already-known implication in receptor binding (25, 27), and Ser-165, located far away from the receptor-binding interface, was used as a negative control (Fig. 5*B*). At each of the selected positions, FOLD-X placed the 20 natural amino acids while moving the neighboring residues, obtaining a total library of 2,720 models (34 amino acid positions × 20 amino acids × 4 receptors). The energy of interaction was obtained by calculating the sum of the individual energies of the receptor and ligand subunits and subtracting them from the global energy of the complex. In this way, a set of predicted energetic values for the complex formation was obtained and compared with the wild-type TRAIL values. After studying these values together with visual inspection of the mutant models, those variants in which a change in selectivity was predicted were selected for experimental studies (Table 1).

Prescreen for Selective Receptor Binding. A fast surface plasmon resonance (SPR)-based receptor-binding prescreen was used to further refine the *in silico* selection. TRAIL-variant cell extracts were evaluated for binding to DR4-, DR5-, and DcR1-immobilized Ig fusion proteins. The ratios of binding to DR4 and DcR1 receptors with respect to the DR5 receptor were calculated and compared with the ratio obtained for wild-type TRAIL. An increase in the DR5/DR4 binding ratio of ≥25% relative to the ratio of wild-type TRAIL was set as indicative of DR5 selectivity. Several variants comprising a substitution (His, Lys, or Arg) at position Asp-269 and variants with double mutation D269H/E195R and D269H/T214R with reduced binding to the DR4 receptor and increased binding to the DR5 receptor were chosen for further analysis. R191E/D269R, R130E, G160M, I200M, and E195R were also selected, because they also showed an increased DR5/DR4 binding ratio. The effects, however, were smaller than that of the Asp-269 variants (data not shown).

Table 1. Predicted difference in binding energy (ΔΔG) of DR5-selective variants binding to different receptors when compared with wild-type TRAIL

Mutations	DR4	DR5	DcR1	DcR2
R130E	0.75	−6.2	1.76	1.52
G160M	−1.11	−1.52	−0.18	−0.65
E195R	0.11	−1.11	0.2	−0.79
T214R	1.85	−0.37	1.94	1.89
D269H	3.52	−1.6	3.78	4.43
D269R	1.95	−1.95	2.45	3.28
D269K	2.43	−1	2.94	3.71

Variants comprising these mutations were selected in the prescreen assay from an initial set of 10 design proposals. Change in energy is measured in kcal/mol and applies to the change of a single binding interface bound to a single receptor.

Determination of Receptor Binding. Selected TRAIL variants were purified as described in ref. 22. Analytical size-exclusion chromatography and dynamic light scattering confirmed that the purified TRAIL variants were in a trimeric state and that higher order oligomeric species or aggregates were absent (data not show). Binding of the purified variants to the immobilized DR4-, DR5-, DcR1-, or DcR2-Ig receptor was assessed in real time by using SPR. The TRAIL proteins were initially analyzed at two concentrations (30 and 60 nM). TRAIL variants R191E/D267R and G160M showed stability and folding problems and were therefore discarded. Binding curves of variants showing a significant change in the ratio of DR5/DR4 binding were subsequently recorded for concentrations ranging from 0.1 to 250 nM. The D269H/T214R variant had an improvement comparable with the D269H single mutant variant in DR5-Ig binding, however no detectable binding to DR4-Ig was found (Fig. 2*A* and *B*). Apparent K_d values for DR5 binding ranged from 0.6 (D269H/E195R) to 2.5 nM (TRAIL) and from 7.2 (TRAIL) to 244 nM (D269H) for DR4 binding. For D269H/T214R, D269K, and D269R, a proper apparent K_d for DR4 binding could not be determined. Binding of D269H and D269H/E195R toward the decoy DcR1-Ig receptor was >20-fold reduced when compared with wild-type TRAIL. Up to the highest concentration tested (250 nM), D269H/T214R did not show any observable binding to DcR1-Ig (Fig. 6*A*, which is published as supporting information on the PNAS web site). D269H and D269H/E195R also showed reduced binding to DcR2-Ig; however, this reduction was much less pronounced than the reduction observed in DcR1 binding. In contrast, D269H/T214R showed a large decrease in binding to DcR2-Ig relative to wild-type TRAIL (Fig. 6*B*). Binding to OPG-Ig was also reduced for these three DR5-selective variants, with D269H/E195R showing the largest decrease in binding to this receptor (Fig. 6*C*). A competition ELISA experiment measuring the binding of TRAIL or variants toward immobilized DR5-Ig in the presence of soluble DR4-, DR5-, or DcR1-Ig corroborated the findings of the receptor-binding experiment. Whereas TRAIL binding to immobilized DR5-Ig could be competed by soluble DR4-, DR5-, and DcR1-Ig, binding of the variants could only be antagonized by soluble DR5-Ig (Fig. 7, which is published as supporting information on the PNAS web site).

Comparison Between Predictions and Experimentally Obtained Results. To calculate the correlation between the predicted and experimentally obtained results of our DR5-selective variants, the

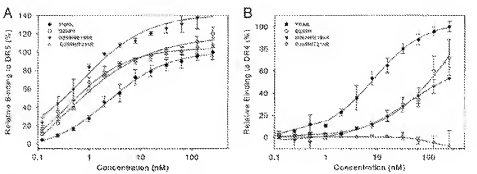

Fig. 2. Receptor binding of TRAIL and DR5-selective variants toward DR5-Ig as determined by SPR (*A*) or toward DR4-Ig (*B*). Receptor binding is calculated relative to the response of TRAIL at 250 nM.

calculated $\Delta\Delta G$ values for DR4 and DR5 binding (Table 1) were compared with the $\Delta\Delta G$ values that stem from the experimentally determined apparent K_d values (see above). The calculated R^2 factor between these predicted and experimental $\Delta\Delta G$ values is 0.9. Adding these values to the alanine scan data set improved the overall calculated R^2 from 0.6 to 0.7 (Fig. 1).

Biological Activity. To assess the biological activity related to DR5 binding, various cancer cells were used. Colo205 colon carcinoma cells and ML-1 chronic myeloid leukemia cells express all four TRAIL receptors on the cell surface, as shown by using FACS analysis, (Fig. 8, which is published as supporting information on the PNAS web site), and are sensitive to TRAIL-induced apoptosis. To test the involvement of DR4 versus DR5 in TRAIL-induced cell death, Colo205 cells were treated with neutralizing anti-DR4 or anti-DR5 antibody for 1 h before the addition of TRAIL. Both antibodies reduced TRAIL-mediated cell death and had an additive effect when used in combination (Fig. 3*A*). However, the DR5-neutralizing antibody was ≈3 times more effective than the DR4-neutralizing antibody, demonstrating that TRAIL-induced apoptosis in Colo205 cells is primarily mediated by DR5. In contrast, the DR4 pathway is the major mediator of TRAIL-induced apoptosis in ML-1 cells (Fig. 3*A*). To examine whether the DR5-specific TRAIL variant induce cell death in Colo205 cells by way of the DR5 receptor, 1 μg/ml neutralizing anti-DR4 or -DR5 antibodies were administered 1 h before ligand treatment. The presence of the anti-DR4 antibody failed to prevent death induced by the DR5-specific variants. However, 1 μg/ml anti-DR5 antibody significantly reduced the amount cell death (Fig. 3*B*).

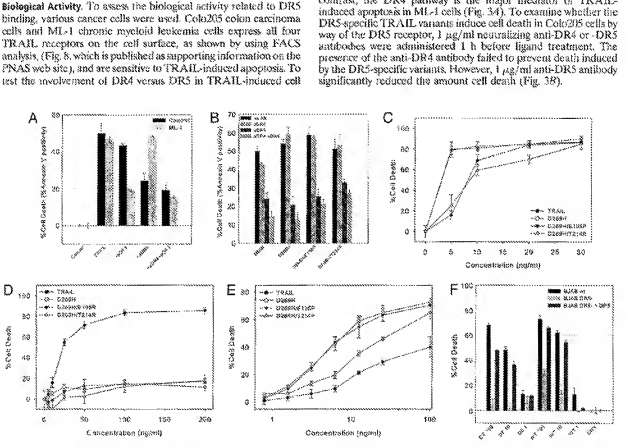

Fig. 3. Biological activity of TRAIL and DR5-selective variants. (*A*) Apoptosis-inducing activity of 100 ng/ml TRAIL in the presence of 1 μg/ml DR4 (aDR4), DR5 (aDR5), or DR4 and DR5 (1 aDR4+ aDR5) receptor-neutralizing antibodies in Colo205 and ML-1 cells. (*B*) Apoptosis-inducing activity in Colo205 cells of 100 ng/ml TRAIL or DR5-selective variants without the presence of neutralizing DR4 or DR5 antibodies (no AB) or in the presence of neutralizing antibody (aDR4, aDR5, or both (aDR4 aDR5)). Shown is the cytotoxic potential (% cell death) of TRAIL or DR5-selective variants in Colo205 (*C*), ML-1 (*D*), and A2780 (*E*) and of 1, 10, or 100 ng/ml TRAIL (WT) or D269H/E195R (DE) relative to cycloheximide control (0.33 μg/ml) in BJAB cells responsive to both DR4- and DR5-mediated cell death (BJAB^{WT}), BJAB cells deficient for DR5 (BJAB^{DR5_DEF}), and BJAB cells deficient for DR5 stably transfected with DR5 (BJAB^{DR5_DEF}+ DR5) (*F*) (31)

Table 2. EC_{50} values of Colo205 and A2780 cells

	Colo205		A2780	
Ligand	EC_{50}, ng/ml	Max effect, % cell death	EC_{50}, ng/ml	Max effect, % cell death
TRAIL	8.6 ± 0.9	78 ± 8	15.6 ± 3	41 ± 3
D269H	1.8 ± 0.5	80 ± 4	4.7 ± 0	70 ± 5
D269H E195R	1.5 ± 0.4	80 ± 6	4.2 ± 1	69 ± 2
D269H T214R	5.1 ± 2.6	66 ± 9	12.1 ± 4	66 ± 11

Results are expressed as ± SD.

Colo205 and ML-1 cells were then treated with increasing concentrations of TRAIL or the DR5-specific variants D269H, D269H/E195R, and D269H/T214R, and their cytotoxic potential was measured with a 3-(4,5-dimethylthiazol-2-yl)-2,5-diphenyl tetrazolium bromide (MTT) assay. In Colo205 cells, all TRAIL ligands were biologically active and induced cell death at levels that were either comparable with that of wild-type TRAIL or were up to 5-fold more active than wild-type TRAIL (Fig. 3C and Table 2). Contrary to Colo205 cells, only TRAIL was able to induce cell death in ML-1 cells (Fig. 3*D*). Similar results were obtained by using EM-2 chronic myeloid leukemia cells expressing only the DR4 receptor and lacking the DR5 receptor and by using the ovarian cancer cell line A2780, which expresses DR5 but lacks DR4 on its surface and is relatively insensitive toward TRAIL-induced cell death (S. de Jong, personal communication). Although EM-2 cells were sensitive to TRAIL-induced cell death (50 ng/ml TRAIL initiating >80% cell death), treatment with any of the DR5 mutants failed to induce significant cell death (Fig. 9, which is published as supporting information on the PNAS web site). In A2780 cells, however, the cytotoxic activity of D269H, D269H/E195R, and D269H/T214R is significantly increased, showing both an increased maximum response and drastically decreased EC_{50} values when compared with wild-type TRAIL (Fig. 3*E* and Table 2). An additional experiment using D269H/E195R in wild-type BJAB cells responsive to both DR4- and DR5-mediated cell death ($BJAB^{wt}$), BJAB cells deficient in DR5 ($BJAB^{DR5\ DEF}$), and BJAB cells deficient in DR5 and stably transfected with DR5 ($BJAB^{DR5\ DEF}$+DR5) (31) confirm our findings. D269H/E195R was able to induce cell death in $BJAB^{wt}$ cells but was unable to induce significant cell death in $BJAB^{DR5\ DEF}$ cells when compared with wild-type TRAIL. In the DR5 transfected $BJAB^{DR5\ DEF}$+DR5 cells, however, the cytotoxic potential was restored (Fig. 3*F*). The cytotoxic effects of these TRAIL variants on noncancerous human umbilical vein endothelial cells was assessed by incubating these cells in the presence of 100 ng/ml TRAIL or TRAIL variants. However, no cytotoxic effects were observed for TRAIL and the receptor-selective TRAIL variants (data not shown). Taken together, the results obtained with the Colo205, ML-1, A2780, and BJAB cell lines show that the biological activity of the D269H, D269H/E195R, and D269H/T214R variants is specifically directed toward the DR5 receptor.

Discussion

Because the DR5 receptor is a good target for TRAIL cancer therapy (see the Introduction), we choose to develop DR5 receptor-selective variants of TRAIL by using a computational design strategy.

Structural Basis for the Changes in Selectivity. This study shows that residue 269 is one of the most important residues for DR5 selectivity. From the crystal structure of TRAIL in complex with DR5, it can be observed that this amino acid is not interacting directly with the receptor. Studying the models of TRAIL in complex with the other three receptors reveals that Asp-269 from TRAIL is

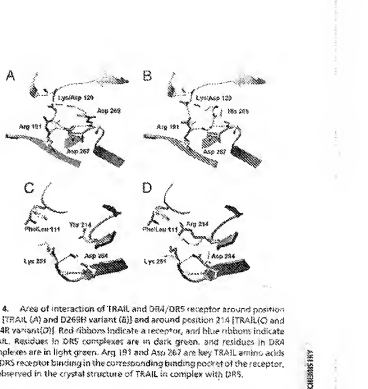

Fig. 4. Area of interaction of TRAIL and DR4/DR5 receptor around position 269 (TRAIL (*A*) and D269H variant (*B*)) and around position 214 (TRAIL (*C*) and T214R variant (*D*)). Red ribbons indicate a receptor, and blue ribbons indicate TRAIL. Residues in DR5 complexes are in dark green, and residues in DR4 complexes are in light green. Arg 191 and Asp 267 are key TRAIL amino acids for DR5 receptor binding in the corresponding binding pocket of the receptor, as observed in the crystal structure of TRAIL in complex with DR5.

interacting with Lys-120 from the receptor. This lysine residue is conserved among the DR4, DcR1, and DcR2 receptors. In contrast, DR5 has an aspartate at this position (Fig. 4 *A* and *B* and Fig. 5*A*).

Changing this amino acid to another with opposite charge shows two cumulative effects. On one hand, breaking the Asp-269–Lys-120 interaction in the complex between TRAIL and receptors DR4, DcR1, and DcR2 would decrease TRAIL affinity toward them; furthermore, Lys-120 has little space for reaccommodation, and this may even introduce some van der Waals clashes in the area. On the other hand, Asp-120 from the DR5 receptor may interact with the protonated His-269 of TRAIL, improving binding toward this receptor. In summary, this combination of effects explains why a single mutation alone can greatly change the selectivity toward DR5, resulting in better binding to the DR5 receptor and a substantial decrease in binding toward the other receptors. Residue 214 is also important for achieving DR5 selectivity. For the T214R mutation, FOLD-X predicts a decrease in binding affinity for all receptors except DR5 (Table 1). This decrease is due to the presence of a phenylalanine at position 111 in DR4 and a proline in DcR1 and DcR2, which prevent proper accommodation of Arg-214 upon complex formation. As a result, the arginine displaces Asp-254 and breaking intramolecular H bonds. In DR5, a leucine at position 111 allows accommodation of Arg-214 without displacement of Asp-254 (Fig. 4 *C* and *D*). An additive effect of mutations toward selectivity can be expected in the cases in which the positions of the mutations are far enough away from each other that they cannot make any unpredictable interaction, e.g., mutations D269H and T214R.

Selective Binding to Different Receptors. Receptor-binding experiments using SPR and competition ELISA experiments confirmed the modeling predictions. Variants D269H, D269H/E195R, D269K, and D269R are between 70- to 150-fold more selective for the DR5 receptor than for the DR4 receptor when compared with wild-type TRAIL. The D269H/T214R variant showed no binding to the DR4 receptor at the highest concentration used in the assay (250 nM). The dissociation rates of TRAIL and the DR5-selective variants in complex with the DR5 and DR4 receptor were, however, too slow to measure accurately by using SPR, thereby precluding the accurate determination of affinity constants. In the competition

ELISA experiments, DR4 was unable to compete with immobilized DR5 for the binding to these designed selective variants, demonstrating that, in the presence of both DR4 and DR5, these variants are markedly more selective toward DR5. The net gain in DR5 selectivity of these variants is the sum of both an increased preference for the DR5 receptor and a reduced preference for the DR4 receptor, exemplifying both positive and negative design principles (13).

Binding of the D269H and D269H/E195R variants to the decoy DcR1 receptor was >20-fold reduced when compared with wild-type TRAIL. The D269H/T214R variant showed no binding to the DcR1 receptor at the highest concentration used in the assay (250 nM). Although binding of the D269H and D269H/E195R variants toward the decoy DcR2 receptor was reduced, the effect was much less pronounced when compared with the reduction in binding as observed with the other receptors. The different environment of Lys-120 in receptor DcR2 when compared with DR4 and DcR1 could explain why the decrease in affinity is smaller in this case in contrast to our predictions. However, the D269H/T214R variant showed an ≈80% decrease in receptor binding to the DcR2 receptor when compared with wild-type TRAIL.

The DR5 Receptor Produces Apoptosis Without Additional Cross-Linking Requirements. By using several different cancer cell lines, receptor-selective behavior of the DR5-selective variants could also be demonstrated in several *in vitro* biological assays. In cells with the DR4 receptor as the major mediator of TRAIL-induced apoptosis (ML-1 and BM-2 cells), DR5-selective variants were unable to induce apoptosis even at high concentrations (200 ng/ml). These variants could, however, induce apoptosis in cells with DR5 as the major mediator of TRAIL-induced apoptosis (Colo205), and this induction could be antagonized by using a neutralizing anti-DR5 antibody. The cell death-inducing activity against Colo205 cells was comparable with wild-type TRAIL (EC_{50} ≈6.6 ng/ml) in the case of D269H/T214R (EC_{50} ≈5.1 ng/ml) or increased >5-fold in the case of D269H/E195R (EC_{50} ≈1.5 ng/ml). In the DR5-positive and DR4-negative A2780 cells, the increase in cell death-inducing activity of the DR5-selective variants was even more pronounced. By using the various BJAB cell lines, it was confirmed that D269H/E195R-mediated induction of cell death was dependent on the presence of the DR5 receptor, and it was observed that the presence of only the DR4 receptor was not sufficient to induce cell death for this DR5-selective variant. Taken together, the *in vitro* biological activity data convincingly demonstrate that differences in receptor selectivity, as measured in the *in vitro* receptor-binding assay, are both relevant and significant in the *in vitro* biological context.

Both our results and results recently published in ref. 32 suggest that cross-linking TRAIL or membrane-bound TRAIL is not an absolute prerequisite for DR5-mediated induction of apoptosis, as was concluded by others (33, 34). A 10-fold improvement in DR5-mediated activity of flag-tagged TRAIL upon cross-linking was demonstrated; however, this also resulted in toxicity in normal cynomolgus monkey hepatocytes (32). Our soluble trimeric DR5-selective TRAIL variants are capable of inducing DR5 receptor-mediated apoptosis at lower concentrations than wild-type TRAIL, thus eliminating any requirement for antibody-mediated cross-linking.

Designed Versus Selected Variants. Other DR5 receptor-selective TRAIL variants were recently isolated by using phage display (32). These variants were selected from saturation mutagenesis libraries that were constructed on the basis of a previously performed alanine scan (30). Remarkably, the best DR5-selective mutant (DR5-E) contained six amino acid substitutions. The mutations we found (e.g., D269H, E195R, and T214R) to induce DR5 selectivity were not identified by the phage-display approach. In a partial dissection to determine the role of each mutation in selectivity, Kelley *et al.* (32) could not eliminate any of the mutations without losing selectivity and/or biological activity. It was concluded that, to achieve receptor selectivity, multiple amino acid substitutions were required. However, our results clearly demonstrate that, in case of the D269H/T214R variant, only two amino acid substitutions are required to obtain complete receptor selectivity. Having fewer mutations relative to the wild-type sequence appears favorable in view of a potential use of the DR5 selective variants as anticancer therapeutics, because fewer mutations are likely to reduce the risk of an immunogenic response.

Conclusion

This study shows that computational redesign of the receptor-binding interface of TRAIL to obtain DR5-selective variants is achievable. *In vitro* analysis demonstrates that our DR5-selective mutants have increased affinity for DR5, whereas they do not bind to DR4. Our DR5-selective variants show high activity toward DR5-responsive cancer cells without the need for additional cross-linking. Consequently, these variants are of interest for development as a potential anticancer therapeutic. Previously, we designed TRAIL variants with improved thermal stability by using a computational redesign strategy (22). Computational protein redesign methods are therefore a valuable addition to other protein engineering methodologies, such as directed evolution or experimental high-throughput approaches, as a tool for the improvement of protein properties. Combining computational and experimental screening methods is a powerful approach in protein engineering; a preliminary computational screening of proteins helps to identify the most important positions involved in protein–protein interactions and therefore decreases the number of variants to screen.

Methods

All reagents were of analytical grade unless specified otherwise. Recombinant TRAIL Ig receptor fusion proteins were ordered from R & D Systems. PBS (pH 7.4) and RPMI medium 1640 were obtained from Invitrogen. All other chemicals were from Sigma. All buffers used in SPR, ELISA, and biological activity assays were of physiological pH and ionic strength.

Computational Design of the Variants. Homology models of DR4, DcR1, and DcR2 were built by using the WHATIF (29) web interface based on human TRAIL in complex with the DR5 ectodomain (26). Afterward, these models were refined by using the protein design options of FOLD-X, removing incorrect torsion angles, eliminating van der Waals clashes, and accommodating TRAIL and receptor residues to their new interface and to build up the putative interactions between TRAIL and the three noncrystallized receptors through rotamer substitution. The crystal complex structure of TRAIL with the DR5 receptor was also refined this way (see *Supporting Methods*, which is published as supporting information on the PNAS web site). A detailed description of the empirical force field FOLD-X is available in ref. 18 and at http://fold-x.embl-heidelberg.de.

In addition, the modified version of FOLD-X used in this work (20) is able to perform amino acid mutations, accommodating his new residue and its surrounding amino acids in the following way. It first mutates the selected position to alanine and annotates the side-chain energies of the neighbor residues. Then it mutates this alanine to the selected amino acid and recalculates the side-chain energies of the same neighboring residues. Those that exhibit an energy difference are then mutated to themselves to see whether another rotamer will be more favorable. This feature allows for proceeding through the whole computational design process by using just a single force field. The method does not guarantee a global minimum, but we have found that it is able to find the wild-type side-chain conformations when doing side-chain reconstruction from a polyAla backbone (F. Stricher and L. Serrano, personal communication).

Side-Directed Mutagenesis, Expression, and Purification of Selectivity Mutants. cDNA corresponding to human soluble TRAIL (amino acids 114–281) was cloned in pET15B (Novagen) by using NcoI and BamHI restriction sites. Mutants were constructed by PCR as described in ref. 22. Homotrimeric TRAIL proteins were purified by using a three-step purification process as described in ref. 22.

SPR Receptor-Binding Assay. Binding experiments were performed by using a SPR-based biosensor, Biacore 3000. Immobilization of the DR4- and DR5-Ig receptors on the sensor surface of a Biacore CM5 sensor chip was performed by following a standard amine-coupling procedure according to the manufacturer's instructions. Receptors were coated at a level of ≈600–800 resonance units. Eighty microliters of TRAIL and variants were injected 3-fold at concentrations ranging from 250 to 0.1 nM at 70 μl/min and at 37°C by using PBS (pH 7.4) supplemented with 0.005% vol/vol P20 (Biacore) as running and sample buffer. Binding of ligands to the receptors was monitored in real time. Due to the very slow dissociation of the TRAIL-receptor complex, only pre-steady state binding data could be obtained. Furthermore, a fast initial dissociation was observed directly after the end of injection, pointing at some heterogeneity in complex formation. To obtain data that represent proper high-affinity complex formation, the response at each concentration was recorded 30 s after the end of the injections (contact time, 30 s). The response data as a function of TRAIL concentration were fitted by using a four-parameter equation to give an apparent affinity constant. Between injections, the receptor/sensor surface was regenerated by using 3 M sodium acetate (pH 5.2) injections. DcR1-, DcR2-, and OPG-Ig were captured by using a protein A-modified (Sigma) CM5 sensor chip, and the protein A sensor surface was regenerated by using 0.5 M glycine (pH 2). For the prescreening assay, 1:50 diluted clarified *Escherichia coli* BL21 extracts were injected at 50 μl/min (see *Supporting Methods*).

Biological Activity. ***Cell lines and treatment.*** Colo205 colon cancer cells, A2780 ovarium cancer cells, ML-1 myeloid leukemia cells, and the BJAB cell lines were maintained in RPMI medium 1640, 10% FCS/1% penicillin/1% streptomycin, in a humidified incubator at 37°C in a 5% CO_2 environment. In the medium of BJAB$^{DR4-,DR5-}$+DR5 cells, puromycin (Sigma) was added to a final concentration of 1 μg/ml. TRAIL receptor inhibitors (neutralizing antibodies) were always added 1 h before TRAIL addition. ***Annexin V staining.*** The Colo205 and ML-1 cells were seeded the day before the experiment at 10^5 cells per ml in 24-well plates (1 ml per well), and were treated with 1 μg/ml anti-DR4- and/or anti-DR5-neutralizing antibodies for 1 h. Wild-type TRAIL, D269H, D269H/E195R, or D269H/T214R (100 ng/ml) was added to the cells and incubated for 2 h and 30 min. After treatment, the cells were harvested by scraping them gently off the wells and then spinning them down. Control or treated Colo205 and ML-1 cells were harvested and collected by centrifugation, washed once in Annexin V incubation buffer, and resuspended in 400 μl of fresh incubation buffer. One microliter of Annexin V was added to the samples, incubated at room temperature for 10 min, and immediately measured on a FACSCalibur flow cytometer (Becton Dickinson). Results were expressed as a percent of Annexin V-positive cells. ***3-(4,5-Dimethylthiazol-2-yl)-2,5-diphenyl tetrazolium bromide (MTT) assay.*** 3-(4,5-Dimethylthiazol-2-yl)-2,5-diphenyl tetrazolium bromide assay was performed as described in ref. 22. BJAB cell lines were incubated with 1, 10, or 100 ng/ml TRAIL or D269H/E195R in the presence of 0.33 μg/ml cycloheximide (Sigma). For the EC_{50} determination, Colo205 cells were treated with serial dilutions (0–25 ng/ml) of TRAIL or mutants, and cytotoxicity was determined as described in ref. 22. EC_{50} values were calculated by using a four-parameter fit.

We thank Dr. Andrew Thorburn (University of Colorado Health Sciences Center, Aurora) for kindly providing the BJAB cell lines; Dr. Steven de Jong and Derk-Jan de Groot (both at University Medical Center, Groningen, The Netherlands) for providing the A2780 cell line and characterizing the BJAB cell lines; and Johanna Vrielink, Dr. Rob van Weeghel, Ron Suk, and Cátia Rodrigues for helpful discussions and technical assistance. This research was partly funded by European Union Fifth Framework Program Grant QLK3-CT-2001-00498. R.H.C. was supported by the European Community Initiative Interreg IIIA.

1. Ashkenazi, A., Pai, R. C., Fong, S., Leung, S., Lawrence, D. A., Marsters, S. A., Blackie, C., Chang, L., McMurtrey, A. E. & Hebert, A., *et al.* (1999) *J. Clin. Invest.* **104,** 155–162.
2. Lawrence, D., Shahrokh, Z., Marsters, S., Achilles, K., Shih, D., Mounho, B., Hillan, K., Totpal, K., DeForge, L. & Schow, P., *et al.* (2001) *Nat. Med.* **7,** 383–385.
3. LeBlanc, H. N. & Ashkenazi, A. (2003) *Cell Death Differ.* **10,** 66–75.
4. Kischkel, F. C., Lawrence, D. A., Chuntharapai, A., Schow, P., Kim, K. J. & Ashkenazi, A. (2000) *Immunity* **12,** 611–620.
5. Sprick, M. R., Weigand, M. A., Rieser, E., Rauch, C. T., Juo, P., Blenis, J., Krammer, P. H. & Walczak, H. (2000) *Immunity* **12,** 599–609.
6. Bodmer, J. L., Holler, N., Reynard, S., Vinciguerra, P., Schneider, P., Juo, P., Blenis, J. & Tschopp, J. (2000) *Nat. Cell Biol.* **2,** 241–243.
7. Kimberley, F. C. & Screaton, G. R. (2004) *Cell Res.* **14,** 359–372.
8. Griffith, T. S., Rauch, C. T., Smolak, P. J., Waugh, J. Y., Boiani, N., Lynch, D. H., Smith, C. A., Goodwin, R. G. & Kubin, M. Z. (1999) *J. Immunol.* **162,** 2597–2605.
9. Ichikawa, K., Liu, W., Zhao, L., Wang, Z., Liu, D., Ohtsuka, T., Zhang, H., Mountz, J. D., Koopman, W. J. & Kimberly, R. P., *et al.* (2001) *Nat. Med.* **7,** 954–960.
10. Chuntharapai, A., Dodge, K., Grimmer, K., Schroeder, K., Marsters, S. A., Koeppen, H., Ashkenazi, A. & Kim, K. J. (2001) *J. Immunol.* **166,** 4891–4898.
11. Wen, J., Ramadevi, N., Nguyen, D., Perkins, C., Worthington, E. & Bhalla, K. (2000) *Blood* **96,** 3900–3906.
12. Chinnaiyan, A. M., Prasad, U., Shankar, S., Hamstra, D. A., Shanaiah, M., Chenevert, T. L., Ross, B. D. & Rehemtulla, A. (2000) *Proc. Natl. Acad. Sci. USA* **97,** 1754–1759.
13. Shifman, J. M. & Mayo, S. L. (2002) *J. Mol. Biol.* **323,** 417–423.
14. Reina, J., Lacroix, E., Hobson, S. D., Fernandez-Ballester, G., Rybin, V., Schwab, M. S., Serrano, L. & Gonzalez, C. (2002) *Nat. Struct. Biol.* **9,** 621–627.
15. Havranek, J. J. & Harbury, P. B. (2003) *Nat. Struct. Biol.* **10,** 45–52.
16. Kortemme, T., Joachimiak, L. A., Bullock, A. N., Schuler, A. D., Stoddard, B. L. & Baker, D. (2004) *Nat. Struct. Mol. Biol.* **11,** 371–379.
17. Steed, P. M., Tansey, M. G., Zalevsky, J., Zhukovsky, E. A., Desjarlais, J. R., Szymkowski, D. E., Abbott, C., Carmichael, D., Chan, C. & Cherry, L., *et al.* (2003) *Science* **301,** 1895–1898.
18. Guerois, R., Nielsen, J. E. & Serrano, L. (2002) *J. Mol. Biol.* **320,** 369–387.
19. Kiel, C., Serrano, L. & Herrmann, C. (2004) *J. Mol. Biol.* **340,** 1039–1058.
20. Schymkowitz, J. W., Rousseau, F., Martins, I. C., Ferkinghoff-Borg, J., Stricher, F. & Serrano, L. (2005) *Proc. Natl. Acad. Sci. USA* **102,** 10147–10152.
21. Kiel, C., Wohlgemuth, S., Rousseau, F., Schymkowitz, J., Ferkinghoff-Borg, J., Wittinghofer, F. & Serrano, L. (2005) *J. Mol. Biol.* **348,** 759–775.
22. van der Sloot, A. M., Mullally, M. M., Fernandez-Ballester, G., Serrano, L. & Quax, W. J. (2004) *Protein Eng. Des. Sel.* **17,** 673–680.
23. Kempkens, O., Médina, E., Fernandez-Ballester, G., Özüyaman, S., Le Bivic, A., Serrano, L. & Knust, E. (2006) *Eur. J. Cell Biol.*, in press.
24. Locksley, R. M., Killeen, N. & Lenardo, M. J. (2001) *Cell* **104,** 487–501.
25. Bodmer, J. L., Schneider, P. & Tschopp, J. (2002) *Trends Biochem. Sci.* **27,** 19–26.
26. Mongkolsapaya, J., Grimes, J. M., Chen, N., Xu, X. N., Stuart, D. I., Jones, E. Y. & Screaton, G. R. (1999) *Nat. Struct. Biol.* **6,** 1048–1053.
27. Hymowitz, S. G., Christinger, H. W., Fuh, G., Ultsch, M., O'Connell, M., Kelley, R. F., Ashkenazi, A. & de Vos, A. M. (1999) *Mol. Cell* **4,** 563–571.
28. Cha, S. S., Sung, B. J., Kim, Y. A., Song, Y. L., Kim, H. J., Kim, S., Lee, M. S. & Oh, B. H. (2000) *J. Biol. Chem.* **275,** 31171–31177.
29. Vriend, G. (1990) *J. Mol. Graphics* **8,** 52–56, 29.
30. Hymowitz, S. G., O'Connell, M. P., Ultsch, M. H., Hurst, A., Totpal, K., Ashkenazi, A., de Vos, A. M. & Kelley, R. F. (2000) *Biochemistry* **39,** 633–640.
31. Thomas, L. R., Johnson, R. L., Reed, J. C. & Thorburn, A. (2004) *J. Biol. Chem.* **279,** 52479–52486.
32. Kelley, R. F., Totpal, K., Lindstrom, S. H., Mathieu, M., Billeci, K., DeForge, L., Pai, R., Hymowitz, S. G. & Ashkenazi, A. (2005) *J. Biol. Chem.* **280,** 2205–2212.
33. Muhlenbeck, F., Schneider, P., Bodmer, J. L., Schwenzer, R., Hauser, A., Schubert, G., Scheurich, P., Moosmayer, D., Tschopp, J. & Wajant, H. (2000) *J. Biol. Chem.* **275,** 32208–32213.
34. Wajant, H., Moosmayer, D., Wuest, T., Bartke, T., Gerlach, E., Schonherr, U., Peters, N., Scheurich, P. & Pfizenmaier, K. (2001) *Oncogene* **20,** 4101–4106.

BIOCHEMISTRY

THE JOURNAL OF BIOLOGICAL CHEMISTRY VOL. 283, NO. 29, pp. 20560–20570, July 18, 2008

DR4-selective Tumor Necrosis Factor-related Apoptosis-inducing Ligand (TRAIL) Variants Obtained by Structure-based Design*[S]

Received for publication, January 17, 2008, and in revised form, April 24, 2008 Published, JBC Papers in Press, May 12, 2008, DOI 10.1074/jbc.M804872200

Vicente Tur[‡1], **Almer M. van der Sloot**[‡§], **Carlos R. Reis**[§¶], **Eva Szegezdi**[‖], **Robbert H. Cool**[‡**], **Afshin Samali**[‖], **Luis Serrano**[**], **and Wim J. Quax**[‡2]

*From the [‡]Centre for Genomic Regulation, CRG-EMBL Systems Biology Unit, Dr Aiguader 88, 08003 Barcelona, Spain, the [§]Department of Pharmaceutical Biology, University of Groningen, Antonius Deusinglaan 1, 9713 AV, Groningen, The Netherlands, [¶]Cell Stress and Apoptosis Research Group, Department of Biochemistry and National Centre for Biomedical Engineering Science, National University of Ireland, Galway, Ireland, [‖]Triskel Therapeutics BV, Antonius Deusinglaan 1, 9713 AV, Groningen, The Netherlands, and **Institució Catalana de Recerca i Estudis Avançats (ICREA), Centre for Genomic Regulation (CRG), EMBL/CRG Systems Biology Research Unit, Universitat Pompeu Fabra, Dr Aiguader 88, 08003 Barcelona, Spain*

Tumor necrosis factor-related apoptosis-inducing ligand (TRAIL) is a potential anticancer agent that selectively induces apoptosis in a variety of cancer cells by interacting with death receptors DR4 and DR5. TRAIL can also bind to decoy receptors (DcR1, DcR2, and osteoprotegerin receptor) that cannot induce apoptosis. Different tumor types respond either to DR4 or to DR5 activation, and chemotherapeutic drugs can increase the expression of DR4 or DR5 in cancer cells. Thus, DR4 or DR5 receptor-specific TRAIL variants would permit new and tumor-selective therapies. Previous success in generating a DR5-selective TRAIL mutant using computer-assisted protein design prompted us to make a DR4-selective TRAIL variant. Technically, the design of DR4 receptor-selective TRAIL variants is considerably more challenging compared with DR5 receptor-selective variants, because of the lack of a crystal structure of the TRAIL·DR4 complex. A single amino acid substitution of Asp at residue position 218 of TRAIL to His or Tyr was predicted to have a favorable effect on DR4 binding specificity. Surface plasmon resonance-based receptor binding tests showed a lowered DR5 affinity in concert with increased DR4 specificity for the designed variants, D218H and D218Y. Binding to DcR1, DcR2, and osteoprotegerin was also decreased. Cell line assays confirmed that the variants could not induce apoptosis in DR5-responsive Jurkat and A2780 cells but were able to induce apoptosis in DR4-responsive EM-2 and ML-1 cells.

Computational protein design methods have been successfully employed to redesign several protein-protein interactions (1–6), but they have as yet hardly been applied to redesign target binding preferences of therapeutic proteins. Computational protein design methods allow the rational design of tailor-made protein therapeutics by modifying the binding characteristics of the protein, for example to reduce target binding promiscuity or to design novel mechanisms of activity.

Tumor necrosis factor (TNF)[4]-related apoptosis-inducing ligand (TRAIL) is a potential protein therapeutic currently attracting great interest because of its anti-cancer activity. TRAIL selectively induces apoptosis in tumor cells *in vitro* and *in vivo* by a death receptor-mediated process. Unlike other apoptosis-inducing TNF family members, soluble TRAIL appears to be inactive against normal healthy tissue (5). TRAIL shows a high degree of promiscuity as it binds to five cognate receptors as follows: DR4 (TRAIL-R1) and DR5 (TRAIL-R2) and three decoy receptors, DcR1 (TRAIL-R3), DcR2 (TRAIL-R4), and osteoprotegerin (OPG) (6). Upon binding to TRAIL, DR4 and DR5 receptors recruit Fas-associated death domain (7–9), which leads to recruitment and activation of caspase-8 and -10 triggering apoptosis (10–13). DcR1 does not contain a death domain, and DcR2 contains a truncated death domain, and thus, binding of TRAIL to these receptors does not induce apoptosis. In contrast, these decoy receptors could prevent apoptosis by sequestering available TRAIL or by interfering with the formation of a TRAIL·DR4 or ·DR5 signaling complex (14).

Use of DR4-selective variants could permit better tumor-specific therapies through escape from the decoy receptor-mediated antagonism, resulting in a higher efficacy with possibly less side effects as compared with wtTRAIL (15–18). Receptors DR4 and/or DR5 were shown to be up-regulated after treatment with DNA-damaging chemotherapeutic drugs, and the response to TRAIL-induced apoptosis was significantly increased (8, 19). Previously, we described the design of DR5-selective TRAIL variants (20). These variants showed an increased affinity for the DR5 receptor and decreased affinities for the DR4 and decoy receptors. A recent study demonstrated

* This work was supported in part by European Union Fifth Framework Program Grant QLK3-CT 2001-00408 and Sixth Framework Program Grant LSH-2005-2.2.0-2. The costs of publication of this article were defrayed in part by the payment of page charges. This article must therefore be hereby marked "*advertisement*" in accordance with 18 U.S.C. Section 1734 solely to indicate this fact.

[S] The on-line version of this article (available at http://www.jbc.org) contains supplemental Figs. 1–3.

[1] These authors contributed equally to this work.

[2] Supported in part by the Dutch STW Valorization Project 7660.

[2] To whom correspondence should be addressed: Dept. of Pharmaceutical Biology, University of Groningen, Antonius Deusinglaan 1, 9713 AV, Groningen, The Netherlands. E-mail: w.j.quax@rug.nl.

[4] The abbreviations used are: TNF, tumor necrosis factor; TRAIL, TNF-related apoptosis-inducing ligand; OPG, osteoprotegerin; WT, wild type; ELISA, enzyme linked immunosorbent assay; rh, recombinant human; CRD, cysteine-rich domain; SPR, surface plasmon resonance.

that primary cells isolated from patients with chronic lymphocytic leukemia and mantle cell lymphoma were almost exclusively sensitive to DR4-mediated apoptosis (21, 22). The existence of certain cancer cells only responding to DR4-mediated apoptosis (20) and favorable results obtained with agonistic anti-DR4 antibodies (23) prompted us to design a DR4-selective TRAIL variant.

Because wild-type TRAIL has higher affinity for DR5 than DR4 (20, 24), the design of an effective DR4-selective TRAIL variant should preferably aim at both an enhanced affinity for DR4 and at decreased affinities for DR5 and decoy receptors. Consequently, it is essential to combine a positive design strategy strengthening the interactions between TRAIL and DR4 with a negative strategy that designs mutations disrupting interactions between TRAIL and the other receptors. Generally, it is less demanding to only disrupt an existing interaction (or create an unfavorable one) by an amino acid substitution than to combine this with the creation of a new favorable interaction. A high quality structural model describing all the relevant interactions between the interacting partners is therefore of paramount importance. As the only crystal structure available is that of the TRAIL-DR5 complex, the design of a DR4-selective variant critically depends on the quality of the homology model of the TRAIL-DR4 complex. We demonstrate here that the design of DR4-specific rhTRAIL variants is possible using homology modeling and computational protein design.

EXPERIMENTAL PROCEDURES

All reagents were of analytical grade unless specified otherwise. Isopropyl β-D-1-thio-galactoside, ampicillin, and dithiothreitol were from Duchefa (Haarlem, The Netherlands). Chromatographic columns and media were from Amersham Biosciences. Restriction enzymes were purchased from New England Biolabs. Recombinant TRAIL receptor Ig fusion proteins formulated with bovine serum albumin were ordered from R & D Systems. All other chemicals were from Sigma. All buffers used in SPR, ELISA, and biological activity assays were of physiological pH and ionic strength.

Modeling of TRAIL-Receptor Complexes—At present only the crystal structure of TRAIL in complex with the DR5 receptor is known. The template selected was Protein Data Bank code 1D4V (25); the structure was at 2.2 Å resolution and of monomeric human TRAIL in complex with the ectodomain of DR5 (TRAIL-R2) receptor. The homotrimer was generated using the protein quaternary structure server from the EBI, having the symmetry coordinates in the Protein Data Bank file. From the sequence alignment of the different TRAIL receptors (26), it is observed that the receptor cysteine-rich domains (CRDs) involved in the interaction with TRAIL (CRD2 and CRD3) are highly conserved, with the exception of the soluble receptor OPG. Indeed, when compared with DR5, the sequence identity of any other membrane-attached TRAIL receptor is higher than 50% in each case, and there are neither insertions nor deletions in the sequence (with the exception of a glycine deletion in the middle of the CRD3 in DcR1). In addition, all the cysteines involved in the formation of internal disulfide bridges are conserved and share the same sequence position. Thus it is possible to build homology models of all TRAIL receptors except for OPG.

The homology model of TRAIL-DR4 was built using the protein design capabilities of FoldX. The DR5 amino acid residues were mutated into the corresponding DR4 amino acids, and subsequently, all amino acid side chain interactions were optimized to accommodate TRAIL and receptor residues to their new interface.

Computational Design of the Mutants—A detailed description of the empirical force field FoldX (version 2.6) is available elsewhere (27, 28) and on line. Briefly, this force field calculates the free energy of unfolding (ΔG) of a target protein or protein complex combining the physical description of the interactions with empirical data obtained from experiments on proteins. Force field components (polar and hydrophobic solvation energies, van der Waals interactions, van der Waals clashes, H-bond energies, and electrostatics in the complex and its effects on the k_{on} and backbone and side chain entropies) were calculated evaluating the properties of the structure, such as its atomic contact map, the accessibility of its atoms and residues, the backbone dihedral angles, the H-bond network, and the electrostatic network of the protein. Water molecules making two or more H-bonds with the protein were also taken into account (29).

FoldX was able to perform amino acid mutations and simultaneously accommodate the new residues and its surrounding amino acids (28). FoldX first mutates the selected position to alanine and annotates the side chain energies of the neighbor residues. Then it mutates this alanine to the selected amino acid and recalculates the side chain energies of the same neighboring residues. Those that exhibit an energy difference are then mutated to themselves to see if another rotamer will be more favorable.

This procedure was also used to reconstruct the binding interface of TRAIL in complex with the modeled DR4 receptor: to repair residues with bad torsion angles, residues having bad van der Waals clashes or to build up the putative interactions between TRAIL and the modeled receptor. The most optimal amino acid conformation was chosen using rotamer substitution (see above). The crystal structure of TRAIL in complex with the DR5 receptor was also refined this way.

Site-directed Mutagenesis, Expression, and Purification of Selectivity Mutants—A cDNA corresponding to human soluble TRAIL (amino acids 114–281) was cloned in pET15B (Novagen) using NcoI and BamHI restriction sites. Mutants were constructed by PCR as described before (30). Homotrimeric TRAIL proteins were purified using a three-step purification as described previously (30). Analytical gel filtration and nonreducing gel electrophoresis confirmed that rhTRAIL WT, D218H, and D218Y are trimeric molecules; they do not form higher degree aggregates and do not contain inter-chain disulfide bridges.

Determination of Receptor Binding—Binding experiments were performed using a surface plasmon resonance-based biosensor Biacore 3000 (Biacore AB, Uppsala, Sweden) at 37 °C. DR4-Ig, DR5-Ig, DcR1-Ig, DcR2-Ig, and OPG-Ig receptor chimeras were captured at a 35 μl/min flow rate using a protein A (Sigma)-modified CM5 sensor chip (Biacore). Receptors chi-

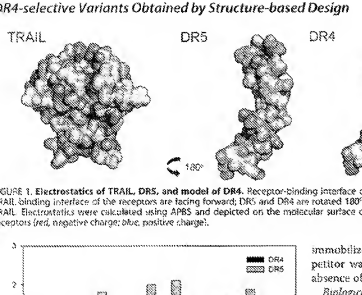

FIGURE 1. **Electrostatics of TRAIL, DR5, and model of DR4.** Receptor-binding interface of TRAIL and the TRAIL-binding interface of the receptors are facing forward; DR5 and DR4 are rotated 180° with respect to TRAIL. Electrostatics were calculated using APBS and depicted on the molecular surface of TRAIL and the receptors (red, negative charge; blue, positive charge).

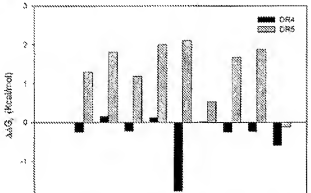

FIGURE 2. **Results of FoldX calculation.** A negative $\Delta\Delta G_f$ indicates an improvement in receptor binding, and a positive $\Delta\Delta G_f$ indicates a decrease in receptor binding.

means were captured at a level of ~500–800 response units. Purified rhTRAIL WT and rhTRAIL variants were injected 3-fold at concentrations ranging from 250 to 2 nM at 70 μl/min flow rate using HBS-EP (Biacore) as running and sample buffer. Binding of ligands to the receptors was monitored in real time. Between injections the protein A sensor surface was regenerated using a 30-s pulse of 10 mM glycine, pH 2.0. The resonance signal measured on the reference cell (containing protein A only) was subtracted from the signal measured on the experimental flow cell. All sensorgrams were corrected for buffer injection. To obtain pre-steady state data that represent proper high affinity complex formation, and assuming the initial fast off-rate to represent lower affinity complexes, the response at each concentration was recorded 30 s after the end of the injections. The response data as a function of TRAIL concentration were fitted by using a four-parameter equation to give an apparent affinity constant.

Selectivity of the variants toward the DR4 receptor was also assessed using a competitive ELISA experiment as described before (20). In short, 10 ng/well rhTRAIL WT or receptor-selective variants were preincubated with 0–500 ng/well DR4 or DR5-Ig for 30 min. Preincubated solutions were added to microtiter plates coated with DR4-Ig. After washing away unbound sample, bound rhTRAIL WT or variants were detected with a polyclonal goat anti-TRAIL antibody (R & D Systems) followed by a horseradish peroxidase-conjugated swine anti-goat antibody (BIOSOURCE) using the one-step turbo 3,3′,5,5′-tetramethylbenzidine-ELISA (Pierce) as detection reagent. Absorbance was measured at 450 nm. Binding of the receptor-selective variants to immobilized DR4-Ig at various concentrations of soluble competitor was calculated relative to the value measured in the absence of soluble receptor.

Biological Activity, Cell Line, and Treatment—A2780, ovarian adenocarcinoma cells were maintained in Dulbecco's modified Eagle's medium, whereas Jurkat T cell leukemia, ML-1 acute myeloid leukemia, and EM-2 chronic myelogenous leukemia cell lines were maintained in RPMI 1640 medium, both supplemented with 10% fetal calf serum, 50 units/ml penicillin, 5 mg/ml streptomycin, 2 mM L-glutamine, and 1 mM sodium pyruvate in a humidified incubator, 37 °C, 5% CO_2 environment.

Annexin V Staining—Cells were seeded the day before the experiment at a density of 3.5×10^5, 5×10^5, and 3×10^5 cells/ml in 24-well plates (0.5 ml/well) for A2780, Jurkat, ML-1 and EM-2 cell types, respectively. 10–250 ng/ml rhTRAIL WT, D269HE195R, D218H, or D218Y was added to the cells and incubated for 24 h. FLAG-tagged TRAIL (Alexis) was preincubated with 1 μg/ml enhancer for 20 min (cross-linking) before adding it to Jurkat cell cultures in a concentration between 10 and 250 ng/ml. A2780 cells were trypsinized gently, and the cells were allowed to recover for 10 min with gentle shaking at 37 °C before pelleting by centrifugation. Jurkat, ML-1, and EM-2 cells were transferred into Eppendorf tubes and spun down. Cell pellets were resuspended in 50 μl of annexin V incubation buffer (10 mM HEPES/NaOH, pH 7.4, 140 mM NaCl, 2.5 mM $CaCl_2$) containing 6 μl of annexin V-fluorescein isothiocyanate (IQ Corp.) for 15 min on ice. The reaction was stopped by adding 300 μl of fresh incubation buffer, and the samples were analyzed immediately using a FACSCalibur flow cytometer (BD Biosciences). Results were expressed as percentage of annexin V-positive cells.

RESULTS

Selectivity Design—For the design of a DR4-selective TRAIL variant, the procedure previously used for the design of DR5-selective TRAIL variants was used (20). In short, the receptor binding interface of TRAIL was screened for single amino acid substitutions that increase the affinity for the DR4 receptor (decreasing interaction energy ($\Delta\Delta G_f$)) or decreasing affinity for DR5. For the TRAIL-DR4-receptor complex, a homology model consisting of TRAIL in complex with CRD2 and -3 of DR4 was constructed based on the TRAIL-DR5-receptor com-

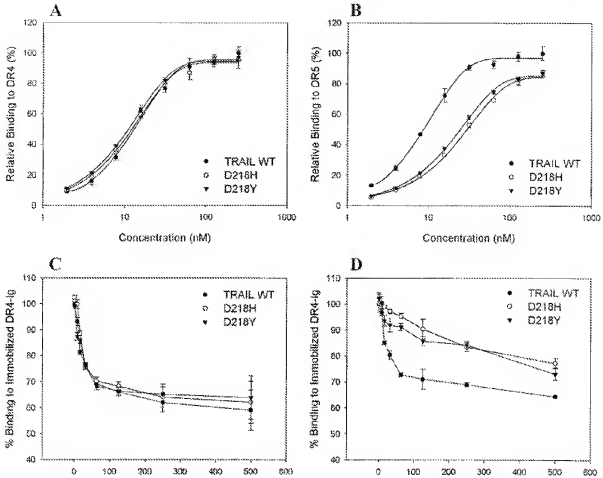

FIGURE 3. **Receptor binding of rhTRAIL WT and DR4-selective mutants as determined by SPR and competitive ELISA.** Receptor binding of rhTRAIL WT, D218H, and D218Y to DR4-Ig was determined by SPR (*A*) or to DR5-Ig (*B*). To obtain pre-steady state data that represent proper high affinity complex formation, and assuming the initial fast off-rate to represent lower complexes, the response at each concentration was recorded 30 s after the end of the injections. Receptor binding was calculated relative to the response of rhTRAIL WT at 250 nM. Competition ELISA used DR4-Ig as competitor (*C*) or soluble DR5-Ig as competitor (*D*). rhTRAIL WT or variants were preincubated with 0–500 ng/well DR4 or DR5 during 30 min. Preincubated solutions were added to microtiter plates coated with DR4-Ig. Binding of the selective variants at various concentrations of soluble receptor toward the immobilized DR4-Ig was calculated relative to the value measured on the presence of 0 ng/well of soluble receptor.

plex. For the TRAIL-DR5-receptor complex, the 1D4V crystal structure was used (25). CRD2 and -3 of DR4 show a considerable degree of sequence identity with DR5 (~50%), and the alignment contains no insertions or deletions (not shown); consequently, it was decided to use a model with an identical amino acid backbone conformation as TRAIL-DR5. FoldX was used to build the TRAIL-DR4 model by mutating DR5 amino acid residues into the corresponding DR4 amino acids, followed by optimization of all amino acid side chain interactions (27, 28). In Fig. 1, electrostatic charges mapped on the solvent-accessible surface of TRAIL, DR5, and the DR4 model are depicted. It can be seen that the surface electrostatics of TRAIL and DR5 are more complementary with each other than the surface electrostatics of TRAIL and DR4. The accuracy of the models and the force field was tested using the affinity data derived from the alanine scanning of rhTRAIL as performed by Hymowitz *et al.* (31). The predictions of the energy change in the complex formation correlate with the changes in the dissociation constants measured (data not shown) (20). This implies that the above method can reliably predict mutations in the binding interface that would alter ligand-receptor interaction.

The FoldX design process (see "Experimental Procedures") proposed several positions in the receptor-binding interface of TRAIL and (single) amino acid substitutions enhancing DR4 selectivity. One of the proposed mutations, K201R, was already present in a sextuple mutant selected by Kelley *et al.* (32) using phage display, underlining the correctness of the DR4 model. In addition, new amino acid substitutions were predicted that have not been described before. Of these, the D218Y and D218H mutations were predicted to result in the highest increase in DR4 selectivity by maintaining or improving the interaction with DR4 and decreasing the interaction with DR5

TABLE 1
Apparent DR4 and DR5 binding affinities and receptor binding capacity of rhTRAIL WT, D218H, and D218Y as determined using a pre-steady state approach

	DR4		DR5	
	Apparent K_d	Receptor binding capacity (% WT)	Apparent K_d	Receptor binding capacity (% WT)
	nM		nM	
WT	18.7 (±1.4)	100 (±3)	7.8 (±1.3)	100 (±1)
D218H	23.3 (±0.6)	99 (±2)	38.9 (±2.7)	93 (±4)
D218Y	10.7 (±0.4)	97 (±3)	23.3 (±0.4)	93 (±3)

(Fig. 2). To assess the effect of pH on receptor binding of D218H, calculations were performed while introducing a charged, neutral, and partially charged histidine at position 218 to reflect acidic, basic, and physiological pH environments, respectively. As shown in Fig. 2, the decreased affinity of D218H for DR5 is partially accounted for by electrostatic repulsion as the $\Delta\Delta G$, increases from 1.2 to 2.0 kcal/mol when going from a neutral to a charged histidine. In contrast, the affinity for DR4 is not dependent on pH (Fig. 2). The D218A mutation has been described previously by Hymowitz *et al.* (31) to reduce the affinity for DR4 (1.3-fold) and, more pronounced, for DR5 (1.9-fold). FoldX also predicts that this variant has a lowered affinity for DR5 (Fig. 2). The D218H and D218Y rhTRAIL mutants were made, produced, and purified as described before (20, 30).

Receptor Binding—Binding of the purified ligands to protein A-immobilized DR4-Ig and DR5-Ig receptor chimeras was assessed in real time using SPR. Receptor binding curves were recorded using rhTRAIL concentrations ranging from 2 to 250 nM at 37 °C (Fig. 3*A* and *B*). Apparent dissociation constants were calculated from pre-steady state response values (Table 1). Although the apparent dissociation constant (K_d) for DR4 of both variants remained unchanged when compared with rhTRAIL WT, both variants showed a 3–3.5-fold increase in their apparent dissociation constant for DR5 (Table 1). Inspection of the sensorgrams recorded at 37 °C for DR4 and DR5 revealed that the k_{off} for rhTRAIL WT was very low (supplemental Fig. 1, *A* and *B*, *left*). On the other hand, both D218H and D218Y variants showed an initial increased off-rate, which in the case of binding to DR4 (supplemental Fig. 1*A*, *middle*, *right*) was much smaller than the off-rate at the DR5 receptor (supplemental Fig. 1*B*, *middle*, *right*).

To assess the selectivity of D218H and D218Y toward the DR4 receptor in the presence of the DR5 receptor, a competitive ELISA experiment was performed. Although soluble DR4-Ig was equally efficient in reducing the binding of both rhTRAIL and the Asp-218 variants toward immobilized DR4-Ig by 50%, soluble DR5-Ig was more than 9-fold less efficient in achieving a 50% reduction in binding toward immobilized DR4 for the Asp-218 variants than for rhTRAIL WT (Fig. 3, *C* and *D*). These results indicate that D218H and D218Y preferentially bind to the DR4 receptor when both DR4 and DR5 receptors are present.

Binding affinities for both variants to the decoy receptors DcR1, DcR2, and OPG were also measured by SPR (Fig. 4, *B* and *C*). D218H and D218Y showed a 2–3-fold reduction in apparent K_d for immobilized DcR2-Ig, mainly because of an increased off-rate. The reduction in binding to immobilized

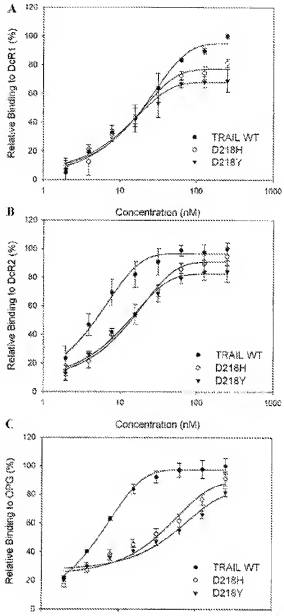

FIGURE 4. **Receptor binding of TRAIL and DR4-selective mutants to DcR1-Ig as determined by SPR (*A*), DcR2-Ig (*B*), or to OPG-Ig (*C*).** Curve fitting was generated from data points derived from the sensorgrams as described in Fig. 3. Receptor binding is calculated relative to the response of TRAIL at 250 nM.

DcR1-Ig was more modest. On both receptors, the increase in off-rate was largest for D218Y (supplemental Fig. 2, *A* and *B*). Binding to immobilized OPG-Ig showed a more complex behavior. Although at concentrations above 125 nM the initial off-rate was still increased for both variants, the maximum level of binding, in particular for D218H, was comparable with the wild-type level. However, at concentrations below 125 nM,

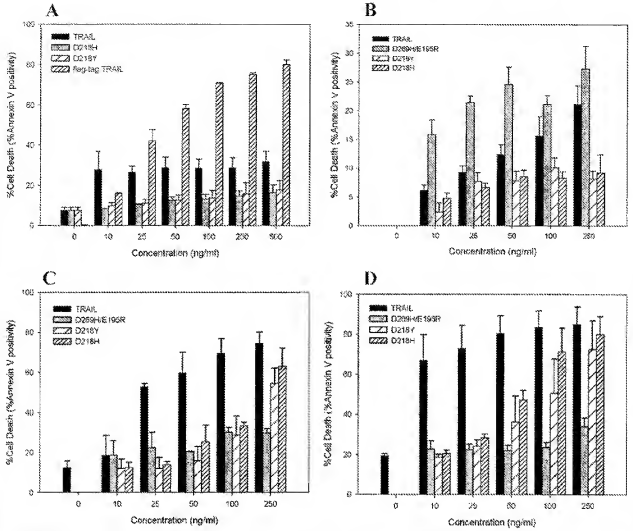

FIGURE 5. **Biological activity of TRAIL, D218Y, and D218H variants and the DR5-selective ligand D269HE195R in DR5-sensitive Jurkat cells (*A*), A2780 cells (*B*), DR4-sensitive ML-1 cells (*C*), and EM-2 cells (*D*).** Percentage apoptosis was measured as percentage annexin V positivity after 3 h of incubation.

binding of both D218H and D218Y to immobilized OPG-Ig was significantly reduced because of a large increase in k_{off} (supplemental Fig. 2*C*). In summary, these results show that the D218Y and D218H mutations provide DR4 selectivity by decreasing the affinity for DR5, DcR2, and OPG while leaving the affinity for DR4 unchanged.

Biological Activity—To test the ability of D218Y and D218H variants to selectively bind and activate DR4, A2780, Jurkat, ML-1, and EM-2 cells were treated with this variant. Previously, it was established that A2780 and Jurkat cells express only DR5 on their surface and hence are only sensitive toward TRAIL-induced apoptosis mediated by DR5 (20, 32). In contrast, ML-1 and EM-2 cells are mainly sensitive toward TRAIL-induced apoptosis mediated by DR4 (supplemental Fig. 3) (20). In Jurkat cells D218Y and D218H showed almost no apoptosis inducing activity (<10%) up to the highest measured concentration of 500 ng/ml compared with rhTRAIL (24% at 500 ng/ml). The restricted apoptosis-inducing ability of D218H and D218Y in Jurkat cells was even more evident when it was compared with the apoptosis inducing activity of cross-linked FLAG-tagged TRAIL (80% at 500 ng/ml) (Fig. 5*A*), a more potent inducer of apoptosis in this particular cell line (33).

In the second DR5-sensitive cell line A2780, the DR5-selective TRAIL variant D269H/E195R displayed the highest apoptosis inducing activity. D218H and D218Y showed significantly lower activity when compared with both the DR5-selective variant and rhTRAIL WT (Fig. 5*B*).

In contrast, in the DR4-responsive cell lines, EM-2 and ML-1, D218H, and D218Y variants were able to efficiently induce apoptosis at concentrations above 100 ng/ml (Fig. 5, *C* and *D*), whereas the DR5-selective variant D269H/E195R essentially lacked apoptosis inducing activity under these conditions. D218H showed higher apoptosis inducing activity in comparison with D218Y, but both variants were less active than rhTRAIL WT. With regard to potential DR4-selective behavior, it is important to correct for this lower

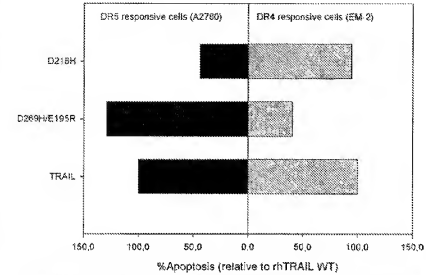

FIGURE 6. **Biological activity of TRAIL, the D218H variant, and the DR5-selective ligand D269HE195R in DR5-sensitive A2780 cells and in DR4-sensitive EM-2 cells.** Percentage apoptosis was measured as percentage of annexin V positivity after 3 h of incubation with 250 ng/ml of TRAIL or variant. Apoptosis inducing activity is calculated relative to the apoptosis inducing activity of TRAIL at these concentrations.

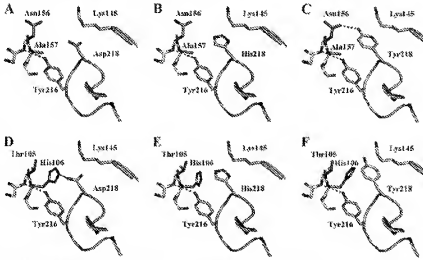

FIGURE 7. **Interactions at the ligand receptor interface surrounding residue 218 of TRAIL, D218H, or D218H and receptors DR4 (*top*) or DR5 (*bottom*).** *A* and *D*, WT; *B* and *E*, D218H; *C* and *F*, D218Y.

agonistic activity. In the DR5-responsive A2780 cell line at a concentration of 250 ng/ml, less than 10% apoptosis is induced by the best performing DR4-selective variant D218H, whereas both rhTRAIL WT and D269H/E195R induced between 20 and 30% apoptosis. In contrast, both rhTRAIL WT and the D218H variant were able to efficiently induce apoptosis (85 and 80%, respectively) in the DR4-responsive cell line EM-2 at this concentration, whereas the DR5-selective variant induced only 34% apoptosis. This is illustrated in Fig. 6 for rhTRAIL WT, D218H, and the DR5-selective variant D269H/E195R. Taken together, these results confirm that the D218H and D218Y variants induce apoptosis preferentially via DR4.

DISCUSSION

TRAIL interacts with five different receptors of the TNF-R family; however, only receptors DR4 and DR5 are able to induce apoptosis. Interestingly, it has been shown that the expression levels of DR4 and/or DR5 were up-regulated in cancer cells in response to a number of chemotherapeutic drugs (6). The existence of certain cancer cells only responding to DR4-mediated apoptosis (20) and favorable results obtained with agonistic anti-DR4 antibodies (23) have encouraged the search for DR4-selective TRAIL variants. Recently, Kelley *et al.* (32) described the use of phage display to select DR4-selective TRAIL variants from a saturation mutagenesis library. However, subsequent analysis revealed that this DR4-selective TRAIL variant containing six mutations was biologically inactive (22). Activity of this mutant could be restored after reverting one of the mutations back to the wild-type amino acid, but how it affected receptor selectivity was not examined (22).

Computational protein design methods have been demonstrated by us and others to represent a valuable tool for the improvement and modification of protein-protein interactions (1–4, 20, 34). From a practical point of view, computational design algorithms enable the modification of several key properties of proteins in a much shorter time frame than any other protein engineering methodologies, such as directed evolution methods.

Previously we used computational protein design to construct a DR5-selective TRAIL variant (20). This stimulated us to design a DR4-selective TRAIL variant using computational protein design despite the lack of a crystal structure for this receptor. In this study we focused on Asp-218 predicted by the FoldX algorithm to be important for selectivity toward the DR4 receptor. Interestingly, this residue has not been identified before with the phage display approach of Kelley *et al.* (32).

From the crystal structure of the TRAIL-DR5 complex and the model of the TRAIL-DR4 complex, it can be observed that Asp-218 forms a hydrogen bond with His-106 of DR5, whereas no hydrogen bond interaction is possible with the equivalent Ala-157 of DR4 (Fig. 7). When mutating Asp-218 to His or Tyr,

the hydrogen bond with His-106 of DR5 is disrupted. In addition, changing Asp-218 into His creates some electrostatic repulsion in this pocket because of two positively charged amino acids in close proximity. In case of the D218Y variant, the substitution of Asp-218 to Tyr introduces van der Waals clashes with His-106 of DR5, forcing one of these residues to be re-accommodated by pushing away the other residue and causing instability to this interaction pocket. Both mutations thus seem to reduce the affinity for DR5.

The DR4 model was built by assuming an identical backbone structure as DR5, as has also been assumed for our 218 mutants in comparison with TRAIL WT. Although this will be true in general, there could be some cases in which small changes in the backbone could affect the predictions. The calculated $\Delta\Delta G$ for the complex of D218Y with DR4 is mainly a consequence of the hydrogen bond that was predicted to be formed between Tyr-218 and DR4 Asn-156. A small change in the modeled coordinates of DR4 would preclude formation of such a hydrogen bond, and such an effect may explain why we could not obtain experimental evidence for an increased DR4 affinity for D218Y. The backbone change is more likely to occur in the coordinates of DR4 than of TRAIL, not only because the many deviations from the DR5 sequence in DR4 but also because the single Asp-218 to Tyr mutation does not introduce any clashes with the TRAIL backbone or neighboring TRAIL residues warranting a potential move. In addition, FoldX correctly predicted a decrease in affinity of D218H and D218Y for DR5.

Both the SPR receptor binding data and the biological activity data indicated that D218Y and D218H variants induce apoptosis preferentially via DR4 and thus are DR4-selective. Receptor binding experiments using SPR showed unchanged affinity for the variants D218H and D218Y toward the DR4-Ig receptor and an increased dissociation rate to DR5-Ig when compared with rhTRAIL WT, resulting in a reduced binding affinity to this receptor. Binding of D218H and D218Y toward the decoy receptors DcR2-Ig, OPG-Ig, and, although less pronounced, to DcR1-Ig also showed a significant reduction in binding affinity when compared with rhTRAIL WT.

In summary, computational protein design can be successfully used to direct TRAIL variants to either the DR5 (20) or DR4 receptor. The computational method used in our study is based on general applicable principles, and it can be used on any other protein as template structure, spanning the whole sequence and structure space of protein families and protein folds. This was convincingly demonstrated in other protein design works using FoldX (2, 20, 29, 30, 35–38). The design predictions for DR4-selective rhTRAIL variants resulted in variants that do show agonistic DR4 specificity in cell line assays. Analytical SPR receptor binding tests showed a lowered DR5 affinity in concert with increased DR4 specificity. These results combined show that the variants D218H and D218Y have become DR4-selective.

REFERENCES

1. Sridhar, J. M., and Mayo, S. L. (2002) *J. Mol. Biol.* **323,** 417–423
2. Reina, J., Lacroix, E., Hobson, S. D., Fernandez-Ballester, G., Rybin, V., Schwab, M. S., Serrano, L., and Gonzalez, C. (2002) *Nat. Struct. Biol.* **9,** 621–627
3. Havranek, J. J., and Harbury, P. B. (2003) *Nat. Struct. Biol.* **10,** 45–52
4. Kortemme, T., Joachimiak, L. A., Bullock, A. N., Schuler, A. D., Stoddard, B. L., and Baker, D. (2004) *Nat. Struct. Mol. Biol.* **11,** 371–379
5. Ashkenazi, A., Pai, R. C., Fong, S., Leung, S., Lawrence, D. A., Marsters, S. A., Blackie, C., Chang, L., McMurtrey, A. E., Hebert, A., DeForge, L., Koumenis, I. L., Lewis, D., Harris, L., Bussiere, J., Koeppen, H., Shahrokh, Z., and Schwall, R. H. (1999) *J. Clin. Invest.* **104,** 155–162
6. LeBlanc, H. N., and Ashkenazi, A. (2003) *Cell Death Differ.* **10,** 66–75
7. Chaudhary, P. M., Eby, M., Jasmin, A., Bookwalter, A., Murray, J., and Hood, L. (1997) *Immunity* **7,** 821–830
8. Schneider, P., Thome, M., Burns, K., Bodmer, J. L., Hofmann, K., Kataoka, T., Holler, N., and Tschopp, J. (1997) *Immunity* **7,** 831–836
9. Kuang, A. A., Diehl, G. E., Zhang, J., and Winoto, A. (2000) *J. Biol. Chem.* **275,** 25065–25068
10. Kischkel, F. C., Lawrence, D. A., Chuntharapai, A., Schow, P., Kim, K. J., and Ashkenazi, A. (2000) *Immunity* **12,** 611–620
11. Sprick, M. R., Weigand, M. A., Rieser, E., Rauch, C. T., Juo, P., Blenis, J., Krammer, P. H., and Walczak, H. (2000) *Immunity* **12,** 599–609
12. Bodmer, J. L., Holler, N., Reynard, S., Vinciguerra, P., Schneider, P., Juo, P., Blenis, J., and Tschopp, J. (2000) *Nat. Cell Biol.* **2,** 241–243
13. Kischkel, F. C., Lawrence, D. A., Tinel, A., LeBlanc, H., Virmani, A., Schow, P., Gazdar, A., Blenis, J., Arnott, D., and Ashkenazi, A. (2001) *J. Biol. Chem.* **276,** 46639–46646
14. Kimberley, F. C., and Screaton, G. R. (2004) *Cell Res.* **14,** 359–372
15. Griffith, T. S., Rauch, C. T., Smolak, P. J., Waugh, J. Y., Boiani, N., Lynch, D. H., Smith, C. A., Goodwin, R. G., and Kubin, M. Z. (1999) *J. Immunol.* **162,** 2597–2605
16. Ichikawa, K., Liu, W., Zhao, L., Wang, Z., Liu, D., Ohtsuka, T., Zhang, H., Mountz, J. D., Koopman, W. J., Kimberly, R. P., and Zhou, T. (2001) *Nat. Med.* **7,** 954–960
17. Chuntharapai, A., Dodge, K., Grimmer, K., Schroeder, K., Marsters, S. A., Koeppen, H., Ashkenazi, A., and Kim, K. J. (2001) *J. Immunol.* **166,** 4891–4898
18. Bin, L., Thorburn, J., Thomas, L. R., Clark, P. E., Humphreys, R., and Thorburn, A. (2007) *J. Biol. Chem.* **282,** 28189–28194
19. Wen, J., Ramadevi, N., Nguyen, D., Perkins, C., Worthington, E., and Bhalla, K. (2000) *Blood* **96,** 3900–3906
20. van der Sloot, A. M., Tur, V., Szegezdi, E., Mullally, M. M., Cool, R. H., Samali, A., Serrano, L., and Quax, W. J. (2006) *Proc. Natl. Acad. Sci. U. S. A.* **103,** 8634–8639
21. MacFarlane, M., Inoue, S., Kohlhaas, S. L., Majid, A., Harper, N., Kennedy, D. B., Dyer, M. J., and Cohen, G. M. (2005) *Cell Death. Differ.* **12,** 773–787
22. MacFarlane, M., Kohlhaas, S. L., Sutcliffe, M. J., Dyer, M. J., and Cohen, G. M. (2005) *Cancer Res.* **65,** 11265–11270
23. Yagita, H., Takeda, K., Hayakawa, Y., Smyth, M. J., and Okumura, K. (2004) *Cancer Sci.* **95,** 777–783
24. Trusek, A., Sharma, S., Silverman, C., Khandekar, S., Reddy, M. P., Deen, K. C., McLaughlin, M. M., Srinivasula, S. M., Livi, G. P., Marshall, L. A., Ahmed, F. E. S., Williams, W. V., and Doyle, M. L. (2000) *J. Biol. Chem.* **275,** 27219–27226
25. Mongkolsapaya, J., Grimes, J. M., Chen, N., Xu, X. N., Stuart, D. I., Jones, E. Y., and Screaton, G. R. (1999) *Nat. Struct. Biol.* **6,** 1048–1053
26. Straussberg, R. L., Feingold, E. A., Grouse, L. H., Derge, J. G., Klausner, R. D., Collins, F. S., Wagner, L., Shenmen, C. M., Schuler, G. D., Altschul, S. F., Zeeberg, B., Buetow, K. H., Schaefer, C. F., Bhat, N. K., Hopkins, R. F., Jordan, H., Moore, T., Max, S. I., Wang, J., Hsieh, F., Diatchenko, L., Marusina, K., Farmer, A. A., Rubin, G. M., Hong, L., Stapleton, M., Soares, M. B., Bonaldo, M. F., Casavant, T. L., Scheetz, T. E., Brownstein, M. J., Usdin, T. B., Toshiyuki, S., Carninci, P., Prange, C., Raha, S. S., Loquellano, N. A., Peters, G. J., Abramson, R. D., Mullahy, S. J., Bosak, S. A., McEwan, P. J., McKernan, K. J., Malek, J. A., Gunaratne, P. H., Richards, S., Worley, K. C., Hale, S., Garcia, A. M., Gay, L. J., Hulyk, S. W., Villalon, D. K., Muzny, D. M., Sodergren, E. J., Lu, X., Gibbs, R. A., Fahey, J., Helton, E., Ketteman, M., Madan, A., Rodrigues, S., Sanchez, A., Whiting, M., Madan, A., Young, A. C., Shevchenko, Y., Bouffard, G. G., Blakesley, R. W., Touchman, J. W., Green, E. D., Dickson, M. C., Rodriguez, A. C., Grimwood, J., Schmutz, J., Myers, R. M., Butterfield, Y. S., Krzywinski, M. I., Skalska, U., Smailus, D. E., Schnerch, A., Schein, J. E., Jones, S. J., and Marra, M. A. (2002) *Proc. Natl. Acad. Sci. U. S. A.* **99,** 16899–16903

27. Guerois, R., Nielsen, J. E., and Serrano, L. (2002) *J. Mol. Biol.* **320,** 369–387
28. Schymkowitz, J. W., Rousseau, F., Martins, I. C., Ferkinghoff-Borg, J., Stricher, F., and Serrano, L. (2005) *Proc. Natl. Acad. Sci. U. S. A.* **102,** 10147–10152
29. Kiel, C., Serrano, L., and Herrmann, C. (2004) *J. Mol. Biol.* **340,** 1039–1058
30. van der Sloot, A. M., Mullally, M. M., Fernandez-Ballester, G., Serrano, L., and Quax, W. J. (2004) *Protein Eng. Des. Sel.* **17,** 673–680
31. Hymowitz, S. G., O'Connell, M. P., Ultsch, M. H., Hurst, A., Totpal, K., Ashkenazi, A., de Vos, A. M., and Kelley, R. F. (2000) *Biochemistry* **39,** 633–640
32. Kelley, R. F., Totpal, K., Lindstrom, S. H., Mathieu, M., Billeci, K., Deforge, L., Fui, P., Hymowitz, S. G., and Ashkenazi, A. (2005) *J. Biol. Chem.* **280,** 2205–2212
33. Wiley, S. R., Schooley, K., Smolak, P. J., Din, W. S., Huang, C. P., Nicholl, J. K., Sutherland, G. R., Smith, T. D., Rauch, C., Smith, C. A., and Goodwin, R. G. (1995) *Immunity* **3,** 673–682
34. Steed, P. M., Tansey, M. G., Zalewsky, J., Zhukovsky, E. A., Desjarlais, J. R., Szymkowski, D. E., Abbott, C., Carmichael, D., Chan, C., Cherry, L., Cheung, P., Charlton, A. J., Chung, H. H., Duberstein, S. K., Eivazi, A., Filikov, A. V., Gao, S. X., Huberty, R. S., Hwang, M., Hyun, L., Kashi, S., Kim, A., Kim, E., Kung, J., Martinez, S. P., Muchhal, U. S., Nguyen, D. H., O'Brien, C., O'Keefe, D., Singer, K., Vafa, O., Viebmeister, L., Yoder, S. C. and Dahiyat, B. I. (2003) *Science* **301,** 1895–1898
35. Wohlgemuth, S., Kiel, C., Kramer, A., Serrano, L., Wittinghofer, F., and Herrmann, C. (2005) *J. Mol. Biol.* **348,** 741–758
36. Kiel, C., Wohlgemuth, S., Rousseau, F., Schymkowitz, J., Ferkinghoff-Borg, J., Wittinghofer, F., and Serrano, L. (2005) *J. Mol. Biol.* **348,** 759–775
37. Kemphens, O., Medina, E., Fernandez-Ballester, G., Ozuyaman, S., Le Blevi, A., Serrano, L., and Knust, E. (2006) *Eur. J. Cell Biol.* **85,** 753–767
38. Szczepek, M., Brondani, V., Buchel, J., Serrano, L., Segal, D. J., and Cathomen, T. (2007) *Nat. Biotechnol.* **25,** 786–793

Cancer Treatment Reviews 35 (2009) 280–288

Contents lists available at ScienceDirect

Cancer Treatment Reviews

journal homepage: www.elsevierhealth.com/journals/ctrv

NEW DRUGS

TRAIL receptor signalling and modulation: Are we on the right TRAIL?

Devalingam Mahalingam [a,b,d], Eva Szegezdi [a,d], Maccon Keane [b,e], Steven de Jong [c,f], Afshin Samali [a,*]

[a] Department of Biochemistry and National Centre for Biomedical Engineering Science, National University of Ireland, Galway, University Road, Galway, Ireland
[b] University College Hospital, Galway, Newcastle Road, Galway, Ireland
[c] Department of Medical Oncology, University Medical Centre Groningen, University of Groningen, Hanzeplein 1, 9713 GZ, Groningen, The Netherlands

ARTICLE INFO

Article history:
Received 27 August 2008
Received in revised form 3 November 2008
Accepted 15 November 2008

Keywords:
Apoptosis
Cancer
DR4
DR5
DcR1
DcR2
TRAIL
Clinical trials
Receptor-selective TRAIL variants
Agonistic antibodies

SUMMARY

Tumour necrosis factor-related apoptosis-inducing ligand or Apo2 ligand (TRAIL/Apo2L) is a member of the tumour necrosis factor (TNF) superfamily of cytokines that induces apoptosis upon binding to its death domain-containing transmembrane receptors, death receptors 4 and 5 (DR4, DR5). Importantly, TRAIL preferentially induces apoptosis in cancer cells while exhibiting little or no toxicity in normal cells. To date, research has focused on the mechanism of apoptosis induced by TRAIL and the processes involved in the development of TRAIL resistance. TRAIL-resistant tumours can be re-sensitized to TRAIL by a combination of TRAIL with chemotherapeutics or irradiation. Studies suggest that in many cancer cells only one of the two death-inducing TRAIL receptors is functional. These findings as well as the aim to avoid decoy receptor-mediated neutralization of TRAIL led to the development of receptor-specific TRAIL variants and agonistic antibodies. These molecules are predicted to be more potent than native TRAIL in vivo and may be suitable for targeted treatment of particular tumours. This review focuses on the current status of TRAIL receptor-targeting for cancer therapy, the apoptotic signalling pathway induced by TRAIL receptors, the prognostic implications of TRAIL receptor expression and modulation of TRAIL sensitivity of tumour cells by combination therapies. The mechanisms of TRAIL resistance and the potential measures that can be taken to overcome them are also addressed. Finally, the status of clinical trials of recombinant TRAIL and DR4-/DR5-specific agonistic antibodies as well as the pre-clinical studies of receptor-selective TRAIL variants is discussed including the obstacles facing the use of these molecules as anti-cancer therapeutics.

Introduction

Despite the significant advances in clinical research, surgical resection, radiotherapy and chemotherapy are still used as the primary method for cancer treatment. Radiation therapy and many chemotherapeutics trigger cancer cell death by inducing DNA damage and cellular stress, blocking DNA replication and tumour cell division. These conventional therapies, however, often induced systemic toxicity, are not entirely effective and eventually contribute to tumour resistance after repeated treatments. In the past decade, a new generation of drugs targeting key, tumour-driving molecules and/or aberrant molecular pathways have been developed (targeted biological molecules). Furthermore, it was recognised that a combination of the conventional therapeutics with the new generation of targeted biological molecules resulted in additive and often even synergistic tumouricidal effects. In combining targeted biological molecules, such as Trastuzumab, a monoclonal antibody that targets the human epidermal growth factor receptor-2 (HER-2) in breast cancer or Rituximab, a chimeric monoclonal antibody against cluster of differentiation 20 (CD20) present in B lymphocytes in treating B-cell lymphomas, with conventional chemotherapy improved survival rates have been achieved.

Tumour necrosis factor-related apoptosis-inducing ligand (TRAIL or Apo2 ligand) is a recently discovered targeted therapeutic. TRAIL is a member of the tumour necrosis factor (TNF) cytokine family that induces apoptosis upon binding to its death domain-containing receptors, TRAIL receptor 1 (death receptor 4, DR4) and TRAIL receptor 2 (death receptor 5, DR5).[1] A further three TRAIL receptors exist, which are unable to induce apoptosis and act as decoys. Decoy receptors 1 (DcR1) and 2 (DcR2), similar to DR4 and DR5, are expressed on the cell surface. While the extracellular, ligand binding domain of DcR1 and DcR2 is highly homologous to that of DR4 and DR5 and is fully functional; neither DcR1 nor DcR2 has a functional intracellular death domain. Thus, overexpression of either DcR1 or DcR2 confers protection against TRAIL-induced apoptosis.[2,3] The fifth TRAIL receptor is osteoprotegerin (OPG), a secreted, low affinity receptor for TRAIL.

* Corresponding author. Tel.: +353 91 492440; fax: +353 91 494506.
E-mail addresses: DevaMrungaboy@gmail.com (D. Mahalingam), Eva.szegezdi@nuigalway.ie (E. Szegezdi), maccon.keane@smail.ie (M. Keane), s.de.jong@int.umcg.nl (S. de Jong), Afshin.Samali@nuigalway.ie (A. Samali).
[d] Tel.: +353 91 495037; fax: +353 91 494596.
[e] Tel.: +353 91 735012; fax: +353 91 758248.
[f] Tel.: +31 50 3612864; fax: +31 50 3614862.

0305-7372/$ – see front matter © 2008 Elsevier Ltd. All rights reserved.
doi:10.1016/j.ctrv.2008.11.005

The physiological function of TRAIL is thought to be the control of autoreactive immune cells and immune surveillance, particularly against tumour development and metastasis.[1] TRAIL has been shown to induce apoptosis in cancer cells with little or no cytotoxicity against non-transformed cells. Although this unique phenomenon was realized a decade ago, the development of TRAIL as an anti-cancer agent was delayed due to reported hepatocyte toxicity.[4] Studies have since found that the observed hepatotoxicity was associated with exogenous tags (polyhistidine or Flag) present on the recombinant soluble human TRAIL (rhTRAIL) molecule used in these studies. These tags altered the tertiary structure of the ligand, which caused receptor aggregation resulting in hepatocyte apoptosis.[5] Determination of the crystal structure of TRAIL identified another key factor important for TRAIL's proper biological activity. The biologically active conformation of TRAIL was found to be stabilized by a zinc ion positioned at the trimer interface.[6] Also it has been reported that the polyhistidine-tagged form of rhTRAIL did not contain as much zinc as the native TRAIL, had a less ordered conformation and was more heterogeneous than untagged TRAIL.[7] The differences in zinc content of the different rhTRAIL formulations might have also contributed to differences in receptor ligation, agonistic properties and hepatotoxicity. Thus, the version of rhTRAIL currently in clinical trials consists of amino acids 114–281, without any oligomerization-enhancing tag and stabilised by a central zinc ion.

TRAIL-induced apoptosis and mechanism of resistance

Binding of death ligands to specific death receptors expressed on the cell surface induces the extrinsic apoptotic pathway. TRAIL is a death ligand with a homotrimeric structure. Upon binding to DR4 or DR5, it induces receptor trimerization and a conformational change in the intracellular death domain (DD) resulting in receptor activation. Activation of the receptor allows the binding of the adaptor molecule, Fas-associated protein with death domain (FADD) via a homotypic, DD–DD interaction. FADD also contains a death effector domain (DED). The DED in FADD binds to the DED of pro-caspase-8/-10 resulting in their oligomerization and autoactivation (Fig. 1).[7] Active caspase-8/-10 in turn activates the effector caspase that executes the apoptotic programme. Caspase-8 can also cleave and activate the pro-apoptotic Bcl-2 protein, Bid, which engages the intrinsic apoptotic pathway.[8] Truncated Bid activates Bax and Bak, leading to their oligomerization and pore formation in the outer mitochondrial membrane. Cytochrome *c* is released through the Bax/Bak megachannels into the cytosol where it induces the assembly of the apoptosome, the activation-platform for pro-caspase-9.[9] Caspase-9 also feeds into the caspase cascade, thus providing a robust, positive feedback loop to the caspase-8/-10-induced apoptotic events (Fig. 1). In some cell types the caspase-8/-10-triggered caspase cascade is sufficient to commit the cell to apoptosis, while in other cell types the intrinsic amplification loop is necessary for the commitment to apoptosis. Depending on the requirement for the intrinsic mitochondrial amplification loop for TRAIL-induced apoptosis, type I (independent) and type II (intrinsic mitochondrial amplification dependent) tumour cells are distinguished.

The intrinsic pathway is also regulated by the tumour suppressor, p53. p53 is activated in response to a wide range of cellular stresses (e.g. DNA damage or oxidative stress following radiation therapy or chemotherapy). p53 acts by inducing cell cycle arrest or apoptosis by regulating the expression of p53-responsive genes (e.g. p21 and p27 to induce cell cycle arrest and Bcl-2 family members; Bax, Puma, Noxa to induce the intrinsic apoptosis pathway).[10] p53 mutations are frequently observed in tumour cells and often account for resistance to genotoxic chemotherapies or irradiation.[11] The fact that TRAIL can induce caspase activation and tumour cell apoptosis independent of the mitochondria (in type I cells) or independent of p53-regulated Bcl-2 family members (in type II cells, via caspase-8 mediated Bid cleavage resulting in direct Bax/Bak activation) offers an approach to target p53-deficient tumours.

Although TRAIL preferentially induces apoptosis in cancerous cells, not all tumour cells are sensitive to TRAIL. Growing evidence suggests that many human cancer types, such as chronic lymphocytic leukemia (CLL), astrocytoma, meningioma and medulloblastoma, are resistant to TRAIL despite the expression of the death-inducing TRAIL receptors on the surface of the tumour cells.[12] The cause of TRAIL resistance is under intense scrutiny and many possible mechanisms have been identified. These mechanisms can contribute to TRAIL resistance to varying extents in different tumour cells. The current challenge is how to identify which of these mechanisms is/are responsible for the resistance in a given tumour. For example, it has been postulated that the decoy receptors can account for TRAIL resistance as overexpression of DcR1 and/or DcR2 protected cancer cells from TRAIL-induced apoptosis.[13] However, other studies have failed to show any correlation between the expression of decoy receptors and TRAIL sensitivity of tumours.[13] Unfortunately, detection of decoy receptors (as well as the death-inducing DR4 and 5) expressed on the cell surface and thus capable of blocking the function of DR4/5 is difficult in primary tumour biopsy sections and thus most studies so far only examined the expression of the decoy receptors by immunohistochemistry.[14] However, a number of studies examined the level of surface-expressed decoy receptors using tumour cell lines but still failed to find significant correlations.[15] As a possible explanation for the lack of correlation, studies revealed that the localization of both the death-inducing and the decoy receptors dynamically changes in tumour cells upon exposure to TRAIL.[15] Additionally a large number of studies examined the intracellular mechanisms of TRAIL resistance and identified an array of anti-apoptotic or pro-survival molecules as factors resulting or contributing to TRAIL-resistance. The following section lists the best characterised inhibitors of the TRAIL-death pathway identified by these pre-clinical studies.

The most characterised inhibitor of TRAIL-mediated apoptosis is cellular FLICE-inhibitory protein (c-FLIP). c-FLIP blocks the transmission of the death signal at the level of the receptor by occupying the caspase-8 binding site on FADD and thus blocking the activation of the caspase cascade (Fig. 1).[16] Further inhibitors, acting downstream of the receptors, were also identified. Activation and/or activity of caspase-9, -3 and -7 can be blocked by inhibitor of apoptosis proteins (IAP), an evolutionarily conserved family of caspase inhibitory proteins.[17] Members include: X-linked IAP (XIAP), c-IAP1, c-IAP2 and survivin. High XIAP expression has been shown to contribute to TRAIL resistance in a number of tumour cell lines (Fig. 1).[18] Anti-apoptotic Bcl-2 proteins can also inhibit TRAIL-induced apoptosis in type II cells. For example, forced Bcl-x_L overexpression conferred TRAIL resistance in pancreatic cancer cell lines.[19] Similarly, increased Bcl-2 expression was found to generate TRAIL resistance in neuroblastoma, glioblastoma and breast carcinoma cell lines.[20] Mcl-1 expression has been linked to TRAIL-resistance of hepatocellular carcinomas and cholangiocarcinomas.[21,22] The expression of these anti-apoptotic proteins is controlled by overactivated pro-survival molecules, such as phosphatidyl inositol 3 kinase (PI3K), Akt, or the nuclear factor-kappa B (NF-κB) family of transcription factors.[23,24] A more in-depth overview of the intracellular regulation of TRAIL resistance is provided in the review of Van Geelen et al.[25]

The expression of many of these apoptosis-inhibitory molecules is often reduced or blocked by chemotherapeutics or newer, biological agents, indicating that combination of these agents with TRAIL may be an effective way to eradicate tumour cells. For

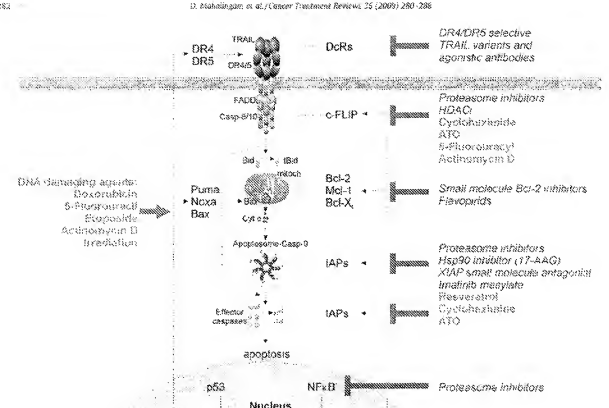

Fig. 1. Mechanisms of resistance and potential therapeutic strategies to re-sensitize tumour cells to TRAIL. TRAIL induces tumour cell apoptosis via binding to its receptors, DR4 and/or DR5. Ligation to DR4/DR5 leads to the recruitment of the adaptor molecule, FADD to which pro-caspase-8/-10 binds resulting in its activation. Active caspase-8/-10 either directly activates the executioner caspases (caspase-3, -6 and -7), or cleaves the BH3-only protein, Bid, leading to formation of Bax/Bak megachannels in the outer mitochondrial membrane through which cytochrome c is released into the cytosol triggering activation of pro-caspase-9 and the executioner caspases. Activation of DR4/DR5 receptors can be blocked by decoy receptors 1 and 2 (DcR1, DcR2), expressed at high levels in some tumour cells, as well as in most non-transformed somatic cells. Novel therapies aim to overcome this inhibition by selectively targeting DR4 and/or DR5 using receptor-selective TRAIL variants or agonistic antibodies. Besides the decoy receptors, DR4/5 function can also be blocked by c-FLIP. Chemotherapeutic (green bold coloured names) and targeted (blue italic coloured names) agents have been shown to down-regulate c-FLIP and could sensitize tumour cells to TRAIL-induced apoptosis. Downstream of DR4/5 the anti-apoptotic Bcl-2 family proteins (Bcl-x_L, Mcl-1 and Bcl-2) can block the transmission of the TRAIL-apoptotic signal. Small molecule Bcl-2 inhibitors and flavopiridols may be used in combination with TRAIL to counteract this effect. Another downstream inhibitor of TRAIL-mediated apoptosis is the inhibitor of apoptosis protein family (IAP), especially XIAP. The therapeutic agents identified to be able to overcome IAP-induced resistance are shown in the figure. In some tumour cells, TRAIL itself, as well as other pro-survival signals can activate the transcription factor NF-κB that directs the transcription of anti-apoptotic genes such as c-FLIP, Bcl-x_L and IAPs. To overcome TRAIL resistance mediated by NF-κB, proteasome inhibitors have been used effectively. Finally, in tumour cells expressing wild type p53, DNA damaging agents and radiation therapy may be used to promote TRAIL-induced apoptosis by upregulating p53 target genes such as DR4/DR5, and the BH3-only proteins Bax, Puma and Noxa (For interpretation of the references to colour in this figure legend, the reader is referred to the web version of this article.).

example, pre-clinical studies found that a number of chemotherapeutic agents are able to sensitize tumour cells to TRAIL downregulated c-FLIP expression (Fig. 1).[26–28] Similarly, targeted agents, such as proteasome inhibitors and histone deacetylase (HDAC) inhibitors, re-sensitized TRAIL-resistant cancer cell lines by decreasing c-FLIP expression (Fig. 1).[28,29] Proteasome inactivation has also been shown to block NF-κB activity and thus reduce the NF-κB-mediated transcription of anti-apoptotic proteins including c-FLIP.[30–32] Agents such as HDAC inhibitors,[30,33] cycloheximide,[34] Imatinib Mesylate (a protein tyrosine kinase inhibitor),[35] proteasome inhibitors,[36] 17-allylamino-17-demethoxygeldanamycin (a Hsp90 inhibitor),[37] arsenic trioxide[38] and a XIAP small-molecule antagonist[39] have all been used to downregulate IAPs to successfully overcome TRAIL resistance in breast, colon, pancreatic, cervical, melanoma and leukemia cell lines. Finally, small-molecule Bcl-2 inhibitors have been developed and shown in pre-clinical testing to sensitize Bcl-2 overexpressing carcinoma cells to TRAIL-induced cell death (Fig. 1).[40]

Trail receptor expression and selective receptor activation

The prognostic implication of TRAIL receptor expression is the subject of intensive investigation as it potentially impacts on the future management of patients. Using immunohistochemistry, we have studied the expression and localization of the TRAIL receptors at different histological grades of cervical, ovarian and colon tumours in comparison to normal tissues.[41–45] In all the three cancer types, the level of TRAIL expression was found to be

reduced in higher grade lesions, while DR4 and DR5 were either more abundant or present in a higher percentage of tumour cells compared to pre-malignant cells, benign tumours and normal epithelium.[41–43]

We have also studied a cohort of 376 stage III colon cancer patients who underwent adjuvant therapy (fluorouracil/levamisole v fluorouracil/levamisole/leucovorin) following resection. Tissue microarrays were constructed and stained immunohistochemically for TRAIL, DR4, and DR5. Log-rank tests and Cox proportional hazard analysis with adjustment for treatment arm, sex, age, N stage, microsatellite instability status, and p53 mutation status were performed. Of the tumour samples, 83% expressed high levels of TRAIL, 92% expressed DR4 and 87% expressed DR5.[44] High DR4 expression was associated with a poor survival rate and a shorter recurrence time. Similarly, tissue microarray analysis of 655 early breast cancer samples found that DR5 expression was associated with a decreased survival rate and higher lymph node involvement in patients.[45] Increased TRAIL receptor expression in tumours with poor prognosis may indicate that these tumours gain advantage and progress more aggressively because they can escape the TRAIL-mediated immune surveillance, for example, by inhibiting the immune response against the tumour or being resistant to TRAIL-induced apoptosis due to the presence of intracellular inhibitory/anti-apoptotic proteins. It has been found that TRAIL resistance increased the rate of metastasis to lymph nodes,[46] but further studies are awaited to clarify the role of TRAIL-sensitivity, as well as TRAIL receptor expression in tumour progression and the aggressiveness of the disease.

In certain cancer cells, despite comparable expression of DR4 and DR5 on the cell surface, DR5 acts as the primary transducer of the TRAIL-death signal.[47–49] Similarly, it is known that normal cells are sensitized to TRAIL when DR5 is upregulated by overexpression of c-myc or oncogenic ras mutants.[51,52] The enhanced sensitivity to TRAIL and the preferential DR5-mediated signalling observed in c-myc-overexpressing tumour cells as well as in tumour cell xenografts may enable the selective targeting of myc-overexpressing tumour cells. Conversely, other studies have found DR4 as the predominant transducer of apoptosis in a number of tumours, such as chronic lymphocytic leukemia and mantle cell lymphoma.[53] While it has been shown that ras- and c-myc-mediated transformation increases DR5 expression and activity (measured by the recruitment and activation of pro-caspase-8), it is still unclear how oncogenic proteins in general regulate TRAIL receptor signalling in different tumour cells, and as yet there are no predictive indicators to determine which death receptor will be preferentially active in a given tumour. It is hoped that further translational research and pharmacodynamic studies in clinical trials may help to answer some of these issues.

To understand why in particular cancers only one of the death-inducing TRAIL receptors can transduce apoptosis, it would be necessary to examine receptor functionality. Although expressed on the cell surface, DR4 and DR5 may not be functional. Unfortunately, only limited data are available on the expression of active TRAIL receptors on the surface of normal and transformed cells due to lack of suitable, high throughput techniques.[10,54,55] Both functional and non-functional TRAIL receptors are detected by Western blot analysis. Likewise, TRAIL receptor mRNA levels cannot reflect the levels of functional death receptors, as post-transcriptional modifications alter receptor functionality.[56] For example, O-glycosylation of the TRAIL receptors has recently been shown to regulate sensitivity of tumour cells to TRAIL.[57] O-linked glycosylation is initiated by N-acetylgalactosamine transferases (GALNT) and further processing is catalysed by fucosyltransferases (FUT). Analysis of TRAIL-sensitive pancreatic cancers, melanomas and non-small cell lung cancers demonstrated high GALNT14 expression in the TRAIL-sensitive tumours, while the expression of GALNT3, FUT3 and FUT6 was found to be high in TRAIL-sensitive colorectal tumours. Overall, the presence of these glycosylating enzymes predicted TRAIL sensitivity in 61% of the cases, while their absence predicted TRAIL resistance in 81% of the cases. The identification of these enzymes in tumour cells may prove useful in future clinical trials to determine receptor functionality and patient suitability for TRAIL therapy.

The clinical TRAIL

In general, a combination therapy can result in an additive tumouricidal effect due to activation of two independent stress pathways or death programmes. As our understanding of the TRAIL-induced signalling pathways and the mechanisms of TRAIL resistance advances, it may be possible to develop even more efficient drug combinations to target specific tumours. For example, the expression of both DR4 and DR5 can be induced by p53[58,59] as well as by other transcription factors, such as NF-κB[60,61] and CHOP (C/EBP-homologous protein).[62,63] Thus, tumour treatment could theoretically be more effective if DNA damaging agents such as radiotherapy and chemotherapy that activate p53 were used in combination with TRAIL. Already, chemotherapeutic agents and/or radiotherapy have been found to restore or enhance TRAIL sensitivity in a range of tumours including breast,[64] prostate[65] and lung cancers[66], and in a number of cases a synergistic effect could be achieved. We and others have demonstrated an increased expression of one death-inducing TRAIL receptor over the other in a variety of cancer cell lines, tumour xenografts in nude mice and primary tumour samples following combination therapies.[41,67] Table 1 summarizes the currently identified chemotherapeutics that induce DR4 and/or DR5 expression and can sensitize TRAIL-resistant tumour cells with references to represent findings on the different types of tumours examined so far. It is hoped that these pre-clinical data will translate to the clinic and identify combinations of TRAIL or selective DR4/DR5 agonists (antibodies or receptor-selective TRAIL variants) and chemo-radiotherapy/biological agents able to reactivate the TRAIL-apoptotic pathway and thus more enable the effective eradication tumours.

Combination therapies enhance TRAIL-induced apoptosis through differential regulation of pro- and anti-apoptotic proteins. These effects though beneficial in cancer, may also be detrimental to normal cells. The potential toxicities on human keratinocytes, endothelial cells and hepatocytes have been realized following studies using proteasome inhibitors and cycloheximide co-treatments.[68–70] How these and other therapeutics affect TRAIL receptor expression in primary, non-transformed cells is largely unknown. Thus, more focused pre-clinical and early clinical trials are required to elucidate the mechanism of TRAIL resistance of non-transformed cells and the safety profile of TRAIL when used in combination with other drugs.

Recombinant human TRAIL (rhTRAIL)

The version of TRAIL currently in phase I/II clinical trials (Genentech, San Francisco, CA, USA) has been purified at a neutral pH and comprises the extracellular region of TRAIL (amino acids 114–281) and zinc to stabilise the biologically active trimeric conformation. Results from the phase I studies are promising. TRAIL (0.5–15 mg/kg) administered as a one hour intravenous (IV) infusion for 5 consecutive days over a 21-day cycle in up to eight cycles demonstrated linear pharmacokinetics, no dose-limiting toxicities or heparotoxicity and a 21–31 min half-life.[71] Among 32 patients with at least one post-baseline tumour assessment, one patient with a chondrosarcoma had a confirmed partial response at 8 mg/kg, 17 patients (53%) experienced stable disease and 13 patients (41%) progressed. An additional phase Ib study of rhTRAIL

Table 1
Effects of anti-cancer drugs shown to enhance TRAIL-induced apoptosis on DR4 and/or DR5 expression.

Receptor regulated	Therapeutics	Mode of action	Tumor type
Upregulation of DR5	Proteasome inhibitors	Inhibition of protein degradation	Cervical,[58] prostate,[59] colon,[60] lung[61]
	HDAC inhibitors	Enabling transcription by blocking gene deacetylation	Leukemia,[62] bladder,[63] renal,[64] breast[65]
	Non-steroidal anti-inflammatory drugs (NSAIDs)	Inhibition of cyclooxygenase-1 and -2 (COX-1/2)	Colon[66] prostate and colon[67] lung[68]
	Radiotherapy	Induction of DNA damage	Prostate,[69] leukemia,[120] breast, lung, colon, head and neck[107]
	Camptothecin/CPT-11/topotecan (topoisomerase-I inhibitor)	Interrupting DNA replication	Colon,[102] colon,[103] renal[104]
	Etoposide (topoisomerase-II inhibitor)	Interrupting DNA replication	Colon,[102] glioma,[67] leukemia[105]
	Doxorubicin (anthracycline antibiotic and topoisomerase II inhibitor)	DNA intercalation and interrupting DNA replication	Leukemia,[105] myeloma,[106] breast[107]
	Cisplatin (alkylating agent)	DNA alkylation and cross-linking	Glioma[67]
	Tunicamycin	Inhibition of N-linked glycosylation	Prostate[68]
	Sulforaphane (chemopreventative agent)	Induction of phase II detoxifying enzymes (e.g. glutathione S-transferase, quinone reductase)	Hepatoma[130]
	Curcumin	Induction of cell cycle arrest and apoptosis	Renal, colon, hepatocellular[109]
Upregulation of DR4	Radiotherapy	Induction of DNA damage	Leukemia[120]
	HDAC inhibitors	Enabling transcription by blocking gene deacetylation	Leukemia[68]
Upregulation of DR4 and DR5	Proteasome inhibitors	Inhibition of protein degradation	Cervical,[58] leukemia[141]
	HDAC inhibitors	Enabling transcription by blocking gene deacetylation	Leukemia,[62] multiple myeloma,[142] breast[143]
	NSAIDs	Inhibition of COX-1/2	Colon[144]
	Camptothecin/CPT-11/topotecan (topoisomerase-I inhibitor)	Interrupting DNA replication	Breast,[145] colon,[146] prostate[147]
	Etoposide (topoisomerase-II inhibitor)	Interrupting DNA replication	Breast,[148] prostate[149]
	Doxorubicin (anthracycline antibiotic and topoisomerase II inhibitor)	DNA intercalation and interrupting DNA replication	Renal,[148] sarcoma,[150] breast/lung/prostate, head and neck[120]
	Cisplatin (alkylating agent)	DNA alkylation and cross-linking	Oesophageal,[151] ovarian[122]
	Chlorambucil (alkylating agent)	DNA alkylation and cross-linking	Leukemia[126]
	Fludarabine (anti-metabolite)	Inhibition of DNA synthesis	Leukemia[125]
	Paclitaxel/Taxotere	Inhibition of microtubule function	Prostate,[68] breast,[152] prostate[147]
	Tunicamycin	Inhibition of N-linked glycosylation	Colon[144]
	Retinoids	Regulation of cell growth and differentiation	Lung[226]

(4 and 8 mg/kg) in combination with Rituximab (administered IV at 375 mg/m^2 weekly for up to eight doses) in previously treated patients with low-grade non-Hodgkin's lymphoma (NHL) was also conducted.[71] No dose-limiting toxicities or adverse events are reported thus far. Of the five patients eligible for response evaluation, two had a complete remission, two experienced partial remission and one had a stable disease.[71]

Although the early clinical trials of rhTRAIL are promising, its short in vivo half-life time and the ubiquitous expression of TRAIL receptors on the surface of non-transformed somatic cells could severely reduce its efficacy. Targeting of TNF ligands to the tumour site either to increase the efficacy or to avoid systemic toxicity has recently become the focus of many pre-clinical studies. Several tumour antigens have been successfully used to direct TNF to the tumour site, such as gp240,[72] EGFR (epidermal growth factor),[73] Her2/Neu[74] and single-stranded DNA released from necrotic tumour cells.[75] To target TRAIL to tumour cells, genetic fusion of rhTRAIL to the tumour-specific CD19 single-chain Fv antibody fragment has been generated.[76] The scFvCD19-rhTRAIL fusion protein selectively bound to and induced apoptosis in CD19 positive tumour cell lines as well as patient-derived acute B-lymphoblastic leukemia (B-ALL) and chronic B-lymphocytic leukemia (B-CLL) cells with normal blood cells remaining unaffected.[76] In addition to fusion proteins, stem cell-mediated delivery systems targeting the tumour stroma are also under development.[77,78] Similarly, rhTRAIL variants capable of selectively targeting DR4, DR5, or DR4 and DR5 but not the decoy receptors, or receptor-selective, agonistic antibodies could avoid decoy receptor-mediated neutralization and could theoretically be more efficient. So far, however, there is insufficient data available to judge this hypothesis and only future studies will answer this question. Table 2 gives a summary of the current status of the development and results of TRAIL variants and agonistic TRAIL receptor antibodies from pre-clinical studies to current clinical trials.

Receptor-selective rhTRAIL variants

We and others have generated receptor-selective TRAIL variants (Table 2).[49,50,79] Using a computational design strategy, we found that mutation of aspartate at position 269 to a histidine and glutamate at position 195 to an arginine (D269H/E195R) in TRAIL generated a variant with a 70–150-fold higher preference for DR5 over DR4 compared to wild type TRAIL.[50] This DR5-specific variant has demonstrated positive anti-tumour activity in DR5-responsive tumour cell lines without any adverse cytotoxicity in non-transformed cells[50] (and authors' unpublished results). This DR5-selective TRAIL variant may be more potent than rhTRAIL due to reduced binding to the decoy receptors or more effective activation of DR5. This could allow a more efficient action on tumour cells, thus compensating for the relatively short half-life time of rhTRAIL molecules. Other TRAIL variants are also being evaluated for anti-tumour efficacy. Kelley and colleagues have developed DR5-selective TRAIL variants with significant anti-tumour activity and DR4-variants with a somewhat lower activity.[49] By omitting one of the six amino acid substitutions used to generate the DR4 variant, its efficacy in DR4-sensitive CLL cells could be greatly increased.[79] We have also generated a DR4-selective TRAIL variant, which is highly selective for DR4 with a pro-apoptotic activity comparable to wild type TRAIL.[80] Pre-clinical and clinical studies are required to prove the advantage of the receptor-selective TRAIL variants over the wild type ligand.

DR4- and DR5-selective agonistic antibodies

Monoclonal antibodies are already used in cancer therapy. Rituximab is used in B-cell non-Hodgkin's lymphoma (NHL) treatment, and Trastuzumab is used for adjuvant and metastatic breast cancer treatment. Recently, agonistic DR4- and DR5-specific antibodies have also been developed. These antibodies, especially

Table 2
Summary of existing recombinant human TRAIL variants and agonistic DR4-, DR5-specific antibodies, their pre-clinical development and current clinical trial status.

Molecule tested	Targeted receptor	Comments and clinical development
His-TRAIL (rhTRAIL variant)	DR4/DR5/decoy receptors	Polyhistidine-tagged rhTRAIL. Induces apoptosis in transformed cell lines. Toxic to primary hepatocytes and keratinocytes[4,126,127]
LZ-TRAIL (rhTRAIL variant)	DR4/DR5/decoy receptors	Leucin-zipper tagged rhTRAIL. Induces apoptosis in transformed cell lines. Toxic to keratinocytes[127,128]
Flag-TRAIL/M2 (rhTRAIL variant)	DR4/DR5/decoy receptors	Flag-tagged rhTRAIL. Induces apoptosis in transformed cell lines when cross-linked. Toxic to primary hepatocytes and keratinocytes[128,129]
Apo2L/TRAIL (rhTRAIL variant)	DR4/DR5/decoy receptors	Non-tagged rhTRAIL. Induces apoptosis in transformed cell lines but not to primary, non-transformed hepatocytes or keratinocytes. Ongoing phase I/II clinical trials as single agent and in combination therapy[3,77,127,130]
TRAIL-CD19 and TRAIL-EGFR (rhTRAIL fusion proteins)	DR4/DR5/decoy receptors with CD19 or EGFR	Selectively targets TRAIL to CD19 or EGFR expressing tumours, respectively. Induces apoptosis in vitro. Good in vivo activity seen with TRAIL-CD19 in pre-clinical studies[78,131]
Apo2L.DR5-8 (rhTRAIL variant)	DR5/DcR2 (?)	Non-tagged, DR5-selective rhTRAIL variant. Induces apoptosis in DR5-responsive cancer cell lines. Toxicity observed following cross-linking[40]
DR5-TRAIL (E195R/D269H) (rhTRAIL variant)	DR5/DcR2 (reduced)	Non-tagged, DR5-selective rhTRAIL. Induces apoptosis in DR5-responsive cancer cell lines. No toxicity in non-transformed fibroblast and endothelial cells. Anti-tumour activity in ovarian cancer xenograft models,[50] (authors' unpublished data)
M413 (agonistic Ab)	DR5	Induces apoptosis in TRAIL-sensitive cancer cell lines selectively through DR5 receptor[132]
TRA-8 (CS-1008) (agonistic Ab)	DR5	Induces apoptosis in DR5-responsive cancer cell lines and primary hepatocellular carcinoma but not toxic to normal hepatocytes (phase I clinical trials),[38] (Sankyo)
AMG 655 (agonistic Ab)	DR5	Induces apoptosis in a number of human cancer cell lines. Phase I trial showing dose linear kinetics with half-life of 10 days and some anti-tumour activity (Amgen)
LBY135 (agonistic Ab)	DR5	Good anti-tumour activity in vitro and in vivo pre-clinical studies. Currently in phase I trials (Novartis)
Lexatumumab (HGS-ETR2, agonistic Ab) HGS-TR2J (agonistic Ab)	DR5	Phase I/Ib trials showing that Lexatumumab can be administered safely and in combination with chemotherapeutic agents. (Human Genome Science)[83,84] HGS-TR2J was voluntarily suspended from clinical development
Apomab (agonistic Ab)	DR5	Phase I trial showing dose proportional pharmacokinetics. Half-life 15–20 days. Currently initiations of phase II trial (Genentech)[133]
TRAIL-R1-5 (rhTRAIL variant)	DR4/decoy receptors (?)	Non-tagged, DR4-selective rhTRAIL. Induces apoptosis in DR4 responsive cancer cell lines. HDACi sensitized primary CLL cells to DR4 mediated apoptosis[79]
M271 (agonistic Ab)	DR4	Induces apoptosis in TRAIL-sensitive cancer cell lines selectively through DR4 receptor[132]
AHG, AG7 (agonistic Ab)	DR4	Induced apoptosis in vitro with cross-linking antibody. Anti-tumour activity in colon cancer xenograft model[81]
2E12 (agonistic Ab)	DR4	Induced apoptosis in vitro with cross-linking antibody[16]
Mapatumumab (HGS-ETR1) (agonistic Ab)	DR4	Phase I – solid malignancies refractory to standard therapy, safely administered up to 10 mg/kg. 39% of patients had SD[85] Phase Ib – combination therapy with paclitaxel and carboplatin: 14% of patients had PR[86] Phase Ib – combination with gemcitabine and cisplatin: 20% of patients had PR, 29% SD[87] Phase II – single treatment in NSCLC: 29% of patients had SD[88]

when cross-linked by secondary antibodies, are very effective activators of the TRAIL receptors.[81]

Currently one chimeric (LBY135 by Novartis) and six human (AMG 655 by Amgen, CS-1008 by Sankyo, Mapatumumab, Lexatumumab, HGS-TR2J by Human Genome Sciences (HGS) and Apomab by Genentech) monoclonal agonistic antibodies against DR4 and DR5 are in phase I/II clinical trials (Table 2). LBY135, AMG 655, Lexatumumab, HGS-TR2J and Apomab are DR5 agonists. Generally, results to date indicate some anti-tumour activity, good safety profile with no hepatotoxicity, linear pharmacokinetics, and relatively long half-life times (10–20 days) with no generation of anti-human antibodies.[82] Lexatumumab, in phase I studies, was safely administered up to a 10 mg/kg dose in a range of solid malignancies with stable disease observed in twelve patients (32%) that lasted a median of 4.5 months.[83] The safety of Lexatumumab in combination with gemcitabine, pemetrexed, doxorubicin or FOLFIRI (leucovorin, fluorouracil, and irinotecan) is also being examined in a phase Ib trial.[84] Tumour shrinkage has been observed, including confirmed partial responses in the FOLFIRI and doxorubicin arms. More detailed results on patient responses are awaited.

Phase I study of Mapatumumab (DR4 agonist) in patients with solid malignancies refractory to standard therapy concluded that it can be safely administered up to 10 mg/kg every 14 days (Table 2). No adverse reactions were observed and out of the forty-nine patients enrolled, nineteen had stable disease with two lasting 9 months.[85] This phase I trial also looked at DR4 receptor expression and found DR4 expressed in 68% of the tumour samples. This study also concluded that DR4 expression alone does not predict responsiveness and suggested other molecular determinants be evaluated.[85] Mapatumumab has also been used safely in combination with paclitaxel and carboplatin in patients with advanced malignancies, where the phase Ib study found that 4/28 patients experienced a confirmed partial response.[86] In another phase Ib study, Mapatumumab could be administered safely up to 30 mg/kg every three weeks in combination with gemcitabine and cisplatin.[87] In this study, 9/45 patients experienced a partial response and 13/45 patients achieved stable disease for more than 18 weeks.[87] A phase II study of Mapatumumab as a single agent in non-small cell lung carcinoma (NSCLC) patients has also been initiated. While the antibody was well tolerated, none of the 32 treated patients showed a response according to the RECIST criteria and nine patients (29%) had stable disease.[88]

Conclusions

TRAIL is now in phase II clinical trials. Whether used as a single agent or in combination therapy, it is hoped that sooner rather than later, it will contribute to improving patient survival. Many questions remain unanswered. Top of the list is why some cells remain resistant to TRAIL? Could the combination of TRAIL receptor agonists with other therapeutics restore cancer cell sensitivity or inadvertently result in the death of normal cells? Why is it that certain tumour cells preferentially transduce apoptosis through one death-inducing TRAIL receptor but not the other; or preferentially induce the expression of only one TRAIL receptor in response

to a given anti-cancer agent? Unfortunately, we are still unable to predict which TRAIL receptors are functional in which tumours and so, as yet, cannot foresee which TRAIL receptor-targeting treatment would be the most appropriate. Ideally, clinical trials showing initial tumour resistance to DR4-selective agonistic antibodies/DR4-selective TRAIL variants would allow subsequent treatment with DR5-antibodies/variants and vice versa. There is no proof as yet that targeting of only DR4 or DR5, rather that both receptors together, is the better approach. When more results emerge from the ongoing clinical trials, a better picture can be obtained enabling the comparison of the anti-tumour efficacy of wild type rhTRAIL to DR4-/DR5-selective agonists. Whether it is possible to develop rhTRAIL variants or agonistic antibodies able to activate both DR4 and DR5 without binding to DcR1/2 is to be seen. Another essential question to ask is whether the differences in the pharmacokinetics and pharmacodynamics of the rhTRAIL variants are problematic *in vivo*? Will a "safe" TRAIL variant be found with potent anti-tumour effects? Given time, through translational research and more extensive clinical trials, we envisage that many of these questions will be answered. In the meantime, however, it appears that we are certainly on the right TRAIL.

Conflict of interest statement

A. Samali is a founder of Triskel Therapeutics Ltd. and a member of its scientific advisory board.

Acknowledgments

Authors are grateful to Dr. Janice Reeve for her help with the preparation of this manuscript. Authors' work is supported by grants from the Framework Programme 6 of the EU, Cancer Research Ireland and Enterprise Ireland.

References

1. LeBlanc HN, Ashkenazi A. Apo2L/TRAIL and its death and decoy receptors. *Cell Death Differ* 2003;10:66–75.
2. Pan G, Ni J, Wei YF, Yu G, Gentz R, Dixit VM. An antagonist decoy receptor and a death domain-containing receptor for TRAIL. *Science* 1997;277:815–8.
3. Sheridan JP, Marsters SA, Pitti RM, et al. Control of TRAIL-induced apoptosis by a family of signaling and decoy receptors. *Science* 1997;277:818–21.
4. Jo M, Kim TH, Seol DW, et al. Apoptosis induced in normal human hepatocytes by tumor necrosis factor-related apoptosis-inducing ligand. *Nat Med* 2000;6:564–7.
5. Lawrence D, Shahrokh Z, Marsters S, et al. Differential hepatocyte toxicity of recombinant Apo2L/TRAIL versions. *Nat Med* 2001;7:383–5.
6. Hymowitz SG, O'Connell MP, Ultsch MH, et al. A unique zinc-binding site revealed by a high-resolution X-ray structure of homotrimeric Apo2L/TRAIL. *Biochemistry* 2000;39:633–40.
7. Kischkel FC, Lawrence DA, Chuntharapai A, Schow P, Kim KJ, Ashkenazi A. Apo2L/TRAIL-dependent recruitment of endogenous FADD and caspase-8 to death receptors 4 and 5. *Immunity* 2000;12:611–20.
8. Green DR. Apoptotic pathways: paper wraps stone blunts scissors. *Cell* 2000;102:1–4.
9. Korsmeyer SJ, Wei MC, Saito M, Weiler S, Oh KJ, Schlesinger PH, et al. Pro-apoptotic cascade activates BID, which oligomerizes BAK or BAX into pores that result in the release of cytochrome c. *Cell Death Differ* 2000;7:1166–73.
10. Yu J, Zhang L. The transcriptional targets of p53 in apoptosis control. *Biochem Biophys Res Commun* 2005;331:851–8.
11. Vogelstein B, Kinzler KW. Cancer genes and the pathways they control. *Nat Med* 2004;10:789–99.
12. Dyer MJ, MacFarlane M, Cohen GM. Barriers to effective TRAIL-targeted therapy of malignancy. *J Clin Oncol* 2007;25:4505–6.
13. Zhang XD, Franco A, Myers K, Gray C, Nguyen T, Hersey P. Relation of TNF-related apoptosis-inducing ligand (TRAIL) receptor and FLICE-inhibitory protein expression to TRAIL-induced apoptosis of melanoma. *Cancer Res* 1999;59:2747–53.
14. Vigneswaran N, Baucum DC, Wu J, et al. Repression of tumor necrosis factor-related apoptosis-inducing ligand (TRAIL) but not its receptors during oral cancer progression. *BMC Cancer* 2007;7:108.
15. Zhang XD, Franco AV, Nguyen T, Gray CP, Hersey P. Differential localization and regulation of death and decoy receptors for TNF-related apoptosis-inducing ligand (TRAIL) in human melanoma cells. *J Immunol* 2000;164:3961–70.
16. Irmler M, Thome M, Hahne M, et al. Inhibition of death receptor signals by cellular FLIP. *Nature* 1997;388:190–5.
17. Deveraux QL, Takahashi R, Salvesen GS, Reed JC. X-linked IAP is a direct inhibitor of cell-death proteases. *Nature* 1997;388:300–4.
18. Schimmer AD, Welsh K, Pinilla C, et al. Small-molecule antagonists of apoptosis suppressor XIAP exhibit broad antitumor activity. *Cancer Cell* 2004;5:25–35.
19. Hinz S, Trauzold A, Boenicke L, et al. Bcl-XL protects pancreatic adenocarcinoma cells against CD95- and TRAIL-receptor-mediated apoptosis. *Oncogene* 2000;19:5477–86.
20. Fulda S, Meyer E, Debatin KM. Inhibition of TRAIL-induced apoptosis by Bcl-2 overexpression. *Oncogene* 2002;21:2283–94.
21. Taniai M, Grambihler A, Higuchi H, et al. Mcl-1 mediates tumor necrosis factor-related apoptosis-inducing ligand resistance in human cholangiocarcinoma cells. *Cancer Res* 2004;64:3517–24.
22. Wirth T, Kuhnel F, Fleischmann-Mundt B, et al. Telomerase-dependent virotherapy overcomes resistance of hepatocellular carcinomas against chemotherapy and tumor necrosis factor-related apoptosis-inducing ligand by elimination of Mcl-1. *Cancer Res* 2005;65:7393–402.
23. Chen C, Edelstein LC, Gelinas C. The Rel/NF-kappaB family directly activates expression of the apoptosis inhibitor Bcl-x(L). *Mol Cell Biol* 2000;20:2687–95.
24. Wang CY, Mayo MW, Korneluk RG, Goeddel DV, Baldwin Jr AS. NF-kappaB antiapoptosis: induction of TRAF1 and TRAF2 and c-IAP1 and c-IAP2 to suppress caspase-8 activation. *Science* 1998;281:1680–3.
25. Van Geelen CM, de Vries EG, de Jong S. Lessons from TRAIL-resistance mechanisms in colorectal cancer cells: paving the road to patient-tailored therapy. *Drug Resist Updat* 2004;7:345–58.
26. Szegezdi E, Cahill S, Meyer M, O'Dwyer M, Samali A. TRAIL sensitisation by arsenic trioxide is caspase-8 dependent and involves modulation of death receptor components and Akt. *Br J Cancer* 2006;94:398–406.
27. Ganten TM, Haas TL, Sykora J, et al. Enhanced caspase-8 recruitment to and activation at the DISC is critical for sensitisation of human hepatocellular carcinoma cells to TRAIL-induced apoptosis by chemotherapeutic drugs. *Cell Death Differ* 2004;11(Suppl. 1):S86–96.
28. Griffith TS, Chin WA, Jackson GC, Lynch DH, Kubin MZ. Intracellular regulation of TRAIL-induced apoptosis in human melanoma cells. *J Immunol* 1998;161:2833–40.
29. Sayers TJ, Brooks AD, Koh CY, et al. The proteasome inhibitor PS-341 sensitizes neoplastic cells to TRAIL-mediated apoptosis by reducing levels of c-FLIP. *Blood* 2003;102:303–10.
30. Guo F, Sigua C, Tao J, et al. Cotreatment with histone deacetylase inhibitor LAQ824 enhances Apo-2L/tumor necrosis factor-related apoptosis inducing ligand-induced death inducing signaling complex activity and apoptosis of human acute leukemia cells. *Cancer Res* 2004;64:2580–9.
31. Adams J. The development of proteasome inhibitors as anticancer drugs. *Cancer Cell* 2004;5:417–21.
32. An J, Sun Y, Fisher M, Rettig MB. Antitumor effects of bortezomib (PS-341) on primary effusion lymphomas. *Leukemia* 2004;18:1699–704.
33. Zhang XD, Gillespie SK, Borrow JM, Hersey P. The histone deacetylase inhibitor suberic bishydroxamate: a potential sensitizer of melanoma to TNF-related apoptosis-inducing ligand (TRAIL) induced apoptosis. *Biochem Pharmacol* 2003;66:1537–45.
34. Kang J, Kisenge RR, Toyoda H, et al. Chemical sensitization and regulation of TRAIL-induced apoptosis in a panel of B-lymphocytic leukaemia cell lines. *British J Haematol* 2003;123:921–32.
35. Nimmanapalli R, Porosnicu M, Nguyen D, et al. Cotreatment with STI-571 enhances tumor necrosis factor alpha-related apoptosis-inducing ligand (TRAIL or apo-2L)-induced apoptosis of Bcr-Abl-positive human acute leukemia cells. *Clin Cancer Res* 2001;7:350–7.
36. Hougardy BM, Maduro JH, van der Zee AG, et al. Proteasome inhibitor MG132 sensitizes HPV-positive human cervical cancer cells to rhTRAIL-induced apoptosis. *Internat J Cancer* 2006;118:1892–900.
37. Vasilevskaya IA, O'Dwyer PJ. 17-Allylamino-17-demethoxygeldanamycin overcomes TRAIL resistance in colon cancer cell lines. *Biochem Pharmacol* 2005;70:580–9.
38. Kerbauy DM, Lesnikov V, Abbasi N, Seal S, Scott B, Deeg HJ. NF-kappaB and FLIP in arsenic trioxide (ATO)-induced apoptosis in myelodysplastic syndromes (MDSs). *Blood* 2005;106:3917–25.
39. Karikari CA, Roy I, Tryggestad E, et al. Targeting the apoptotic machinery in pancreatic cancers using small-molecule antagonists of the X-linked inhibitor of apoptosis protein. *Mol Cancer Ther* 2007;6:957–66.
40. Hao JH, Yu M, Liu FT, Newland AC, Jia L. Bcl-2 inhibitors sensitize tumor necrosis factor-related apoptosis-inducing ligand-induced apoptosis by uncoupling of mitochondrial respiration in human leukemic CEM cells. *Cancer Res* 2004;64:3607–16.
41. Arts HJ, de Jong S, Hollema H, ten Hoor K, van der Zee AG, de Vries EG. Chemotherapy induces death receptor 5 in epithelial ovarian carcinoma. *Gynecol Oncol* 2004;92:794–800.
42. Koornstra JJ, Kleibeuker JH, van Geelen CM, et al. Expression of TRAIL (TNF-related apoptosis-inducing ligand) and its receptors in normal colonic mucosa, adenomas, and carcinomas. *J Pathol* 2003;200:327–35.
43. Reesink-Peters N, Hougardy BM, van den Heuvel FA, et al. Death receptors and ligands in cervical carcinogenesis: an immunohistochemical study. *Gynecol Oncol* 2005;96:705–13.
44. van Geelen CM, Westra JL, de Vries EG, et al. Prognostic significance of tumor necrosis factor-related apoptosis-inducing ligand and its receptors in

adjuvantly treated stage III colon cancer patients. *J Clin Oncol* 2006;24:4998–5004.
45. McCarthy MM, Sznol M, DiVito KA, Camp RL, Rimm DL, Kluger HM. Evaluating the expression and prognostic value of TRAIL-R1 and TRAIL-R2 in breast cancer. *Clin Cancer Res* 2005;11:5188–94.
46. Grosse-Wilde A, Voloshanenko O, Bailey SL, et al. TRAIL-R deficiency in mice enhances lymph node metastasis without affecting primary tumor development. *J Clin Invest* 2008;118:100–10.
47. Ashkenazi A. Targeting death and decoy receptors of the tumour-necrosis factor superfamily. *Nat Rev Cancer* 2002;2:420–30.
48. Ichikawa K, Liu W, Zhao L, et al. Tumoricidal activity of a novel anti-human DR5 monoclonal antibody without hepatocyte cytotoxicity. *Nat Med* 2001;7:954–60.
49. Kelley RF, Totpal K, Lindstrom SH, et al. Receptor-selective mutants of apoptosis-inducing ligand 2/tumor necrosis factor-related apoptosis-inducing ligand reveal a greater contribution of death receptor (DR) 5 than DR4 to apoptosis signaling. *J Biol Chem* 2005;280:2205–12.
50. van der Sloot AM, Tur V, Szegezdi E, et al. Designed tumor necrosis factor-related apoptosis-inducing ligand variants initiating apoptosis exclusively via the DR5 receptor. *Proc Natl Acad Sci USA* 2006;103:8634–9.
51. Nesterov A, Nikrad M, Johnson T, Kraft AS. Oncogenic Ras sensitizes normal human cells to tumor necrosis factor-alpha-related apoptosis-inducing ligand-induced apoptosis. *Cancer Res* 2004;64:3922–7.
52. Wang Y, Engels IH, Knee DA, Nasoff M, Deveraux QL, Quon KC. Synthetic lethal targeting of MYC by activation of the DR5 death receptor pathway. *Cancer cell* 2004;5:501–12.
53. MacFarlane M, Inoue S, Kohlhaas SL, et al. Chronic lymphocytic leukemic cells exhibit apoptotic signaling via TRAIL-R1. *Cell Death Differ* 2005;12:773–82.
54. Younes M, Georgakis GV, Rahmani M, Beer D, Younes A. Functional expression of TRAIL receptors TRAIL-R1 and TRAIL-R2 in esophageal adenocarcinoma. *Eur J Cancer* 2006;42:542–7.
55. Melloni E, Secchiero P, Celeghini C, et al. Functional expression of TRAIL and TRAIL-R2 during human megakaryocytic development. *J Cell Physiol* 2005;204:975–82.
56. Horak P, Pils D, Haller G, et al. Contribution of epigenetic silencing of tumor necrosis factor-related apoptosis inducing ligand receptor 1 (DR4) to TRAIL resistance and ovarian cancer. *Mol Cancer Res* 2005;3:335–43.
57. Wagner KW, Punnoose EA, Januario T, et al. Death-receptor O-glycosylation controls tumor-cell sensitivity to the proapoptotic ligand Apo2L/TRAIL. *Nat Med* 2007;13:1070–7.
58. Takimoto R, El-Deiry WS. Wild-type p53 transactivates the KILLER/DR5 gene through an intronic sequence-specific DNA-binding site. *Oncogene* 2000;19:1735–43.
59. Liu X, Yue P, Khuri FR, Sun SY. P53 upregulates death receptor 4 expression through an intronic p53 binding site. *Cancer Res* 2004;64:5078–83.
60. Chen X, Kandasamy K, Srivastava RK. Differential roles of RelA (p65) and c-Rel subunits of nuclear factor kappa B in tumor necrosis factor-related apoptosis-inducing ligand signaling. *Cancer Res* 2003;63:1059–66.
61. Sheikh MS, Burns TF, Huang Y, et al. P53-dependent and -independent regulation of the death receptor KILLER/DR5 gene expression in response to genotoxic stress and tumor necrosis factor alpha. *Cancer Res* 1998;58:1593–8.
62. Shiraishi T, Yoshida T, Nakata S, et al. Tunicamycin enhances tumor necrosis factor-related apoptosis-inducing ligand-induced apoptosis in human prostate cancer cells. *Cancer Res* 2005;65:6364–70.
63. Yamaguchi H, Wang HG. CHOP is involved in endoplasmic reticulum stress-induced apoptosis by enhancing DR5 expression in human carcinoma cells. *J Biol Chem* 2004;279:45495–502.
64. Keane MM, Ettenberg SA, Nau MM, Russell EK, Lipkowitz S. Chemotherapy augments TRAIL-induced apoptosis in breast cell lines. *Cancer Res* 1999;59:734–41.
65. Nimmanapalli R, Perkins CL, Orlando M, O'Bryan E, Nguyen D, Bhalla KN. Pretreatment with paclitaxel enhances apo-2 ligand/tumor necrosis factor-related apoptosis-inducing ligand-induced apoptosis of prostate cancer cells by inducing death receptors 4 and 5 protein levels. *Cancer Res* 2001;61:759–63.
66. Jin H, Yang R, Fong S, et al. Apo2 ligand/tumor necrosis factor-related apoptosis-inducing ligand cooperates with chemotherapy to inhibit orthotopic lung tumor growth and improve survival. *Cancer Res* 2004;64:4900–5.
67. Nagane M, Pan G, Weddle JJ, Dixit VM, Cavenee WK, Huang HJ. Increased death receptor 5 expression by chemotherapeutic agents in human gliomas causes synergistic cytotoxicity with tumor necrosis factor-related apoptosis-inducing ligand in vitro and in vivo. *Cancer Res* 2000;60:847–53.
68. Leverkus M, Neumann M, Mengling T, et al. Regulation of tumor necrosis factor-related apoptosis-inducing ligand sensitivity in primary and transformed human keratinocytes. *Cancer Res* 2000;60:553–9.
69. Li JH, Kirkiles-Smith NC, McNiff JM, Pober JS. TRAIL induces apoptosis and inflammatory gene expression in human endothelial cells. *J Immunol* 2003;171:1526–33.
70. Koschny R, Ganten TM, Sykora J, et al. TRAIL/bortezomib cotreatment is potentially hepatotoxic but induces cancer-specific apoptosis within a therapeutic window. *Hepatology* 2007;45:649–58.
71. Ashkenazi A, Holland P, Eckhardt SG. Ligand-based targeting of apoptosis in cancer: the potential of recombinant human apoptosis ligand 2/Tumor necrosis factor-related apoptosis-inducing ligand (rhApo2L/TRAIL). *J Clin Oncol* 2008;26:3621–30.
72. Liu Y, Zhang W, Cheung LH, et al. The antimelanoma immunocytokine scFvMEL/TNF shows reduced toxicity and potent antitumor activity against human tumor xenografts. *Neoplasia* 2006;8:384–93.
73. Christ O, Matzku S, Burger C, Zoller M. Interleukin 2-antibody and tumor necrosis factor-antibody fusion proteins induce different antitumor immune responses in vivo. *Clin Cancer Res* 2001;7:1385–97.
74. Rosenblum MG, Horn SA, Cheung LH. A novel recombinant fusion toxin targeting HER-2/NEU-over-expressing cells and containing human tumor necrosis factor. *Int J Cancer* 2000;88:267–73.
75. Sharifi J, Khawli LA, Hu P, Li J, Epstein AL. Generation of human interferon gamma and tumor Necrosis factor alpha chimeric TNT-3 fusion proteins. *Hybrid Hybridom* 2002;21:421–32.
76. Stieglmaier J, Bremer E, Kellner C, et al. Selective induction of apoptosis in leukemic B-lymphoid cells by a CD19-specific TRAIL fusion protein. *Cancer Immunol Immunother* 2008;57:233–46.
77. Mohr A, Lyons M, Deedigan L, et al. Mesenchymal stem cells expressing TRAIL lead to tumour growth inhibition in an experimental lung cancer model. *J Cell Mol Med* 2008 [Epub ahead of print].
78. Szegezdi E, O'Reilly A, Davy Y, et al. Stem cells are resistant to TRAIL receptor-mediated apoptosis. *J Cell Mol Med* 2008. in press.
79. MacFarlane M, Kohlhaas SL, Sutcliffe MJ, Dyer MJ, Cohen GM. TRAIL receptor-selective mutants signal to apoptosis via TRAIL-R1 in primary lymphoid malignancies. *Cancer Res* 2005;65:11265–70.
80. Tur V, van der Sloot AM, Reis CR, et al. DR4-selective tumor necrosis factor-related apoptosis-inducing ligand (TRAIL) variants obtained by structure-based design. *J Biol Chem* 2008;283:20560–8.
81. Chuntharapai A, Dodge K, Grimmer K, et al. Isotype-dependent inhibition of tumor growth in vivo by monoclonal antibodies to death receptor 4. *J Immunol* 2001;166:4891–8.
82. Oldenhuis C, Stegehuis J, Walenkamp A, de Jong S, de Vries E. Targeting TRAIL death receptors. *Curr Opin Pharmacol* 2008;8:433–9.
83. Plummer R, Attard G, Pacey S, et al. Phase 1 and pharmacokinetic study of lexatumumab in patients with advanced cancers. *Clinic Cancer Res* 2007;13:6187–94.
84. Sikic BI, Wakelee HA, von Mehren M, et al. A phase 1b study to assess the safety of lexatumumab, a human monoclonal antibody that activates TRAIL-R2, in combination with gemcitabine, pemetrexed, doxorubicin or FOLFIRI. *Mol Cancer Ther* 2007;6:3434s–5s.
85. Tolcher AW, Mita M, Meropol NJ, et al. Phase I pharmacokinetic and biologic correlative study of mapatumumab, a fully human monoclonal antibody with agonist activity to tumor necrosis factor-related apoptosis-inducing ligand receptor-1. *J Clin Oncol* 2007;25:1390–5.
86. Chow LQ, Eckhardt SG, Gustafson DL, et al. HGS-ETR1, an antibody targeting TRAIL-R1, in combination with paclitaxel and carboplatin in patients with advanced solid malignancies: Results of a phase I and PK study. *J Clinic Oncol* 2006;24:103s.
87. Oldenhuis C, Mom C, Sleijfer S, et al. A phase I study with the agonistic TRAIL-R1 antibody, mapatumumab, in combination with gemcitabine and cisplatin. *J Clin Oncol* 2008:3540. [ASCO Meeting Abstracts].
88. Greco FA, Bonomi P, Crawford J, et al. Phase 2 study of mapatumumab, a fully human agonistic monoclonal antibody which targets and activates the TRAIL receptor-1, in patients with advanced non-small cell lung cancer. *Lung Cancer* 2008;61:82–90.
89. Yoshida T, Shiraishi T, Nakata S, et al. Proteasome inhibitor MG132 induces death receptor 5 through CCAAT/enhancer-binding protein homologous protein. *Cancer Res* 2005;65:5662–7.
90. He Q, Huang Y, Sheikh MS. Proteasome inhibitor MG132 upregulates death receptor 5 and cooperates with Apo2L/TRAIL to induce apoptosis in Bax-proficient and -deficient cells. *Oncogene* 2004;23:2554–8.
91. Voortman J, Resende TP, Abou El Hassan MA, Giaccone G, Kruyt FA. TRAIL therapy in non-small cell lung cancer cells: sensitization to death receptor-mediated apoptosis by proteasome inhibitor bortezomib. *Molecul Cancer Therapeutic* 2007;6:2103–12.
92. Nakata S, Yoshida T, Horinaka M, Shiraishi T, Wakada M, Sakai T. Histone deacetylase inhibitors upregulate death receptor 5/TRAIL-R2 and sensitize apoptosis induced by TRAIL/APO2-L in human malignant tumor cells. *Oncogene* 2004;23:6261–71.
93. Earel Jr JK, VanOosten RL, Griffith TS. Histone deacetylase inhibitors modulate the sensitivity of tumor necrosis factor-related apoptosis-inducing ligand-resistant bladder tumor cells. *Cancer Res* 2006;66:499–507.
94. VanOosten RL, Moore JM, Karacay B, Griffith TS. Histone deacetylase inhibitors modulate renal cell carcinoma sensitivity to TRAIL/Apo-2L-induced apoptosis by enhancing TRAIL-R2 expression. *Cancer Biol Therapy* 2005;4:1104–12.
95. Butler LM, Liapis V, Bouralexis S, et al. The histone deacetylase inhibitor, suberoylanilide hydroxamic acid, overcomes resistance of human breast cancer cells to Apo2L/TRAIL. *Internat J Cancer* 2006;119:944–54.
96. Tang X, Sun YJ, Half E, Kuo MT, Sinicrope F. Cyclooxygenase-2 overexpression inhibits death receptor 5 expression and confers resistance to tumor necrosis factor-related apoptosis-inducing ligand-induced apoptosis in human colon cancer cells. *Cancer Res* 2002;62:4903–8.
97. Huang Y, He Q, Hillman MJ, Rong R, Sheikh MS. Sulindac sulfide-induced apoptosis involves death receptor 5 and the caspase 8-dependent pathway in human colon and prostate cancer cells. *Cancer Res* 2001;61:6918–24.
98. Liu X, Yue P, Zhou Z, Khuri FR, Sun SY. Death receptor regulation and celecoxib-induced apoptosis in human lung cancer cells. *J Nation Cancer Inst* 2004;96:1769–80.

99. Shankar S, Singh TR, Srivastava RK. Ionizing radiation enhances the therapeutic potential of TRAIL in prostate cancer in vitro and in vivo: Intracellular mechanisms. *The Prostate* 2004;**61**:35–49.
100. Gong B, Almasan A. Apo2 ligand/TNF-related apoptosis-inducing ligand and death receptor 5 mediate the apoptotic signaling induced by ionizing radiation in leukemic cells. *Cancer Res* 2000;**60**:5754–60.
101. Marini P, Schmid A, Jendrossek V, et al. Irradiation specifically sensitises solid tumour cell lines to TRAIL mediated apoptosis. *BMC cancer* 2005;5:5.
102. LeBlanc H, Lawrence D, Varfolomeev E, et al. Tumor-cell resistance to death receptor-induced apoptosis through mutational inactivation of the proapoptotic Bcl-2 homolog Bax. *Nature Medicine* 2002;8:274–81.
103. Naka T, Sugamura K, Hylander BL, Widmer MB, Rustum YM, Repasky EA. Effects of tumor necrosis factor-related apoptosis-inducing ligand alone and in combination with chemotherapeutic agents on patients' colon tumors grown in SCID mice. *Cancer Res* 2002;**62**:5800–6.
104. Dejosez M, Ramp U, Mahotka C, et al. Sensitivity to TRAIL/APO-2L-mediated apoptosis in human renal cell carcinomas and its enhancement by topotecan. *Cell Death Different* 2000;7:1127–36.
105. Wen J, Ramadevi N, Nguyen D, Perkins C, Worthington E, Bhalla K. Antileukemic drugs increase death receptor 5 levels and enhance Apo-2L-induced apoptosis of human acute leukemia cells. *Blood* 2000;**96**:3900–6.
106. Mitsiades CS, Treon SP, Mitsiades N, et al. TRAIL/Apo2L ligand selectively induces apoptosis and overcomes drug resistance in multiple myeloma: therapeutic applications. *Blood* 2001;**98**:795–804.
107. Wang TT, Jeng J. Coordinated regulation of two TRAIL-R2/KILLER/DR5 mRNA isoforms by DNA damaging agents, serum and 17beta-estradiol in human breast cancer cells. *Breast Cancer Res Treat* 2000;**61**:87–96.
108. Kim H, Kim EH, Eom YW, et al. Sulforaphane sensitizes tumor necrosis factor-related apoptosis-inducing ligand (TRAIL)-resistant hepatoma cells to TRAIL-induced apoptosis through reactive oxygen species-mediated up-regulation of DR5. *Cancer Res* 2006;**66**:1740–50.
109. Jung EM, Park JW, Choi KS, et al. Curcumin sensitizes tumor necrosis factor-related apoptosis-inducing ligand (TRAIL)-mediated apoptosis through CHOP-independent DR5 upregulation. *Carcinogenesis* 2006;**27**:2008–17.
110. Di Pietro R, Secchiero P, Rana R, et al. Ionizing radiation sensitizes erythroleukemic cells but not normal erythroblasts to tumor necrosis factor-related apoptosis-inducing ligand (TRAIL)–mediated cytotoxicity by selective up-regulation of TRAIL-R1. *Blood* 2001;**97**:2596–603.
111. Kabore AF, Sun J, Hu X, McCrea K, Johnston JB, Gibson SB. The TRAIL apoptotic pathway mediates proteasome inhibitor induced apoptosis in primary chronic lymphocytic leukemia cells. *Apoptosis* 2006;**11**:1175–93.
112. Fandy TE, Shankar S, Ross DD, Sausville E, Srivastava RK. Interactive effects of HDAC inhibitors and TRAIL on apoptosis are associated with changes in mitochondrial functions and expressions of cell cycle regulatory genes in multiple myeloma. *Neoplasia (New York, NY)* 2005;7:646–57.
113. Singh TR, Shankar S, Srivastava RK. HDAC inhibitors enhance the apoptosis-inducing potential of TRAIL in breast carcinoma. *Oncogene* 2005;**24**:4609–23.
114. Sinicrope FA, Penington RC. Sulindac sulfide-induced apoptosis is enhanced by a small-molecule Bcl-2 inhibitor and by TRAIL in human colon cancer cells overexpressing Bcl-2. *Molecul Cancer Therapeut* 2005;4:1475–83.
115. Singh TR, Shankar S, Chen X, Asim M, Srivastava RK. Synergistic interactions of chemotherapeutic drugs and tumor necrosis factor-related apoptosis-inducing ligand/Apo-2 ligand on apoptosis and on regression of breast carcinoma in vivo. *Cancer Res* 2003;**63**:5390–400.
116. Xiang H, Fox JA, Totpal K, et al. Enhanced tumor killing by Apo2L/TRAIL and CPT-11 co-treatment is associated with p21 cleavage and differential regulation of Apo2L/TRAIL ligand and its receptors. *Oncogene* 2002;**21**:3611–9.
117. Shankar S, Chen X, Srivastava RK. Effects of sequential treatments with chemotherapeutic drugs followed by TRAIL on prostate cancer in vitro and in vivo. *The Prostate* 2005;**62**:165–86.
118. Wu XX, Kakehi Y, Mizutani Y, et al. Enhancement of TRAIL/Apo2L-mediated apoptosis by adriamycin through inducing DR4 and DR5 in renal cell carcinoma cells. *Internat J Cancer* 2003;**104**:409–17.
119. Evdokiou A, Bouralexis S, Atkins GJ, et al. Chemotherapeutic agents sensitize osteogenic sarcoma cells, but not normal human bone cells, to Apo2L/TRAIL-induced apoptosis. *Internat J Cancer* 2002;**99**:491–504.
120. Guan B, Yue P, Clayman GL, Sun SY. Evidence that the death receptor DR4 is a DNA damage-inducible, p53-regulated gene. *J Cell Physiol* 2001;**188**:98–105.
121. Kondo K, Yamasaki S, Sugie T, et al. Cisplatin-dependent upregulation of death receptors 4 and 5 augments induction of apoptosis by TNF-related apoptosis-inducing ligand against esophageal squamous cell carcinoma. *Int J Cancer* 2006;**118**:230–42.
122. Siervo-Sassi RR, Marrangoni AM, Feng X, et al. Physiological and molecular effects of Apo2L/TRAIL and cisplatin in ovarian carcinoma cell lines. *Cancer Lett* 2003;**190**:61–72.
123. Johnston JB, Kabore AF, Strutinsky J, et al. Role of the TRAIL/APO2-L death receptors in chlorambucil- and fludarabine-induced apoptosis in chronic lymphocytic leukemia. *Oncogene* 2003;**22**:8356–69.
124. Jin Z, McDonald 3rd ER, Dicker DT, El-Deiry WS. Deficient tumor necrosis factor-related apoptosis-inducing ligand (TRAIL) death receptor transport to the cell surface in human colon cancer cells selected for resistance to TRAIL-induced apoptosis. *J Biological Chemist* 2004;**279**:35829–39.
125. Sun SY, Yue P, Hong WK, Lotan R. Augmentation of tumor necrosis factor-related apoptosis-inducing ligand (TRAIL)-induced apoptosis by the synthetic retinoid 6-[3-(1-adamantyl)-4-hydroxyphenyl]-2-naphthalene carboxylic acid (CD437) through up-regulation of TRAIL receptors in human lung cancer cells. *Cancer Res* 2000;**60**:7149–55.
126. Pitti RM, Marsters SA, Ruppert S, Donahue CJ, Moore A, Ashkenazi A. Induction of apoptosis by Apo-2 ligand, a new member of the tumor necrosis factor cytokine family. *J Biol Chem* 1996;**271**:12687–90.
127. Qin J, Chaturvedi V, Bonish B, Nickoloff BJ. Avoiding premature apoptosis of normal epidermal cells. *Nat Med* 2001;7:385–6.
128. Walczak H, Miller RE, Ariail K, et al. Tumoricidal activity of tumor necrosis factor-related apoptosis-inducing ligand in vivo. *Nat Med* 1999;5:157–63.
129. Schneider P, Holler N, Bodmer JL, et al. Conversion of membrane-bound Fas(CD95) ligand to its soluble form is associated with downregulation of its proapoptotic activity and loss of liver toxicity. *J Exp Med* 1998;**187**:1205–13.
130. Ashkenazi A, Pai RC, Fong S, et al. Safety and antitumor activity of recombinant soluble Apo2 ligand. *J Clin Invest* 1999;**104**:155–62.
131. Bremer E, van Dam GM, de Bruyn M, et al. Potent systemic anticancer activity of adenovirally expressed EGFR-selective TRAIL fusion protein. *Mol Ther* 2008;**16**(12):1919–26.
132. Griffith TS, Rauch CT, Smolak PJ, et al. Functional analysis of TRAIL receptors using monoclonal antibodies. *J Immunol* 1999;**162**:2597–605.
133. Ashkenazi A. Targeting the extrinsic apoptosis pathway in cancer. *Cytokine Growth Factor Rev* 2008;**19**:325–31.

Enhanced Antitumor Efficacy of a DR5-Specific TRAIL Variant over Recombinant Human TRAIL in a Bioluminescent Ovarian Cancer Xenograft Model

Evelien W. Duiker,[1] Elisabeth G.E. de Vries,[1] Devalingam Mahalingam,[2] Gert Jan Meersma,[1] Wytske Boersma-van Ek,[1] Harry Hollema,[2] Marjolijn N. Lub-de Hooge,[3] Go M. van Dam,[4] Robbert H. Cool,[5,7] Wim J. Quax,[5] Afshin Samali,[6] Ate G.J. van der Zee,[2] and Steven de Jong[1]

Abstract **Purpose:** Recombinant human tumor necrosis factor-related apoptosis-inducing ligand (rhTRAIL) is clinically evaluated as novel anticancer drug. rhTRAIL-DR5, a rhTRAIL variant that specifically binds to DR5 receptor, has recently been developed. We investigated whether rhTRAIL-DR5 is more efficient than rhTRAIL in combination with cisplatin in DR5-expressing human A2780 ovarian cancer cells.

Design: Effect of cisplatin alone or in combination with rhTRAIL or rhTRAIL-DR5 on DR5 surface expression, apoptosis, and cell survival of A2780 was measured. Biodistribution analysis was done in mice with ^{125}I-rhTRAIL administered intravenously versus intraperitoneally. Antitumor efficacy of rhTRAIL-DR5 versus rhTRAIL was determined in an intraperitoneally growing bioluminescent A2780 xenograft model.

Results: Cisplatin strongly enhanced DR5 surface expression. Both rhTRAIL and rhTRAIL-DR5 in combination with cisplatin induced high levels of caspase-3 activation, apoptosis, and cell kill, with rhTRAIL-DR5 being most potent. Intraperitoneal administration of ^{125}I-rhTRAIL resulted in a 1.7-fold higher area under the curve in serum, increased tumor exposure, and more caspase-3 activation in the tumor than intravenous administration. Intraperitoneal administration of rhTRAIL-DR5 delayed A2780 tumor progression, reflected in a mean light reduction of 68.3% ($P = 0.015$), whereas rhTRAIL or rhTRAIL-DR5 plus cisplatin resulted in 85% ($P = 0.003$) and 97% ($P = 0.002$) reduction compared with A2780 tumor progression in vehicle-treated animals. Combination of rhTRAIL-DR5 with cisplatin was more effective than cisplatin alone ($P = 0.027$).

Conclusion: rhTRAIL-DR5 was superior over rhTRAIL *in vitro* and *in vivo* against DR5-expressing ovarian cancer also in combination with cisplatin. Intraperitoneal administration of rhTRAIL-DR5 warrants further exploration in ovarian cancer.

In developed countries, ovarian cancer is the fifth leading cause of deaths related to cancer in women (1). Although initial response rates to first-line treatment are up to 80% in advanced stage patients, the overall 5-year survival is low due to the occurrence of drug resistance (2). A reduced tendency of cancer cells to undergo apoptosis is due to defects in the intrinsic apoptosis pathway, which contributes to drug resistance (3, 4). Therefore, an attractive strategy for targeting cancer cells involves shifting cellular balance in favor of cell death. Such a shift can be achieved by targeting the extrinsic apoptotic pathway. This pathway is activated after binding of death ligands of the tumor necrosis factor family to their respective receptors at the cell membrane (5). The recombinant human form of the death ligand tumor necrosis factor-related apoptosis-inducing ligand (TRAIL) is regarded as the most promising death ligand due to its selective toxicity against tumor cells while sparing most normal tissues (6). rhTRAIL (Apo2L) is currently evaluated in clinical trials. A recent phase I study showed that rhTRAIL can be administered safely and is well tolerated (7). This ligand binds four membrane-bound receptors, of which death receptor 4 (DR4) and death receptor 5 (DR5) act as agonistic receptors and decoy receptor 1 (DcR1) and decoy receptor 2 (DcR2) act as antagonist receptors (8).

Besides rhTRAIL, we and others have developed alternative strategies for targeting death receptors such as agonistic antibodies (9) and TRAIL variants that selectively activate DR4 or DR5 (10, 11). By avoiding competition with other

Authors' Affiliations: Departments of [1]Medical Oncology, [2]Pathology, [3]Nuclear Medicine and Molecular Imaging, [4]Surgical Oncology, [5]Pharmaceutical Biology, and [6]Gynecological Oncology, University Medical Center Groningen, University of Groningen; [7]Ratel Therapeutics BV, Groningen, The Netherlands and [8]Cell Stress and Apoptosis Research Group, Department of Biochemistry and National Centre for Biomedical Engineering Science, National University of Ireland, Galway, Ireland

Received 8/22/08; revised 12/3/08; accepted 12/5/08; published OnlineFirst 3/10/09.

Grant support: Dutch Cancer Society grant 2003-2932 and EUFP6 programme LSHC-CT-2006-037985.

The costs of publication of the article were defrayed in part by the payment of page charges. This article must therefore be hereby marked *advertisement* in accordance with 18 U.S.C. Section 1734 solely to indicate this fact.

Note: Supplementary data for this article are available at Clinical Cancer Research Online (http://clincancerres.aacrjournals.org/).

Requests for reprints: Steven de Jong, Department of Medical Oncology, University Medical Center Groningen, University of Groningen, P.O. Box 30.001, 9700 RB Groningen, The Netherlands. Phone: 31-50-3612984; Fax: 31-50-3618862; E-mail: s.de.jong@int.umcg.nl

doi:10.1158/1078-0432.CCR-08-3335

Translational Relevance

Although overall initial response rates to first-line treatment are up to 80% in advanced-stage ovarian cancer patients, the overall 5-year survival is low due to the occurrence of resistance to platinum-based therapies. The recombinant human form of the tumor necrosis factor-related apoptosis-inducing ligand (rhTRAIL) is toxic against tumor cells via the death receptors DR4 and DR5. Cisplatin induces DR5 expression in cancer cells and is more effective in combination with rhTRAIL. rhTRAIL is currently evaluated in clinical trials. Recently, a rhTRAIL variant (rhTRAIL-DR5) that specifically binds to DR5 receptor has been developed. rhTRAIL-DR5 showed enhanced efficacy *in vitro* and *in vivo* against DR5-expressing human ovarian cancer cells, with maximal efficacy in combination with cisplatin. As the peritoneal cavity is the main site of disease in ovarian cancer, it was interesting that intraperitoneal administration of rhTRAIL resulted in higher area under the curve and more apoptosis in the intraperitoneally growing tumor than intravenous administration. Thus, intraperitoneal administration of rhTRAIL-DR5 in combination with cisplatin warrants further exploration in ovarian cancer.

TRAIL receptors, we showed that specific targeting of DR5 using DR5-selective TRAIL variants resulted in enhanced apoptosis in several cancer cell lines, including the A2780 ovarian cancer cell line. In these cell lines, rhTRAIL-induced apoptosis was primarily mediated by DR5 (11). The DR5-selective rhTRAIL variants possess increased binding capacities for the designated receptor, which may enhance efficacy and improve the therapeutic window (11). The role of DR5 has been implied in ovarian cancer, because hypermethylation of the DR4 promoter and reduced expression of DR4 frequently occur in ovarian cancers (12). Moreover, univariate analysis showed an association for high DR5 expression with decreased survival in ovarian cancers (13). In addition, use of rhTRAIL combined with cisplatin enhanced apoptosis and growth inhibition in several ovarian cancer cell lines, which was related to cisplatin-induced DR4 and DR5 cell surface expression (14). Taken together, these results present DR5 as an interesting target in ovarian cancer. Thus far, studies combining chemotherapeutic drugs with DR5 targeting drugs have not been done in ovarian cancer models.

Clinical efficacy of death receptor targeted therapies in ovarian cancer depends on their biological activity and pharmacologic behavior. As the peritoneal cavity is the main site of disease in ovarian cancer, intraperitoneal drug administration may result in increased tumor penetration and drug exposure with reduced systemic toxicity (15). Intraperitoneal cisplatin administration increases survival compared with intravenous administration in advanced-stage ovarian cancer patients (16). As intravenous rhTRAIL administration in humans results in rapid renal clearance with a half-life of ~30 min (17), intraperitoneal administration may delay its clearance and lead to increased antitumor activity.

The aim of the present study was to compare the *in vitro* and *in vivo* efficacy of a novel rhTRAIL variant directed at DR5 (rhTRAIL-DR5) with that of rhTRAIL alone and in combination with cisplatin in a bioluminescent human A2780 intraperitoneal ovarian cancer model. The rhTRAIL variant, obtained by computational design, contains two amino acid mutations, D269H and E195R, which ensure high affinity binding specifically to DR5 (11). The optimal route of *in vivo* variant or rhTRAIL administration, intravenously or intraperitoneally, was evaluated by biodistribution analysis with radiolabeled rhTRAIL. *In vivo* efficacy was determined by bioluminescence.

Materials and Methods

Cell lines and transfection procedure The human ovarian cancer cell line A2780, a kind gift from Dr. Hamilton (Fox Chase Cancer Center), forms intraperitoneal xenografts mimicking peritonitis carcinomatosis in nude mice (18). The A2780-luc cell line was generated as follows: the luciferase gene was excised from pGL3-basic (Promega) with *Hin*dIII and *Xba*I restriction enzymes (Roche Applied Science) and ligated into a pcDNA3 vector under the control of the cytomegalovirus promoter. A2780 cells were cultured to 70% confluency and transfected by incubation with 2.5 μg plasmid DNA and 5 μL Fugene6 (Roche) in 250 μL Opti-MEM (Invitrogen). Two days after transfection, transfectants were selected by adding geneticin (1 mg/mL) (Roche Applied Science). Stable transfectants were obtained with a clonogenic assay followed by subcloning of positive clones by limiting dilution. The cell lines were cultured in RPMI 1640 (Life Technologies) supplemented with 10% heat-inactivated FCS (Bodinco) and 0.1 mol/L L-glutamine in a humidified atmosphere with 5% CO_2 at 37°C. Geneticin was added once a month to the A2780-luc culture. Luciferase expression was regularly tested with the luciferase assay (Promega) and the Bio-Rad ChemiDoc XRS system (Bio-Rad).

Cytotoxicity assays and determination of apoptosis The microculture tetrazolium assay, done as described earlier (19), was used to measure cytotoxicity. The cells were cultured in Ham's/F-12 and DMEM supplemented with 20% FCS and 0.1 mol/L L-glutamine. rhTRAIL and rhTRAIL-DR5 were produced as we have described earlier (11, 20). Binding capacity to DR4 and DcR1 is virtually absent for TRAIL-DR5, whereas affinity for DcR2 is reduced (11). Treatments consisted of continuous incubation with 0 to 100 ng/mL rhTRAIL-DR5 or rhTRAIL. In cell viability assays assessing combination treatment with cisplatin, the cells were preincubated for 4 h with 2.5 μmol/L cisplatin (inhibitory concentration 20%, IC_{20}), before addition of 0 to 25 ng/mL rhTRAIL or rhTRAIL-DR5.

Caspase-3/7 activity was used as an early apoptosis marker. Caspase-3/7 activity was determined with a caspase-3/7 fluorometric assay (Zebra Biosciences). For the fluorometric detection of DEVDase activity, cells were plated in 6-well plates and left to adhere overnight. The cells were exposed to 2.5 μmol/L cisplatin for 4 h, after which cisplatin was washed away with PBS [6.4 mmol/L Na_2HPO_4, 1.5 mmol/L KH_2PO_4, 0.14 mmol/L NaCl, 2.7 mmol/L KCl (pH 7.2)] and fresh medium was added to the cells. Twenty hours later, 50 ng/mL rhTRAIL-DR5 or rhTRAIL was added for various times. Thereafter, the cells were harvested with trypsin and washed twice with ice-cold PBS. Before performing the caspase-3 activity assay according to the manufacturer's protocol, protein content of the lysates was determined with Bradford analysis (21).

The acridine orange staining served as a marker for end-stage apoptosis. For the apoptosis assay, 10,000 cells were incubated in 96-well tissue culture plates. The cells were exposed to 2.5, 10, or 30 μmol/L cisplatin for 4 h, after which they were washed with PBS twice and incubated in regular culture medium. Twenty hours thereafter, cells were incubated in regular culture medium with or without 100 or 250 ng/mL rhTRAIL-DR5 or rhTRAIL for an additional 4 h. The same procedure was done in the presence of 2.5 μg/mL mouse anti-DcR2 antibody (R&D Systems), with the exception that

1 h preincubation with the blocking antibody preceded rhTRAIL-DR5 and rhTRAIL incubation. With this anti-DcR2 antibody, an enhanced effect of rhTRAIL was observed in Colo205 human colon carcinoma cells.[8] After drug incubation, acridine orange was added to each well to distinguish apoptotic cells from viable cells. Staining intensity was determined by fluorescence microscopy. Apoptosis was defined by the appearance of apoptotic bodies and/or chromatin condensation and expressed as the percentage of apoptotic cells counted in three fields containing minimally 300 cells.

To quantitatively express the efficacy of combination therapy (cisplatin + rhTRAIL or rhTRAIL-DR5) compared with both agents alone, we calculated enhancement ratios for cell kill and apoptosis as follows: enhancement ratio = [% induced by combination therapy / (% induced by cisplatin alone + % induced by ligand)].

Flow cytometry. Analysis of TRAIL receptor membrane expression was done by fluorescence-activated cell sorting analysis as described previously (22). For death receptor expression after cisplatin exposure, cells were exposed for 4 h, washed with PBS, and incubated for 20 h in regular culture medium, after which fluorescence-activated cell sorting analysis was done. Cells were subsequently washed twice with cold PBS containing 2% FCS and 0.1% sodium azide and incubated with phycoerythrin-conjugated mouse monoclonal antibodies against DR4, DR5, DcR1, and DcR2. Mouse phycoerythrin-labeled IgG1 and IgG2B were used as isotype controls. All phycoerythrin-labeled antibodies were purchased from R&D Systems. Membrane receptor expression was analyzed with Winlist and Winlist 32 software (Verity Software House) and shown as mean fluorescent intensity of all analyzed cells.

DR5 RNA interference and Western blotting. Small interfering RNA (siRNA) specific for human DR5 were designed and synthesized by Eurogentec. The double-stranded siRNA specific for human DR5 was 5′-GACCCUUGUGCUCGUUGUC-dTdT-3′ (sense) and 5′-GACAACGAGCACAAGGGUC-dTdT-3′ (antisense). Double-stranded luciferase siRNA sequence was 5′-CUUACGCUGAGUACUUCGA-dTdT-3′ (sense) and 5′-UCGAAGUACUCAGCGUAAG-dTdT-3′ (antisense). A2780 cells were transfected in 6-well plates (at 30-50% confluency) with siRNA duplexes (133 nmol/L) using Oligofectamine transfection reagent according to the manufacturer's instructions (Invitrogen/Life Technologies). After 24 h, medium was aspired and cells were harvested and plated. Then, cells were exposed to various cisplatin concentrations for 4 h, washed with PBS, and incubated for 20 h in regular culture medium. Finally, cells were harvested and used for flow cytometry or Western blotting. For the apoptosis assay, cells were incubated in regular culture medium with or without rhTRAIL-DR5 or rhTRAIL (100 ng/mL) for an additional 4 h and apoptosis was determined with the acridine orange assay.

For Western blotting, cells were washed in ice-cold PBS and lysed in SDS sample buffer [4% SDS, 20% glycerol, 0.5 mol/L Tris-HCl (pH 6.8), 0.002% bromophenol blue] containing 10% 2-β-mercaptoethanol by boiling for 5 min in a water bath. Proteins were separated on a SDS-polyacrylamide gel and transferred to a polyvinylidene difluoride membrane (Millipore) by wet blotting. Western blotting was done using skim milk as blocking agent (19). The following antibodies were applied: rabbit anti-DR5 antibody (Cell Signaling Technology) and mouse-anti-actin as the control for equal protein loading (ICN Biomedicals). Secondary antibodies conjugated with horseradish peroxidase were obtained from DAKOCytomation. Chemiluminescence was detected using BM Chemiluminescence Blotting Substrate (POD) or Lumi-LightPLUS Western blotting substrate (Roche Diagnostics).

Animals and bioluminescence imaging procedure. Female nude mice (Hsd:athymic nude-nu) were obtained from Harlan Nederland at age 6 to 8 weeks (~21 g). Inoculation was done 10 days after acclimatization. All animal studies were conducted in accordance with the Law on Animal Experimentation and local guidelines and approved by the local ethical committee.

Imaging was conducted with the IVIS 100 series (Xenogen) composed of a cooled charge-coupled device camera connected to a light-tight black chamber. Before in vivo imaging, animals were anesthetized with 4% isoflurane and injected intraperitoneally with D-luciferin (150 mg/kg, Xenogen) reconstituted in sterile PBS. Mice were placed in prone position on a warmed stage (37°C) in the imaging chamber, and grayscale reference images were obtained under dim illumination. Pseudocolor images representing bioluminescent intensity were acquired with LivingImage software (version 2.50, Xenogen) 10 and 15 min after D-luciferin injection in complete darkness. These images were superimposed on the grayscale images for analysis with Igor Pro software (version 4.09, WaveMetrics). All bioluminescence imaging (BLI) data are depicted in radiance units (photons/s/cm^2/sr) enabling absolute comparisons between bioluminescent images and represent final data obtained after subtraction of the background signal.

Characterization of the intraperitoneal bioluminescent model. The A2780-Luc peritonitis carcinomatosis model, characterized in 45 mice, showed exponential tumor growth from 5 days after intraperitoneal inoculation with 2×10^6 A2780-Luc cells. Approximately 10 days later, the increment of the bioluminescence signal was delayed, characterized by a flattening of the BLI log-growth curve that evolved in an almost flat slope. This flattening preceded the development of macroscopic disease, bloody ascites formation, and deterioration of general condition. Animal survival based on clinical condition was, on average, 4 weeks after inoculation. Flattening was most likely due to superposed tumor tissue that absorbed and scattered light emitted from tumor cells situated deeply in the peritoneal cavity. To employ flattening of the BLI growth curve in the definition of a uniform endpoint, we used logistic regression analysis. The exponential curve was represented by, $y = a \cdot e^{bx}$, where y stands for the bioluminescent signal (in radiance), a for the intercept with the y axis (BLI signal at day 5), e for the uniform mathematical constant, x for time (in days), and b for the equation-specific constant, which is calculated by logistic regression. The equation can be used to predict BLI signal on consecutive imaging days. Definition of flattening, which serves as a surrogate endpoint for survival, was a bioluminescent signal of <50% as the expected signal based on the equation. We used this endpoint in the efficacy studies with one refinement. Treatment induced alterations in the log growth which did not allow determining an equation representing the BLI curve for each mouse during treatment. The time from cessation of treatment to flattening was too short to reliably employ logistic regression analysis. Therefore, the mean signal at flattening in the vehicle-treated group minus 1 × SD was defined as absolute cutoff value (3.1×10^6 photons/s/cm^2/sr), which was valid as a uniform survival endpoint in 85% of the mice.

In vivo biodistribution with ^{125}I-rhTRAIL. Radio-iodination of rhTRAIL was done with a rhTRAIL solution of 1 mg/mL in Tris (pH 7.4), containing 100 μmol/L zinc sulfate and 10% glycerol. rhTRAIL (45 μg) and chloramine T (50 μg; Merck) were allowed to react with 70 MBq ^{125}I-NaI in 0.05 mol/L NaOH (pH 9.0; GE Healthcare) during 3 min at pH 8.0. The labeling reaction was terminated with sodium metabisulfite (Acros Organics). Nonbound ^{125}I was removed by gel filtration chromatography. The PD-10 column (Sephadex G-25M; Amersham Biosciences) was eluted with Tris containing 100 μmol/L zinc sulfate, 10% glycerol, and 0.5% human serum albumin. The biodistribution study was conducted in 50 mice after establishment of A2780-Luc intraperitoneal xenografts. ^{125}I-rhTRAIL (0.15 mL; 150 kBq, 0.5 μg) was administered intravenously through retro-orbital injection in 25 mice and intraperitoneally in 25 mice. At t = 15, 30, 60, 90, and 360 min, groups of 5 mice were sacrificed and organs and tissues were excised, rinsed for residual blood, and weighed. Tumor tissue was additionally fixed in 10% buffered formalin for histologic assessment. Samples were counted for radioactivity in a calibrated well-type LKB-1282-CompuGamma counter. Tissue activity was expressed as %ID/g. Tumor-to-blood and tumor-to-muscle ratios were also calculated. All data were corrected for physical decay and compared with a known standard sample. Pharmacokinetic parameters

[8] Szegezdi et al., manuscript submitted.

were derived using the KINFIT module of the MW/PHARM computer program package (version 3.50; MediWare). Clearance rates of ^{125}I-rhTRAIL from the circulation were calculated using nonlinear regression analysis.

Immunohistochemistry. Tissues were fixed in 10% buffered formalin, embedded in paraffin, and cut in 4 μm sections, which were mounted on APES-coated glass slides and deparaffinized in xylene. Antigen retrieval was done by microwave treatment for 8 min in 0.01 mol/L citric buffer (pH 6.0). For active caspase-3 staining, the slides were incubated overnight at 4°C with a polyclonal rabbit anti-cleaved caspase-3 antibody (Asp^{175}, 1:200; Cell Signaling Technology). The antibody detects endogenous levels of the large fragment (17/19 kDa) of activated caspase 3 resulting from cleavage adjacent to Asp^{175}. Biotinylated swine anti-rabbit (DAKO) was used as a secondary antibody (1:300 dilution), after which streptavidin/horseradish peroxidase (DAKO; 1:300 dilution) was applied. Negative controls were obtained by omission of the primary antibody and by incubation with normal rabbit IgG1. Slides were counterstained with hematoxylin. Immunohistochemical staining for cleaved caspase-3 was semiquantitatively scored as follows: 0, no positive staining cells; +/-, focal staining in one small field; +, scattered staining of few cells/focal staining in a larger field; and ++, scattered staining of multiple cells/focal staining in several large fields.

Histologic assessment of liver tissue was carried out on H&E-stained slides.

In vivo imaging of antitumor activity. A2780 luc cells (2×10^6) were injected intraperitoneally into 60 nude mice. Five days after inoculation, the mice were randomized in groups of 10 mice per treatment arm. Treatment consisted of intraperitoneal injection with vehicle (NaCl, 5 mice, days 5 and 12, and rhTRAIL-buffer, 5 mice, days 5-10 and 12-16), cisplatin (4 mg/kg at days 5 and 12), rhTRAIL or rhTRAIL-DR5 (5 mg/kg, days 5-10 and 12-16), or the combination of cisplatin with rhTRAIL or rhTRAIL-DR5. Cisplatin in the combination therapy was administered 4 h before rhTRAIL or rhTRAIL-DR5 injections. We determined the maximum tolerated dose of cisplatin (4 mg/kg intraperitoneally, weekly × 2, ref. 23) in a pilot study based on maximum 15% weight loss in tumor-bearing mice. In rat, a single intraperitoneal dose of 4 mg/kg resulted in a total platinum peak concentration of ~10 μmol/L in plasma and ~100 μmol/L in the peritoneal cavity (23), whereas a peak serum concentration of ~50 μmol/L was reached in patients at the maximum tolerated dose (intravenous dose 100 mg/m^2, ref. 24). Mice were monitored daily for general condition and weight. Bli was done at 2- to 3-day intervals. When the signal reached a value $\geq 3 \times 10^5$ photons/s/cm^2/sr, mice were sacrificed. Tumor and liver tissue samples were excised for histologic assessment.

Statistical analysis. *In vitro* data and biodistribution results were assessed for differences with unpaired two-tailed Student's *t* test or χ^2 analysis. Results from the *in vivo* efficacy study, with bioluminescence signals depicted in radiance (photons/s/cm^2/sr), are represented as

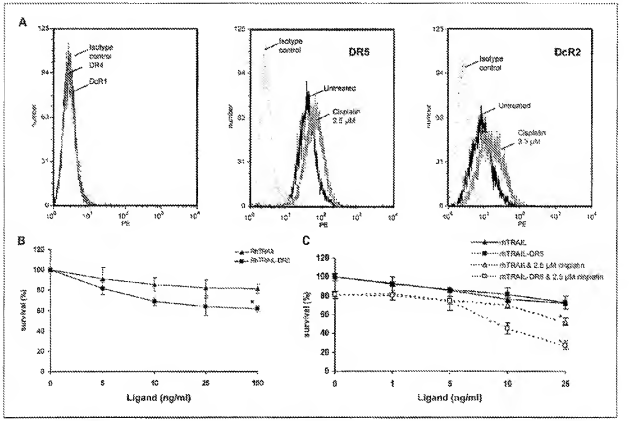

Fig. 1. *A*, levels of TRAIL receptor membrane expression on A2780 before and after exposure to 2.5 μmol/L determined by flow cytometry analysis. Cells were incubated with cisplatin for 4 h and cultured in normal medium for an additional 20 h. TRAIL receptor expression is expressed as the fluorescence intensity (photons/s/sr/cm^2). *B*, survival of A2780 assessed with a cytotoxicity assay after 96 h exposure to 0 to 100 ng/mL rhTRAIL and rhTRAIL-DR5. *, $P = 0.008$. *C*, survival of A2780 determined with a cytotoxicity assay. Cells were preincubated for 4 h with 2.5 μmol/L cisplatin, after which the cells were washed, cultured in medium for 20 h, and exposed to 0 to 25 ng/mL rhTRAIL or rhTRAIL-DR5 for an additional 72 h. *, $P < 0.01$, rhTRAIL versus cisplatin and rhTRAIL + *, $P < 0.01$, rhTRAIL-DR5 versus cisplatin and rhTRAIL-DR5. *, $P < 0.001$, cisplatin and rhTRAIL versus cisplatin and rhTRAIL-DR5. Mean ± SD of at least three independent experiments.

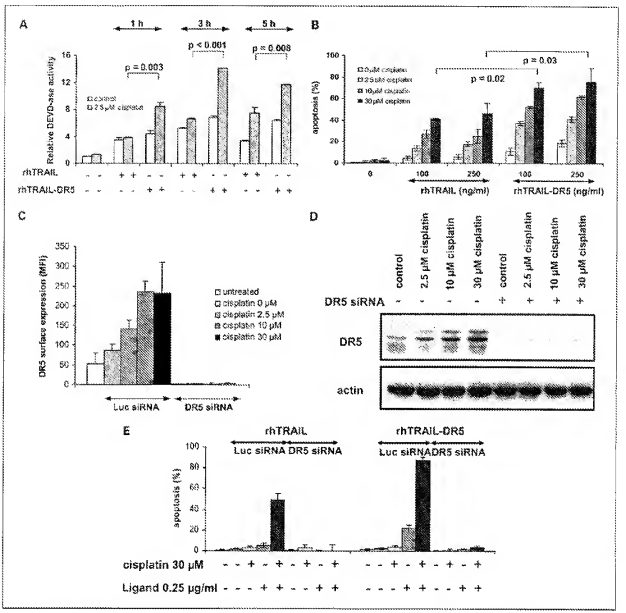

Fig. 2. *A*, induction of apoptosis after exposure to 50 ng/mL rhTRAIL or rhTRAIL-DR5 alone or after preincubation with 2.5 μmol/L cisplatin for 4 and 20 h before rhTRAIL or rhTRAIL-DR5 administration. Caspase activation was determined with a caspase-3 activity assay after 1, 3, and 5 h treatment. *B*, cells were preincubated with medium and 2.5, 10, and 30 μmol/L cisplatin for 4 h and washed. After 20 h, the cells were exposed for 4 h to 100 or 250 ng/mL rhTRAIL or rhTRAIL-DR5, and apoptosis was assessed by means of acridine orange staining. For clarity, only significance between apoptosis levels in cells treated with 30 μmol/L cisplatin in combination with rhTRAIL-DR5 versus 30 μmol/L cisplatin in combination with rhTRAIL was indicated. Apoptosis levels were significantly higher for rhTRAIL-DR5 versus rhTRAIL ($P < 0.001$) for 100 and 250 ng/mL. Apoptosis levels were also significantly higher ($P < 0.01$) for 2.5 and 10 μmol/L cisplatin in combination with rhTRAIL-DR5 versus 2.5 and 10 μmol/L cisplatin in combination with rhTRAIL. *C*, DR5 membrane expression in A2780 cells transfected with siRNA against luciferase (*Luc siRNA*) or siRNA against DR5 (*DR5 siRNA*). Cells were preincubated with cisplatin for 4 h, washed, and cultured in medium for 20 h and DR5 membrane expression was determined with flow cytometry. Mean fluorescence intensities were corrected for staining with a nonspecific isotype control. *D*, DR5 cellular protein expression in A2780 cells transfected with siRNA against luciferase or siRNA against DR5 (*DR5 siRNA*). Cells were preincubated with cisplatin for 4 h, washed, and cultured in medium for 20 h and DR5 protein expression was determined with Western blotting using actin as a control for protein loading. *E*, A2780 cells transfected with siRNA against luciferase (*Luc siRNA*) or siRNA against DR5 (*DR5 siRNA*) were preincubated with medium or 30 μmol/L cisplatin for 4 h and then washed. After 20 h, the cells were exposed for 4 h to 250 ng/mL rhTRAIL or rhTRAIL-DR5, and apoptosis was assessed by means of acridine orange staining. Mean ± SD of three independent experiments.

mean ± SE. Percent signal reduction compared with vehicle-treated mice at the end of treatment (day 16) was calculated according to the formula: 100 - (signal intensity at day 16) / (mean signal intensity vehicle group at day 16) × 100. One-way ANOVA was done to determine differences in signal intensity between groups and between differences in percent signal reduction. Significant differences were subjected to post hoc analysis with Tamhane's T2 and Dunnett's T3 tests assuming unequal variances. Survival (days) was estimated by

Kaplan-Meier analysis and compared with log-rank tests. $P < 0.05$ was considered significant. Statistical analyses were generated using Graph Pad Prism software version 4.0 (GraphPad software) and SPSS 14.0 for Windows (SPSS).

Results

In vitro activity of rhTRAIL-DR5, rhTRAIL, and cisplatin on A2780. A2780 cells express DR5 and low DcR2 cell surface levels, whereas DR4 and DcR1 are undetectable (Fig. 1A). Long-term exposure (96 h) of A2780 cells to relatively low concentrations of rhTRAIL and rhTRAIL-DR5 induced a loss of viability, reaching a maximum effect between 25 and 100 ng/mL (Fig. 1E). rhTRAIL-DR5 was more effective than rhTRAIL at the highest ligand concentration. Short treatment with cisplatin for 4 h resulted in a clearly detectable increase in DR5 and DcR2 cell surface expression after 24 h without substantially affecting cell growth in a survival assay (Fig. 1A and C). Therefore, we preincubated cells with cisplatin (2.5 μmol/L) for 4 h and cultured the cells for an additionally 20 h, allowing enhanced DR5 cell surface expression. Cells were continuously treated with rhTRAIL or rhTRAIL-DR5 for an additional 72 h (Fig. 1C). rhTRAIL-DR5 decreased cell survival more effectively than rhTRAIL both as a single agent ($P < 0.01$) and in combination with cisplatin ($P < 0.001$). Cisplatin sensitized A2780 cells to rhTRAIL-DR5- or rhTRAIL-induced cell kill with enhancement ratios of 1.6 and 1, respectively.

Taking into account the short half-life of rhTRAIL in mice and human (17), we assessed apoptosis using a caspase-3 activity assay in A2780 cells following short exposure to rhTRAIL and rhTRAIL-DR5. Caspase activity was enhanced within 1 h after exposure of the cells to rhTRAIL or TRAIL-DR5 (Fig. 2A). Preincubation with 2.5 μmol/L cisplatin for 4 h further enhanced caspase-3 activation. Cisplatin followed by rhTRAIL-DR5 was more effective than cisplatin followed by rhTRAIL after 1 h ($P < 0.003$). The fast activation of caspase-3, detectable within 1 h after start of treatment with rhTRAIL or TRAIL-DR5, probably resulted in an underestimation of caspase-3 activation at the last time point (5 h) due to degradation of active caspase-3 in late apoptotic cells. With an acridine orange assay detecting late apoptotic cells, we showed that rhTRAIL-DR5 was more effective than rhTRAIL following pretreatment with cisplatin for 4 h with clinically relevant concentrations up to 30 μmol/L (Fig. 2B; ref. 24). Cisplatin (30 μmol/L) combined with rhTRAIL or rhTRAIL-DR5 gave enhancement ratios of 8.2 and 5, respectively.

The involvement of the DR5 in inducing apoptosis in these cells was further assessed in cells in which the DR5 had been knocked down by siRNA. A strong cisplatin concentration-dependent increase in DR5 surface expression, as well as DR5 cellular protein expression, was observed in the luciferase siRNA-treated cells, whereas DR5 siRNA resulted in complete down regulation of DR5 in the presence of cisplatin up to 30 μmol/L (Fig. 2C and D). In addition, DR5 siRNA completely protected A2780 cells against TRAIL- and TRAIL-DR5-induced apoptosis also in the presence of cisplatin (Fig. 2E). The apoptosis assays for rhTRAIL and rhTRAIL-DR5 were also done with coincubation of a DcR2 blocking antibody, which had no effect on the apoptosis levels (Supplementary Figure).

These data show that the DR5 pathway is important for rhTRAIL- and rhTRAIL-DR5-induced apoptosis, which is further activated by cisplatin in ovarian cancer cells.

^{125}I-rhTRAIL biodistribution in tumor-bearing mice. Tissue biodistribution and tumor uptake of intravenously (Supplementary Table S1A) and intraperitoneally (Supplementary Table S1B) administered ^{125}I-rhTRAIL were compared in nude mice with intraperitoneal A2780-Luc xenografts. The administration route influenced the disposition of ^{125}I-rhTRAIL. Blood activity (%ID/g) was higher at 15 min (43.39 ± 11.04 versus 25.30 ± 5.04) and 30 min (30.51 ± 12.40 versus 15.33 ± 3.78) after intravenous versus intraperitoneal injection, whereas it was lower at 90 min (7.52 ± 1.22 versus 23.74 ± 6.85) and 360 min (2.63 ± 0.56 versus 8.26 ± 1.74). The blood kinetics of ^{125}I-rhTRAIL in blood could be described by a two-compartment model. The resulting blood activity versus time profiles (Fig. 3A) showed a higher area under the time curve

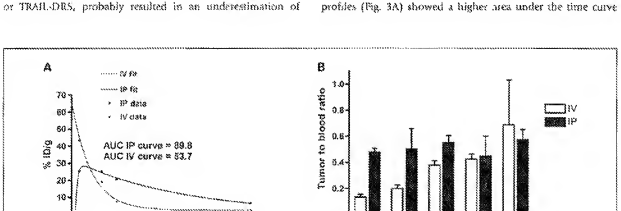

Fig. 3. *A*, area under the blood activity versus times curves for intraperitoneal and intravenous ^{125}I-rhTRAIL. Blood activity was determined at 15, 30, 60, 90, and 360 min after administration of ^{125}I-rhTRAIL. %ID/g was calculated and averaged for 3 to 5 mice per time point and pharmacokinetic profiles were fitted with a two-compartment model. *B*, tumor-to-blood ratio versus time of ^{125}I-rhTRAIL administered intravenously or intraperitoneally. Tumor-to-blood ratios were calculated by dividing the average tumor activity in %ID/g per time point through the average blood activity in %ID/g per time point. *In vivo* biodistribution study was conducted in mice after establishment of A2780-Luc intraperitoneal xenografts.

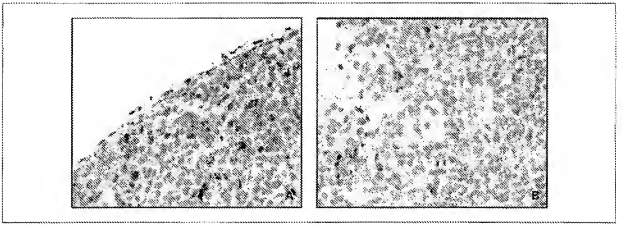

Fig. 4. Intraperitoneally growing A2780 xenografts were excised 15 to 360 min after ^{125}I-rhTRAIL was administered intravenously or intraperitoneally. Immunohistochemical staining of active caspase-3 in xenografts at 360 min after intraperitoneal (*A*) and intravenous (*B*) ^{125}I-rhTRAIL administration. Sample of the subgroup of tumors with scattered staining of multiple cells/focal staining in several large fields following intraperitoneal or intravenous administration of rhTRAIL. Active caspase-3 staining near the blood vessels is visible in a xenograft from the intravenous group.

after intraperitoneal administration than after intravenous administration. After intraperitoneal injection, the peak blood activity is lower than after intravenous injection but remains higher for a longer period. Kidney uptake (%ID/g) showed the same pattern as blood pool activity with higher activity after intravenous versus intraperitoneal administration at 15 min (199.2 ± 40.69 versus 19.83 ± 1.38) and 30 min (126.6 ± 19.68 versus 21.45 ± 1.90) and lower activity at 90 min (12.73 ± 2.47 versus 17.87 ± 1.28) and 360 min (7.06 ± 0.56 versus 4.45 ± 0.31). Activity in well-perfused organs such as lung, liver, and spleen displayed similar kinetics as the blood pool activity in both administration routes. Stomach activity increased over time, which can be attributed to *in vivo* dehalogenation. Intraperitoneal administration resulted in high tumor activity at 15 min (11.31 ± 1.51) and 60 min (12.91 ± 3.29) with a gradual decrease to 360 min, whereas after intravenous administration tumor activity remained largely unchanged up to 60 min (6.85 ± 1.29) and then gradually decreased to 360 min. At all time points, tumor uptake (%ID/g) was higher after intraperitoneal administration versus intravenous administration but only reached significance at 90 min. The tumor-to-blood ratios were higher after intraperitoneal versus intravenous administration at 15 min (0.48 ± 0.03 versus 0.13 ± 0.02) and 60 min (0.55 ± 0.06 versus 0.38 ± 0.04). Tumor-to-blood ratios remained constant over time after intraperitoneal injection, whereas tumor-to-blood ratios after intravenous administration gradually increased to ratios observed with intraperitoneal administration (Fig. 3B). These results indicate that intraperitoneal administration of rhTRAIL may have advantages compared with intravenous administration in this intraperitonially growing tumor model.

Assessment of caspase-3 activity in tumors. To determine whether intraperitoneal and/or intravenous administration resulted in ^{125}I-rhTRAIL-induced cleavage of procaspase-3 into active caspase-3, paraffin-embedded tumor tissues obtained at 15, 30, 60, 90, and 360 min after ^{125}I-rhTRAIL injection were stained for active caspase-3. Whereas almost no active caspase-3 was detected in samples obtained at 15 min, tumors obtained between 30 and 360 min showed low but clearly visible active caspase-3–positive tumor cells following either intraperitoneal or intravenous administration of ^{125}I-rhTRAIL. Focal staining as well as scattered staining of tumor cells often just below the tumor surface was observed following intraperitoneal administration (Fig. 4A), whereas focal staining or scattered staining throughout the tumor was observed following intravenous administration. Active caspase-3 staining was found near blood vessels in two tumors from the intravenous group (Fig. 4B). Semiquantitative analyses of the tumors, taking together the staining in tumors from sacrificed mice between 30 and 360 min after administration of ^{125}I-rhTRAIL, revealed that scattered staining of multiple cells or focal staining in several fields was more often observed in tumors following intraperitoneal than intravenous administration (7 of 15 evaluable tumors in the intraperitoneal group versus 1 of 16 evaluable tumors in the intravenous group; $P = 0.01$). The low levels of active caspase-3 in both intraperitoneal and intravenous groups were probably due to the relatively low concentration of ^{125}I-rhTRAIL (0.5 μg/mice) used in the biodistribution study.

In vivo efficacy of rhTRAIL, rhTRAIL-DR5, and cisplatin on intraperitoneal xenografts. The response of intraperitoneal A2780-Luc xenografts to treatment with rhTRAIL, rhTRAIL-DR5, and cisplatin or a combination of either rhTRAIL or rhTRAIL-DR5 with cisplatin was assessed by BLI. Tumor regression was not visible within the first 48 h after treatment initiation at day 5 but was clearly evident at the end of the first treatment period (day 9), with the largest signal reduction seen after combination of rhTRAIL or rhTRAIL-DR5 with cisplatin (Fig. 5A). Signals rose in the days between both treatments. All treatment groups, except the rhTRAIL-treated arm, had significantly smaller tumors at day 16 than the vehicle-treated group. This is reflected in the mean signal reduction as to vehicle-treated mice, whereas rhTRAIL alone did not result in a significant decrease (48.8% range, 32.8-64.6%; $P = 0.097$); rhTRAIL-DR5 and cisplatin gave a reduction of 68.5% (range, 61.8-74.8%, $P = 0.015$) and 72.3% (range, 59.8-84.9%, $P = 0.009$), respectively. Combination therapies were highly effective: rhTRAIL plus cisplatin caused a decline in signal intensity of 84.8% (range, 73.5-96.1; $P = 0.003$) and

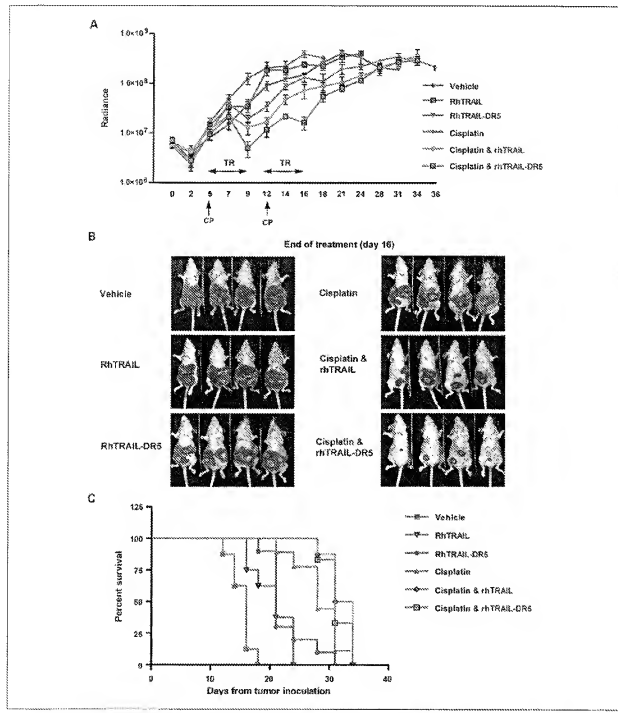

Fig. 5. Visualization of response to rhTRAIL, mTRAIL, DR5, cisplatin, and the combination of either ligand with cisplatin by means of BLI. Nude mice were inoculated intraperitoneally with 2×10^6 AZ/50-Luc cells. After 5 days, treatment was initiated: cisplatin (4 mg/kg intraperitoneally) or vehicle at days 5 and 12, rhTRAIL and mTRAIL-DR5 (3 mg/kg intraperitoneally) or vehicle at days 5 to 10 and 12 to 16, or a combination of rhTRAIL or mTRAIL-DR5 with cisplatin. *CP*, cisplatin; *TR*, rhTRAIL / mTRAIL-DR5. *A*, change in light emission (in radiance units) over time per treatment arm. Bioluminescent signals at each time point were averaged per treatment group. Mean ± SE. Significant differences in signal intensities at day 16 were observed between vehicle ($4.6 \times 10^8 \pm 6.7 \times 10^7$) vs. rhTRAIL ($2.3 \times 10^8 \pm 3.1 \times 10^7$) $P = 0.037$, vehicle vs. mTRAIL-DR5 ($1.4 \times 10^8 \pm 1.2 \times 10^7$) $P = 0.018$, vehicle vs. cisplatin ($1.3 \times 10^8 \pm 2.4 \times 10^7$) $P = 0.009$, vehicle vs. cisplatin and rhTRAIL ($8.7 \times 10^7 \pm 2.1 \times 10^7$) $P = 0.003$, and vehicle vs. cisplatin and mTRAIL-DR5 ($1.6 \times 10^7 \pm 4.6 \times 10^6$) $P = 0.002$. *B*, bioluminescent images at the end of treatment (day 16) of each 4 mice representative for 10 mice per experimental arm. Images are displayed and quantified in log radiance (photons/s/cm^2/sr). *C*, Kaplan-Meier survival analysis of all mice. A bioluminescent signal $>3.1 \times 10^8$ was used as surrogate endpoint for survival as described in Materials and Methods.

rhTRAIL-DR5 plus cisplatin resulted in 96.5% (range, 93.7-99.4%, $P = 0.002$) signal reduction. The decline in signal intensity after rhTRAIL-DR5 plus cisplatin was higher than the mean light reduction after cisplatin alone ($P = 0.07$). Thus, all therapies, except rhTRAIL monotherapy, exhibited significant antitumor activity at the end of treatment, with the combination therapies displaying the highest activity.

In general, light intensity at the end of treatment was inversely associated with survival (Fig. 5B). Animals were sacrificed when a bioluminescent signal $\geq 3.1 \times 10^6$ photons/s/cm^2/sr was reached as a surrogate marker for survival. The median survival of the vehicle controls was 16 days, with no mice surviving after 18 days (Fig. 5C). Monotherapy with rhTRAIL and rhTRAIL-DR5 prolonged median survival to 21 days ($P < 0.001$) and with cisplatin to 28 days ($P < 0.0001$). rhTRAIL-DR5 in combination with cisplatin resulted in a median survival of 31 days ($P < 0.0001$), and rhTRAIL plus cisplatin resulted in a median survival of 32.5 days ($P < 0.0001$). The latter was also significant compared with cisplatin monotherapy ($P = 0.033$). Liver histology at sacrifice did not show any signs of liver damage.

Discussion

In this study, we show that rhTRAIL-DR5, a rhTRAIL variant designed to specifically bind DR5, induced higher levels of apoptosis and growth inhibition in ovarian cancer cells than rhTRAIL. Pretreatment with cisplatin strongly enhanced apoptosis and cytotoxicity induced by rhTRAIL-DR5 or rhTRAIL, with the combination of cisplatin and rhTRAIL-DR5 being most effective. Intraperitoneal administration of these drugs in an orthotopic bioluminescent mouse model of human ovarian peritonitis carcinomatosis delayed tumor growth, with superior efficacy of cisplatin combined with rhTRAIL-DR5 over cisplatin alone.

Whereas rhTRAIL can bind to DR4 and DR5, agents that specifically target one death receptor are in various stages of development. Using receptor-selective rhTRAIL variants, we and others have recently defined that cancer cells can display a preference for either DR4 or DR5 for apoptosis signaling, resulting in enhanced apoptosis when the dominant receptor is targeted. Colon and breast cancer cell lines were reported to signal primarily through DR5 (10, 11), whereas primary lymphoid malignancies do so through DR4 (25, 26). Interestingly, DR5-selective TRAIL variants, including rhTRAIL-DR5, caused higher levels of apoptosis than wild-type rhTRAIL in DR5-expressing Jurkat and A2780 cells as well as in BJAB cells when DR5 was reexpressed (10, 11). In the present study, we used the rhTRAIL variant that contains two amino acid mutations, D269H and E195R, with high-affinity binding for DR5 and almost no affinity for DR4 (11). We showed that pretreatment of A2780 cells with cisplatin augmented rhTRAIL-DR5- or rhTRAIL-induced cytotoxicity and apoptosis, with the highest efficacy of cisplatin combined with rhTRAIL-DR5. Combinations of anticancer agents with receptor targeted drugs are often more effective than the single agents in preclinical models. Death receptor up-regulation induced by chemotherapeutic drugs or irradiation in a p53-dependent (27-29) or p53-independent (30) matter is regarded as one of the mechanisms contributing to enhanced effects of combinatory regimens. In our model, cisplatin induced DR5 and DcR2 up-regulation. Drug-induced DR5 up-regulation is more frequently reported than DR4 up-regulation (22, 27, 31). Several other studies have reported the important role of DR5 in ovarian cancer (12, 13). Moreover, in ovarian cancer specimens obtained before and after cisplatin treatment, DR5 expression increased from 37% to 74% after chemotherapy, whereas DR4 staining remained unaltered (32). This might imply that combinatory strategies with DR5 targeted agents are more effective than combinational regimes with DR4 targeted drugs in ovarian cancer.

Additionally, agents binding only one receptor will cause exclusively the formation of DR4 or DR5 homotrimers, whereas TRAIL binding may cause homotrimer and heterotrimer formation. Whether this affects apoptosis induction is not well established. Immunoprecipitation of death-inducing signaling complexes after treatment with TRAIL showed fewer heterotrimeric than homotrimeric complexes, which might indicate that homotrimers are favored over heterotrimers (33). Moreover, targeting a single receptor may induce enhanced apoptosis due to a lack of competition with decoy receptors (34, 35). A2780 cells express DR5 and low levels of DcR2. Blocking antibodies against DcR2 did not enhance rhTRAIL-induced apoptosis, indicating that another mechanism is responsible for the superior efficacy of rhTRAIL-DR5 over rhTRAIL. Increased binding capacities for DR5 of the mutant over rhTRAIL might be involved (11), although the exact kinetics of receptor binding of rhTRAIL-DR5 need to be established in further detail. Other TRAIL mutants showed that increased affinity for the targeted receptor might play a role (10). Alternatively, a recent study showed that the extracellular domains of DR4, but not of DR5, can interact with the extracellular domain of DcR1 and DcR2 (36). The absence of DR4 in A2780 may then explain why DcR2 antibodies had no effect on rhTRAIL in these cells. This indicates that, in cell lines positive for DR4 and DR5 surface expression, the differences in apoptosis induction between rhTRAIL and rhTRAIL-DR5 might be larger. Loss of affinity for decoy receptors may result in toxicity of rhTRAIL-DR5. However, a clear correlation between decoy receptor expression and resistance to rhTRAIL in normal cells has not been established (37) and monoclonal antibodies devoid of binding capacity to decoy receptors can be safely administered in clinical trials.

The rationale behind intraperitoneal drug administration is to increase local drug exposure while lowering plasma clearance (38). We show that intraperitoneal rhTRAIL administration resulted in a higher area under the curve and a reduced clearance. The high kidney activity confirms the function of the kidney as main site of rhTRAIL clearance, which is not influenced by intraperitoneal administration. Activity in most organs followed that of blood pool activity, suggesting that distribution to normal tissues was limited, which corresponds to previous studies (39). Our results indicate that intraperitoneal administration of rhTRAIL may result in favorable tumor uptake in intraperitoneally growing tumors. Moreover, we found active caspase-3 staining after intraperitoneal injection at this nontherapeutic dose of rhTRAIL. Whether this is caused by local rhTRAIL penetration into the tumor, a limiting factor for intraperitoneal administration of antibodies (40), needs to be established. To further investigate the efficacy of intravenous versus intraperitoneal administration on intraperitoneally growing tumors, therapeutic doses of rhTRAIL or rhTRAIL variants have to be used and related to tumor

responses. Additionally, those experiments should focus on the relation between caspase-3 activation and tumor responses and the molecular characteristics of the surviving tumor cells.

In the present study, we used BLI to assess tumor response, because no reliable methods based on clinical features exist to accurately evaluate intraperitoneal tumor proliferation over time. The BLI data clearly visualized the differences in response to the applied treatments. Furthermore, we used bioluminescence to define an endpoint for survival. As survival of mice with intraperitoneal xenografts is mostly based on assessment of clinical condition, our method ensured the definition of a uniform and objective early endpoint. The response to treatment in each arm reflected the *in vitro* results with high accuracy. At the end of treatment, tumor burden in mice treated with low-dose cisplatin together with rhTRAIL-DR5 was lower than after cisplatin alone. These results were associated with a survival advantage, although this advantage was limited. This may be due to the cell line model we used, which is not extremely sensitive to cisplatin combined with ligands *in vitro* and which is growing extremely rapidly *in vivo*. Our study comprising two cycles of therapy was, however, not designed to primarily assess survival but to show a proof of concept. The cisplatin dose used in mice is comparable with clinically achievable doses (24), but no more cycles could be given to these mice due to toxic side effects. Further studies in mice and finally in patients are warranted to define optimal dosage schedules for maximal survival benefit.

In summary, our data indicate that a receptor selective variant of rhTRAIL, rhTRAIL-DR5, displays better antitumor efficacy than rhTRAIL. The combination of rhTRAIL-DR5 together with cisplatin might offer a new strategy for more effective ovarian cancer treatment.

Disclosure of Potential Conflicts of Interest

W.J. Quax, A. Samali, founders/directors, Trskel Therapeutics.

References

1. Jemal A, Siegel R, Ward E, et al. Cancer statistics, 2007. CA Cancer J Clin 2007;57:43–66.
2. Agarwal R, Kaye SB. Ovarian cancer: strategies for overcoming resistance to chemotherapy. Nat Rev Cancer 2003;3:502–16.
3. Pommier Y, Sordet O, Antony S, Hayward RL, Kohn KW. Apoptosis defects and chemotherapy resistance: molecular interaction maps and networks. Oncogene 2004;23:2934–49.
4. Wernyj RP, Morin PJ. Molecular mechanisms of platinum resistance: still searching for the Achilles' heel. Drug Resist Updat 2004;7:227–32.
5. Hengartner MO. The biochemistry of apoptosis. Nature 2000;407:770–6.
6. Duiker EW, Mom CH, de Jong S, et al. The clinical trail of TRAIL. Eur J Cancer 2006;42:2233–40.
7. Herbst RS, Mendelson DS, Ebbinghaus S, et al. A phase I safety and pharmacokinetic (PK) study of recombinant Apo2L/TRAIL, an apoptosis-inducing protein in patients with advanced cancer. J Clin Oncol 2006; Proc Am Soc Clin Oncol Pt I. 24:3013.
8. Ashkenazi A. Targeting death and decoy receptors of the tumour-necrosis factor superfamily. Nat Rev Cancer 2002;2:420–30.
9. Takeda K, Stagg J, Yagita H, Okumura K, Smyth MJ. Targeting death-inducing receptors in cancer therapy. Oncogene 2007;26:3745–57.
10. Kelley RF, Totpal K, Lindstrom SH, et al. Receptor-selective mutants of apoptosis-inducing ligand 2/tumor necrosis factor-related apoptosis-inducing ligand reveal a greater contribution of death receptor (DR) 5 than DR4 to apoptosis signaling. J Biol Chem 2005;280:2205–12.
11. Van der Sloot AM, Tur V, Szegezdi E, et al. Designed tumor necrosis factor-related apoptosis-inducing ligand variants initiating apoptosis exclusively via the DR5 receptor. Proc Natl Acad Sci U S A 2006;103:8634–9.
12. Horak P, Pils D, Haller G, et al. Contribution of epigenetic silencing of tumor necrosis factor-related apoptosis inducing ligand receptor 1 (DR4) to TRAIL resistance and ovarian cancer. Mol Cancer Res 2005;3:335–43.
13. Ouellet V, Le PC, Madore J, et al. An apoptotic molecular network identified by microarray: on the TRAIL to new insights in epithelial ovarian cancer. Cancer 2007;110:297–308.
14. Siervo-Sassi RR, Marrangoni AM, Feng X, et al. Physiological and molecular effects of Apo2L/TRAIL and cisplatin in ovarian carcinoma cell lines. Cancer Lett 2003;190:61–72.
15. Petignat P, du BA, Bruchim I, Fink D, Provencher DM. Should intraperitoneal chemotherapy be considered as standard first-line treatment in advanced stage ovarian cancer? Crit Rev Oncol Hematol 2007;62:137–47.
16. Armstrong DK, Bundy B, Wenzel L, et al. Intraperitoneal cisplatin and paclitaxel in ovarian cancer. N Engl J Med 2006;354:34–43.
17. Ling J, Herbst RS, Mendelson DS, et al. Apo2L/TRAIL pharmacokinetics in a phase Ia trial in advanced cancer and lymphoma. J Clin Oncol 2006; Proc Am Soc Clin Oncol Pt I. 24:3047.
18. Shaw TJ, Senterman MK, Dawson K, Crane CA, Vanderhyden BC. Characterization of intraperitoneal, orthotopic, and metastatic xenograft models of human ovarian cancer. Mol Ther 2004;10:1032–42.
19. Van Geelen CM, de Vries EG, Le TK, van Weeghel RP, de Jong S. Differential modulation of the TRAIL receptors and the CD95 receptor in colon carcinoma cell lines. Br J Cancer 2003;89:363–73.
20. Ashkenazi A, Pai RC, Fong S, et al. Safety and antitumor activity of recombinant soluble Apo2 ligand. J Clin Invest 1999;104:155–62.
21. Bradford MM. Rapid and sensitive method for quantitation of microgram quantities of protein utilizing principle of protein-dye binding. Anal Biochem 1976;72:248–54.
22. Hougardy BM, Maduro JH, van der Zee AG, et al. Proteasome inhibitor MG132 sensitizes HPV-positive human cervical cancer cells to rhTRAIL-induced apoptosis. Int J Cancer 2006;118:1892–900.
23. Los G, Mutsaers PH, van der Vijgh WJ, Baldew GS, de Graaf PW, McVie JG. Direct diffusion of *cis*-diamminedichloroplatinum(II) in intraperitoneal rat tumors after intraperitoneal chemotherapy: a comparison with systemic chemotherapy. Cancer Res 1989;49:3380–4.
24. Van Hennik MB, van der Vijgh WJ, Klein I, et al. Comparative pharmacokinetics of cisplatin and three analogues in mice and humans. Cancer Res 1987;47:5297–301.
25. MacFarlane M, Kohlhaas SL, Sutcliffe MJ, Dyer MJ, Cohen GM. TRAIL receptor-selective mutants signal to apoptosis via TRAIL-R1 in primary lymphoid malignancies. Cancer Res 2005;65:11265–70.
26. MacFarlane M, Inoue S, Kohlhaas SL, et al. Chronic lymphocytic leukemic cells exhibit apoptotic signaling via TRAIL-R1. Cell Death Differ 2005;12:773–82.
27. Chinnaiyan AM, Prasad U, Shankar S, et al. Combined effect of tumor necrosis factor-related apoptosis-inducing ligand and ionizing radiation in breast cancer therapy. Proc Natl Acad Sci U S A 2000;97:1754–9.
28. Liu X, Yue P, Khuri FR, Sun SY. p53 upregulates death receptor 4 expression through an intronic p53 binding site. Cancer Res 2004;64:5078–83.
29. Takimoto R, El Deiry WS. Wild-type p53 transactivates the KILLER/DR5 gene through an intronic sequence-specific DNA binding site. Oncogene 2000;19:1735–43.
30. Meng RD, El Deiry WS. p53-Independent upregulation of KILLER/DR5 TRAIL receptor expression by glucocorticoids and interferon-gamma. Exp Cell Res 2001;262:154–69.
31. Nagane M, Pan GH, Weddle JJ, et al. Increased death receptor 5 expression by chemotherapeutic agents in human gliomas causes synergistic cytotoxicity with tumor necrosis factor-related apoptosis-inducing ligand *in vitro* and *in vivo*. Cancer Res 2000;60:847–53.
32. Arts HJ, de Jong S, Hollema H, et al. Chemotherapy induces death receptor 5 in epithelial ovarian carcinoma. Gynecol Oncol 2004;92:794–800.
33. Kischkel FC, Lawrence DA, Chuntharapai A, et al. Apo2L/TRAIL-dependent recruitment of endogenous FADD and caspase-8 to death receptors 4 and 5. Immunity 2000;12:611–20.
34. Bouralexis S, Findlay DM, Atkins GJ, et al. Progressive resistance of BTK-143 osteosarcoma cells to Apo2L/TRAIL-induced apoptosis is mediated by acquisition of DcR2/TRAIL-R4 expression: resensitisation with chemotherapy. Br J Cancer 2003;89:206–14.
35. Merino D, Lalaoui N, Morizot A, et al. Differential inhibition of TRAIL-mediated DR5-DISC formation by decoy receptors 1 and 2. Mol Cell Biol 2006;26:7046–55.
36. Lee H-W, Lee S-H, Lee H-W, Ryu Y-W, Kwon M-H, Kim Y-S. Homomeric and heteromeric interactions of the extracellular domains of death receptors and death decoy receptors. Biochem Biophys Res Commun 2005;330:1205–12.
37. Held J, Schulze-Osthoff K. Potential and caveats of TRAIL in cancer therapy. Drug Resist Updat 2001;4:243–52.
38. Hofstra LS, de Vries EG, Mulder NH, Willemse PH. Intraperitoneal chemotherapy in ovarian cancer. Cancer Treat Rev 2000;26:133–43.
39. Xiang H, Nguyen CB, Kelley SK, Dybdal N, Escandon E. Tissue distribution, stability, and pharmacokinetics of Apo2 ligand/tumor necrosis factor-related apoptosis-inducing ligand in human colon carcinoma COLO 205 tumor-bearing nude mice. Drug Metab Dispos 2004;32:1230–8.
40. Flessner MF, Choi J, Credit K, Deverkadra R, Henderson K. Resistance of tumor interstitial pressure to the penetration of intraperitoneally delivered antibodies into metastatic ovarian tumors. Clin Cancer Res 2005;11:3117–25.

BIOCHEMISTRY
including biophysical chemistry & molecular biology

Article

Enhancement of Antitumor Properties of rhTRAIL by Affinity Increase toward its Death Receptors

Carlos R. Reis, Almer M. van der Sloot, Eva Szegezdi, Alessandro Natoni, Vicente Tur, Robbert H. Cool, Afshin Samali, Luis Serrano, and Wim J. Quax

Biochemistry, **2009**, 48 (10), 2180-2191• DOI: 10.1021/bi801627x • Publication Date (Web): 23 February 2009

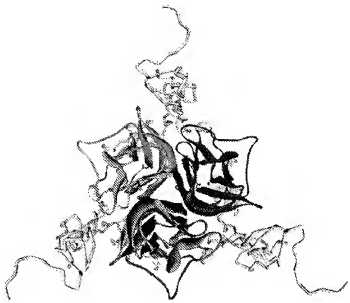

Enhancement of Antitumor Properties of rhTRAIL by Affinity Increase toward Its Death Receptors†

Carlos R. Reis,[‡,§] Almer M. van der Sloot,[‡,||] Eva Szegezdi,[⊥,#] Alessandro Natoni,[⊥] Vicente Tur,[||] Robbert H. Cool,[‡,▽] Afshin Samali,[⊥] Luis Serrano,[○] and Wim J. Quax*[,‡]

Department of Pharmaceutical Biology, University of Groningen, Antonius Deusinglaan 1, 9713 AV, Groningen, The Netherlands, Centre for Genomic Regulation, CRG-EMBL Systems Biology Unit, Dr. Aiguader 88, 08003, Barcelona, Spain, Department of Biochemistry and National Centre for Biomedical Engineering Science, National University of Ireland, Galway, Ireland, Trixtel Therapeutics BV, Antonius Deusinglaan 1, 9713 AV, Groningen, The Netherlands, and Institució Catalana de Recerca I Estudis Avançats (ICREA), Centre for Genomic Regulation (CRG), EMBL/CRG Systems Biology Research Unit, Universitat Pompeu Fabra, Dr. Aiguader 88, 08003 Barcelona, Spain

Received October 14, 2008; Revised Manuscript Received January 8, 2009

ABSTRACT: Tumour necrosis factor-related apoptosis-inducing ligand (TRAIL) is a potent and selective inducer of apoptosis in various tumor types, raising enthusiasm for TRAIL as a potential anticancer agent. TRAIL-induced apoptosis is mediated by death receptors 4 (DR4) and DR5. The design of rhTRAIL variants either with improved affinity or selectivity toward one or both death-inducing receptors is thought to enhance the therapeutical potential of TRAIL. Here we demonstrate that a single amino acid mutation at the position of glycine 131 to lysine or arginine in wild-type rhTRAIL significantly improved the affinity of rhTRAIL toward its death receptors, with the highest affinity increase observed for the DR4 receptor. These variants were able to induce higher *in vitro* levels of apoptosis in cancer cells responsive to only DR4 or to both death receptors and could therefore increase the potential use of rhTRAIL as an anticancer therapeutic agent.

Targeting and activation of death receptors belonging to the tumor necrosis factor (TNF)[1]receptor family open a window to a unique therapeutic strategy by extrinsically inducing p53-independent apoptosis in cancer cells (*1*). Tumor necrosis factor (TNF) related apoptosis-inducing ligand (TRAIL) is attracting great interest as a potential anticancer therapeutic agent because of its ability to selectively trigger receptor-mediated apoptosis in cancer cells but not in normal cells (*2*, *3*).

TRAIL is unique within the TNF ligand family as it interacts with an intricate receptor system consisting of two apoptosis-inducing or agonistic death receptors, death receptor 4 (DR4/TRAIL-R1) and death receptor 5 (DR5/TRAIL-R2), and three antagonistic or decoy receptors, decoy receptor 1 (DcR1/TRAIL-R3), decoy receptor 2 (DcR2/TRAIL-R4), and the soluble receptor osteoprotegerin (OPG) (*4*). Binding of TRAIL to the two apoptosis-inducing receptors (DR4 and DR5) leads to recruitment of Fas-associated death domain (FADD) (*5*−*7*), which in turn allows binding and activation of the initiator caspases-8 and -10 and induction of apoptosis (*8*−*10*). DcR1 and DcR2 lack a death domain or contain a truncated death domain, respectively. Thus, binding of TRAIL to these receptors does not induce apoptosis but could instead prevent apoptosis by sequestering available TRAIL or by interfering with the formation of a TRAIL-DR4 or -DR5 signaling complex (*11*). Recently, it was demonstrated that DcR2 is not merely a decoy receptor. DcR2 was shown to inhibit DR5-mediated apoptosis through ligand-independent association with DR5 via the preligand assembly domain (PLAD) (*12*) or to inhibit TRAIL-DR5 signaling in a ligand-dependent fashion by forming heteromeric ligand−receptor complexes (*13*). In addition, it is clear that the sensitivity toward this apoptosis signaling pathway is not defined solely by these components, since cell surface expression of the decoy receptors does not necessarily correlate with sensitivity of tumor cells to TRAIL (*14*).

Although TRAIL signals via DR4 and DR5, many studies suggest that DR5 is the primary receptor leading to apoptosis (*14*−*17*). In this light, it is perhaps expected that DR5 is the highest affinity receptor of TRAIL (*18*, *19*). However, it has been recently shown that in primary cells from patients with chronic lymphocytic leukemia and mantle cell lymphoma the death-mediating receptor is DR4, not DR5 (*20*, *21*).

† This research was partly funded by European Union Fifth Framework Program Grant QLK3-CT 2001-00498 and Sixth Framework Program Grant LSH-2005-2.2.0-2. R.H.C. was in part supported by the Technology Foundation STW, Applied Science Division of NWO, and the technology program of the Dutch Ministry of Economic Affairs.

* To whom correspondence should be addressed. E-mail: w.j.quax@rug.nl. Phone: +3150 363 2558. Fax: +3150 363 3000.

‡ These authors contributed equally to this work.

§ Department of Pharmaceutical Biology, University of Groningen.

|| Centre for Genomic Regulation, Barcelona.

⊥ Department of Biochemistry, National University of Ireland.

Trixtel Therapeutics BV, Groningen.

○ Institució Catalana de Recerca I Estudis Avançats, Universitat Pompeu Fabra, Barcelona.

▽ Trixtel Therapeutics BV, Groningen.

[1] Abbreviations: TNF, tumor necrosis factor; TRAIL, TNF-related apoptosis-inducing ligand; DR4, death receptor 4; DR5, death receptor 5; SPR, surface plasmon resonance; ELISA, enzyme-linked immunosorbent assay.

10.1021/bi801927x CCC: $40.75
Published on Web 02/23/2009

Improving a high-affinity protein−protein interaction is a challenging problem that has practical implications in the development of protein-based therapeutics. Redesign of several protein−protein interactions have been successfully accomplished by using computational protein design methods in order to modify binding characteristics (*19*, *22*−*24*). Previously, we used computational protein design to generate DR5-selective TRAIL variants (*19*) and DR4-selective variants (*25*). Although DR4-selective variants showed an increase in specificity, the biological activity on DR4-responsive cells was lower when compared to wild-type rhTRAIL (*25*).

Designing a TRAIL variant having an increased binding affinity toward DR4 and unchanged (or increased) affinity toward DR5 could therefore be of therapeutic interest for TRAIL-sensitive cancer cells. Such a mutant would not differentiate between DR4- and DR5-sensitive tumor cells, allowing treatment of a broader range of cancer cells. In order to improve the efficiency of rhTRAIL, variants mediating apoptosis via DR4, we set out to improve the affinity for DR4 without emphasizing the selectivity aspect. Here we demonstrate that such an approach is feasible, having designed TRAIL variants containing a single mutation leading to an improved affinity for both DR4 and DR5. Replacement of glycine 131 to lysine or arginine was sufficient to increase the death-inducing potency of rhTRAIL, which led to a significant improvement in biological activity.

EXPERIMENTAL PROCEDURES

All reagents were of analytical grade unless specified otherwise. Isopropyl-*β*-D-1-thiogalactoside (IPTG), ampicillin, and dithiothreitol (DTT) were purchased from Duchefa. Chromatographic columns and media were from Amersham Biosciences. Restriction enzymes used were purchased from New England Biolabs. Recombinant TRAIL-receptor Ig fusion proteins were ordered from R&D Systems. Anti-caspase-3 and anti-caspase-8 were from Cell Signaling Technology. All other chemicals were from Sigma. All buffers used in SPR and ELISA or biological activity assays were of physiological pH and ionic strength.

Modeling of TRAIL−*Receptor Complexes.* At present only the crystal structure of TRAIL in complex with the DR5 receptor is known. The template selected was 1D4V (*26*), the structure at 2.2 Å resolution and of monomeric human TRAIL in complex with the ectodomain of DR5 (TRAIL-R2) receptor. The homotrimer was generated using the protein quaternary structure server from the EBI (http://pqs.ebi.ac.uk), having the symmetry coordinates in the PDB file. From the sequence alignment of the different TRAIL receptors it is observed that the receptor cysteine-rich domains (CRDs) involved in the interaction with TRAIL (CRD2 and CRD3) are highly conserved, with the exception of the soluble receptor OPG. Indeed, when compared to DR5, the sequence identity of any other membrane-attached TRAIL receptor is higher than 50% in each case, and there are neither insertions nor deletions in the sequence (with the exception of a glycine deletion in the middle of the CRD3 in DcR1). In addition, all of the cysteines involved in the formation of internal disulfide bridges are conserved and share the same sequence position. Thus, it was possible to build homology models of all TRAIL receptors except for OPG.

The homology model of TRAIL-DR4 was built using the protein design capabilities of FoldX. The DR5 amino acid residues were mutated into the corresponding DR4 amino acids, and subsequently, all amino acid side chain interactions were optimized in order to accommodate TRAIL and receptor residues to their new interface.

Computational Design of the Mutants. A detailed description of the empirical force field FoldX (version 3.0) is available elsewhere (*27*, *28*) (and at http://foldx.crg.es). Briefly, this force field calculates the free energy of unfolding (ΔG) of a target protein or protein complex combining the physical description of the interactions with empirical data obtained from experiments on proteins. Force field components (polar and hydrophobic solvation energies, van der Waals interactions, van der Waals clashes, H-bond energies, electrostatics in the complex and its effects on the k_{on} and backbone and side chain entropies) are calculated evaluating the properties of the structure, such as its atomic contact map, the accessibility of its atoms and residues, the backbone dihedral angles, the H-bond network, and the electrostatic network of the protein. Water molecules making two or more H-bonds with the protein are also taken into account (*29*).

FoldX is able to perform amino acid mutations and simultaneously accommodate the new residues and its surrounding amino acids (*28*). FoldX first mutates the selected position to alanine and annotates the side chain energies of the neighbor residues. Then it mutates this alanine to the selected amino acid and recalculates the side chain energies of the same neighboring residues. Those that exhibit an energy difference are then mutated to themselves to see if another rotamer will be more favorable.

This procedure was also used to reconstruct the binding interface of TRAIL in complex with the modeled DR4 receptor. In order to repair residues with bad torsion angles, residues having bad van der Waals clashes, or to build up the putative interactions between TRAIL and the modeled receptor, the most optimal amino acid conformation was chosen using rotamer substitution (see above). The crystal structure of TRAIL in complex with the DR5 receptor was also refined in this way.

Site-Directed Mutagenesis, Expression, and Purification of rhTRAIL Variants. cDNA corresponding to human soluble TRAIL (aa 114−281) was cloned in pET15b (Novagen) using *Nco*I and *Bam*HI restriction sites. Mutants were constructed by polymerase chain reaction (PCR) using the QuikChange site-directed mutagenesis (Stratagene) method. The polymerase used was *Pfu* Turbo supplied by Stratagene. Introduction of mutations was confirmed by DNA sequencing. Wild-type rhTRAIL and variants cloned into pET15b were transformed into *Escherichia coli* BL21(DE3). Homotrimeric TRAIL proteins were overproduced, and the harvested cells were resuspended in 3 mL/g of wet cells in extraction buffer [PBS, pH 8, 10% (*w*/*v*) glycerol, 7 mM *β*-mercaptoethanol]. Cells were disrupted using sonication, and extracts were clarified by centrifugation for 60 min at 40000*g*. Subsequently, the supernatant was loaded on a nickel-charged HisPrep FF 16/10 column (GE Healthcare), and wild-type TRAIL and TRAIL mutants were further purified by cation-exchange chromatography on a HiTrap SP HP column (GE Healthcare) as described before (*30*). Analytical gel filtration using a Hiload Superdex 75 16/60 column (GE Healthcare) (Supporting Information Figure S1).

dynamic light scattering, and nonreducing gel electrophoresis were used to confirm that wild-type TRAIL and variants were trimeric molecules, not forming higher degree aggregates and not containing interchain disulfide bridges. Purified protein solutions were flash frozen in liquid nitrogen and stored at −80 °C.

Determination of Receptor Binding by Surface Plasmon Resonance. Binding experiments were performed using a surface plasmon resonance-based biosensor Biacore 3000 (Biacore AB). Research grade CM5 sensor chips, *N*-hydroxysuccinimide (NHS), *N*-ethyl-*N*′-(3-diethylaminopropyl)carbodiimide (EDC), ethanolamine hydrochloride, and standard buffers, e.g., HBS-N and HBS-EP, were purchased from the manufacturer. All of the buffers were filtered and degassed. Immobilization of DR4-Ig and DR5-Ig receptors (R&D Systems) on the sensor surface of a Biacore CM5 sensor chip was performed following a standard amine coupling procedure according to the manufacturer's instructions. Receptors were coated at a level of ~800 response units. Activated, coupled surfaces were then quenched of reactive sites with 1 M ethanolamine (pH 8). Reference surfaces consisted of activated CM dextran, subsequently blocked with ethanolamine. A 50 μL aliquot of TRAIL and variants was injected in 3-fold at concentrations ranging from 250 to 0.5 nM at 70 mL/mL and at 37 °C using HBS-N supplemented with 0.005% surfactant P20 (Biacore) as running and sample buffer. Binding of ligands to the receptors was monitored in real time. Between injections the receptor/sensor surface was regenerated using 1:1 10 mM glycine, 1.5 M NaCl, pH 2:ethylene glycol and a contact time of 30 s.

Determination of Receptor Binding by ELISA and Competitive ELISA Assay. To estimate the fold difference in affinity of mutants versus wild-type rhTRAIL, we used a competitive ELISA in addition to ELISA assay. Nunc maxisorb plates were coated for 2 h with DR4-Ig (100 ng per well) in 0.1 M sodium carbonate/bicarbonate buffer (pH 8.6), and the remaining binding places were subsequently blocked with 2% BSA for 1 h. After being washed for six times with Tris-buffered saline/0.5% Tween 20 (TBST) (pH 7.5), serial dilutions of soluble DR4-, DR5-, DcR1-, or DcR2-Ig (0−500 ng per well) and wild-type rhTRAIL or mutants (10 ng per well) in PBS (pH 7.4) preincubated for 1 h at room temperature were added to the wells and incubated for 1 h at room temperature. For the ELISA assay serial dilutions of wild-type rhTRAIL and variants (0−1000 ng per well) were added to the well coated with DR4-Ig and DR5-Ig and incubated at room temperature for 1 h. After being washed for six times with TBST, a 1:200 dilution of anti-TRAIL antibody (R & D Systems) was added and incubated for 1 h at room temperature, and, after being washed six times with TBST, subsequently incubated with a 1:25000 dilution of a horse radish peroxidase-conjugated swine anti-goat antibody. After being washed six times with TBST, 100 μL of 1-step Turbo TMB solution (Pierce) was added, and after 20 min, the reaction was quenched with 100 μL of 1 M sulfuric acid. The absorbance was measured at 450 nM on a microplate reader (Thermo Labsystems). Binding of rhTRAIL or variants to immobilized DR4-Ig with 0 ng per well of the soluble receptors was taken as 100%, and binding at other concentrations of soluble receptors was calculated relative to 0 ng per well of soluble receptor.

Cell Line and Treatment. Colon carcinoma Colo205 and HCT15, BxPC pancreatic carcinoma, ML-1 acute myeloid leukemia, EM-2 chronic myelogenous leukemia, and Burkitt's lymphoma BJAB cell lines were maintained in RPMI1640 medium, supplemented with 10% FBS, 50 units/mL penicillin, 5 mg/mL streptomycin, 2 mM L-glutamine, and 1 mM sodium pyruvate in a humidified incubator at 37 °C and 5% CO_2 environment. HepG2 hepatocellular carcinoma cells were cultured in DMEM, with 10% FBS, 50 units/mL penicillin, 5 mg/mL streptomycin, and glutamine. Colon carcinoma SW948 cells were cultured in Leibovitz L15-RPMI 1640 (1:1) enriched with 10% FBS, 0.05 M pyruvate, 0.1 M glutamine, and 0.025% β-mercaptoethanol at 37 °C in a humidified atmosphere with 5% CO_2. Human dermal fibroblasts were grown in low glucose DMEM (Sigma) supplemented with 10% fetal calf serum, 50 units/mL penicillin, and 5 mg/mL streptomycin; human umbilical vein endothelial cells (HUVEC, PromoCell) were cultured in endothelial cell growth medium with SupplementMix (PromoCell). All cells were seeded at 50% confluency 24 h prior to treatment. Cells were cultured in a humidified atmosphere at 37 °C and 5% CO_2 and treated with recombinant human TRAIL or rhTRAIL variants G131K and G131R.

Annexin V Staining. Cells were seeded the day before the experiment in 24-well plates (0.5 mL/well) for ML-1, EM-2, HCT15, BxPC, and HepG2 cell types. Wild-type rhTRAIL, G131R, or G131K (5−250 ng/mL) was added to the cells and incubated for 24 h. Cells were transferred into Eppendorf tubes and spun down. Cell pellets were resuspended in 50 μL of annexin V incubation buffer (10 mM HEPES/NaOH, pH 7.4, 140 mM NaCl, 2.5 mM $CaCl_2$) containing 6 μL of annexin V-fluorescein isothiocyanate (IQ Corp.) for 15 min on ice. The reaction was stopped by adding 300 μL of fresh incubation buffer, and the samples were analyzed immediately using a FACSCalibur flow cytometer (BD Biosciences). Results were expressed as percentage of annexin V-positive cells.

Cytotoxicity and Caspase Activity. BJAB, Colo205, and SW948 cells were seeded in 96-well plates the day before the experiment. Ligands (wild-type rhTRAIL and Gly-131 variants) were serially diluted in cell culture medium (1.5−100 ng/mL) and then added to each well of a 96-well tissue culture microplate (Greiner) containing cells. Mixtures were incubated for 24 h at 37 °C in a humidified atmosphere containing 5% CO_2. Subsequently, 20 μL of MTS (Promega) reagent was added. Cell viability was determined after 1 h of incubation by measuring the absorption at 490 nm on a microplate reader (Thermo Labsystems). BJAB cell lines were incubated with concentrations ranging from 1.5 to 100 ng/mL TRAIL or variants in the presence of 0.33 μg/mL cycloheximide (Sigma) or without cycloheximide for the $BJAB^{WT}$ cell line. Caspase activity was determined using a Caspase-Glo 3/7 assay (Promega) in a 96-well plate. SW948 colon carcinoma cells were plated in a 96-well plate and treated with wild-type rhTRAIL and Gly-131 variants (100 ng/mL) for 20 h or left untreated. The Caspase-Glo 3/7 reagent was added to wells, and luminescence was recorded at 1 h with a luminometer.

For immunoblotting, ML-1 cells were seeded in 6-well plates at the usual density. After treatment with rhTRAIL and the Gly-131 variants and pretreatment with z-VAD.fmk (Enzyme Systems Products), the cells were harvested, and

cells were used for annexin V assay, and the rest were washed once in PBS and lysed in 100 μL of lysis buffer (1% Triton X, 10% glycerol, 150 mM NaCl, 20 mM Tris-HCl, pH 7.6). Cells were incubated on ice for 5 min and then spun down for 5 min. The supernatant was collected, and protein concentration was determined by the BCA method (Pierce). Thirty micrograms of proteins was loaded onto 12% SDS−PAGE. After electrophoresis, proteins were transferred into a polyvinylidene fluoride membrane. The membrane was blocked for 1 h at room temperature in blocking buffer (5% nonfat dry milk in PBS/0.05% Tween 20) and incubated overnight with rabbit anti-caspase-3 polyclonal antibody at 4 °C (1:500 in blocking buffer). The membrane was then washed three times for 5 min in washing buffer (PBS/0.05% Tween 20) and incubated with goat anti-rabbit IgG HRP-conjugated secondary antibody (Pierce) for 1 h at room temperature in blocking buffer. After incubation, the membrane was washed three times in washing buffer and once in PBS for 5 min. The membrane was developed using SuperSignal West Pico chemiluminescent substrate (Pierce) according to the manufacturer's instructions.

Western Blotting. For antigen detection membranes were incubated with antibodies to actin (1:500, Sigma) and caspase-3 and -8 (1:500, Cell Signaling Technologies) overnight at 4 °C followed by 2 h incubation at room temperature with appropriate secondary antibodies (1:5000; Pierce). Protein bands were visualized using Supersignal Ultra chemiluminescent substrate (Pierce) on X-ray film (Agfa).

RESULTS

Design of High-Affinity TRAIL−Death Receptor Complexes. Several crystal structures of TRAIL in complex with the DR5 receptor are available (*26*, *31*, *32*), while the crystal structure of TRAIL in complex with the DR4 receptor is still not determined. Consequently, a TRAIL-DR4 homology model was constructed based on the crystal structure of the TRAIL-DR5−receptor complex with PDB coordinates 1D4V (*26*) as described before (*19*, *25*). We previously validated the constructed TRAIL-DR4 model and the FoldX design process with experimentally available mutant data (*19*, *25*). The TRAIL-DR5 and TRAIL-DR4 structural models were used in the FoldX design process to screen the receptor binding interface of TRAIL for single amino acid substitutions that would increase the affinity for the DR4 receptor (decreasing interaction energy ($\Delta\Delta G_i$)) in concert with an increased or unchanged affinity for DR5.

The FoldX *in silico* screening of the TRAIL receptor binding interface yielded several amino acid positions and (single) amino acid substitutions for enhancement of DR4 and DR5 binding affinity. From this screen, a mutant with a single amino acid replacement of glycine at position 131 to arginine appeared to be of particular interest. This variant was predicted to have increased affinity for both DR4 and DR5. Mutating to Lys instead of Arg was predicted to be less favorable, showing a smaller increase in affinity for DR4 and unchanged affinity for DR5 (Figure 1A). Models of TRAIL in complex with DcR1 and DcR2 were constructed, and the effect of the G131R and G131K mutations on binding affinity toward decoy receptors 1 and 2 was assessed. These models predicted both G131R and G131K to increase or maintain the binding affinity of TRAIL toward DcR1 and DcR2.

Structural Basis for the Changes in Affinity. In the TRAIL-DR5 crystal structure (PDB coordinates 1D4V) Gly-131 is located at the N-terminal part of the AA″ loop between two arginines (Arg-130 and Arg-132), and its Cα is in close proximity to Cγ and Cδ of Arg-118 of the DR5 receptor (Figure 1B,C). The side chain conformation of Arg-118 is stabilized through an intrachain hydrogen bond interaction with Gln-101 of the receptor. The equivalent position to Arg-118 of DR5 in the DR4 receptor is Ala-169 (and Gln-101 of DR5 is Val-152 in DR4), and compared to the TRAIL-DR5 complex, this results in a pocket around position Gly-131 in the TRAIL-DR4 complex. Structural alignment of individual TRAIL and DR5 receptors present in the asymmetric crystal cell units from available crystal structures of TRAIL-DR5 complexes (1D4V, 1D0G, and 1DU3, respectively) reveals considerable structural heterogeneity in the region surrounding residue Gly-131 (Figure 1C). The AA″ loop is very flexible, and the position of the Gly-131 Cα in 1D0G and 1DU3 differs up to 8 Å when compared to the Cα position in 1D4V, and the side chain of Arg-118 of DR5 also shows a wide range of conformations. For the design process the highest resolution structure of a TRAIL-DR5 complex (1D4V) was used as a template, and this structure is also the only that has a complete AA″ loop. The φ,ψ angles of Gly-131 are within the allowed region of the Ramachandran plot.

Upon mutating Gly-131 to Arg, the Arg-131 side chain in the G131R-DR4 complex forms an intermolecular hydrogen bond in the G131R-DR4 complex bond with the main chain oxygen of Gly-151 of DR4 and partially fills the pocket (Figure 2B). In the G131R-DR5 complex, the side chain of Arg-118 moves out of the interface, and Arg-131 establishes a double interchain hydrogen bond with the Gly-100 main chain oxygen of DR5 and fills up the pocket (Figure 2A). In the case of the G131K substitution, the Arg-118 side chain of DR5 moves out of the interface as well, and in both DR4 and DR5 complexes Lys-131 occupies the pocket (Figure 2). In contrast to the G131R substitution, G131K does not seem to establish any hydrogen bond interaction with residues from the DR4 or DR5 receptor. In opposition to what might be expected from creating a highly charged patch on the surface of TRAIL (Arg-130, Arg/Lys-131, Arg-132) by substituting Gly-131 with Arg or Lys, the contribution of electrostatics to the gain in interaction energy is negligible. Decomposing the FoldX interaction energy term reveals that rather hydrophobic solvation and an increase in van der Waals interactions account for most of the gain in interaction energy. The gain in interaction energy due to hydrogen bond formation of Arg-131 with the DR4 and DR5 receptors is almost completely counterbalanced because of a large entropic penalty. However, the ability to participate in hydrogen bond formation with the DR4 and DR5 receptors causes the G131R variant to be slightly more favorable than the G131K variant. As can be appreciated from Figure 1C the conformational freedom of Arg-118 of the DR5 receptor is considerable; the entropic cost of forcing this Arg-118 into another conformation(s) is one of the main reasons for the predicted increase in affinity of G131R and G131K variants for DR4 compared to DR5.

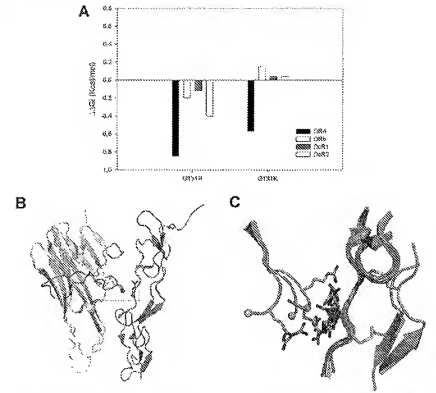

FIGURE 1: Binding energy predictions and structural overview of area surrounding Gly-131. (A) Predicted difference in binding energy (ΔΔG) of Gly-131 variants binding to different death receptors when compared with wild-type rhTRAIL, as determined by FoldX. The change in energy is measured in kcal/mol and applies to the change of a single binding interface bound to a single receptor. A negative ΔΔG indicates an improvement in receptor binding, and a positive ΔΔG indicates a decrease in receptor binding. (B) Ribbon drawing of a monomer TRAIL subunit (114−281) and DR5 monomer showing the various β strands and loops and the location of position G131 (blue box). (C) Structure heterogeneity around position 131 between different monomer TRAIL structures (left) and monomer DR5 structures (right) of known PDB coordinates for TRAIL or TRAIL-DR5 (PDB coordinates 1D0G in cyan, 1DU3 in green, and 1D4V in purple). Depicted are Arg130 of TRAIL and the Cα of Gly-131 (orange sphere) together with Arg118 of the DR5 receptor.

The binding pocket of the DcR1 and DcR2 receptor is more similar to that of the DR4 than of the DR5 receptor: the positions equivalent to Gln-101 and Arg-118 in DR5 are valines in both DcR1 and DcR2 (data not shown). The absence of Arg in DcR1 and DcR2 at the position equivalent to Arg118 in DR5 results in no additional entropic cost upon mutation of Gly-131 toward Arg or Lys, thus resulting in interactions similar to the one observed in the TRAIL-DR4 complex.

Receptor Binding of rhTRAIL Variants. Binding of the purified ligands to immobilized DR4-Ig and DR5-Ig receptor chimeras was assessed in real time using surface plasmon resonance (SPR). Receptor binding curves were recorded using rhTRAIL concentrations ranging from 0.5 to 250 nM at 37 °C (Figure 3A,B). Apparent dissociation constants were calculated from pre-steady-state response values (Table 1). Data were fitted using a standard four-parameter equation. Both variants G131R and G131K showed ~3- and ~1.7-fold increase in apparent affinity for binding to DR4-Ig, respectively, mainly due to a higher association to the directly immobilized receptors DR4-Ig (Supporting Information Figure S2). The increase in affinity to DR5-Ig was slightly more modest with ~2.4- and 1.5-fold increase in apparent affinity to immobilized DR5-Ig for G131R and G131K, respectively. ELISA assays confirmed the increase in affinity toward both death receptors. Receptor response curves were recorded using rhTRAIL concentrations ranging from 0 to 1000 ng per well (Figure 3C,D), with both variants displaying an approximate 3-fold increase in affinity toward DR4 (Figure 3C, Table 1). Similarly to the SPR assay we observed for both variants a smaller increase in affinity for DR5 than for DR4 (Figure 3D, Table 1). An increase in apparent affinity was also observed to the decoy receptors DcR1- and DcR2-Ig as measured by SPR (Supporting Information Figure S3).

To assess the binding preference of the Gly-131 variants, a competitive ELISA assay was performed using coated DR4-Ig plates and competitive soluble receptors DR4-, DR5-, DcR1-, and DcR2-Ig (Figure 4). Soluble DR4-Ig was shown to be very efficient in reducing the binding of the variants G131R and G131K (by ~7-fold) when compared to wild-type rhTRAIL (Figure 4A), indicating an increased affinity to soluble competitive DR4-Ig leading to a lower binding to immobilized DR4-Ig. Soluble DR5-Ig was less efficient than DR4-Ig in neutralizing binding of the Gly-131 variants, however, with a nearly similar competitive behavior as observed for wild-type rhTRAIL (Figure 4B). DcR1-Ig was also able to compete for binding of the variants to DR4-Ig with an almost 3-fold reduction in binding when compared with wild-type rhTRAIL (Figure 4C). A nearly equivalent ratio was observed for wild-type rhTRAIL and variants for DcR2-Ig competition to DR4-Ig binding, with the variants

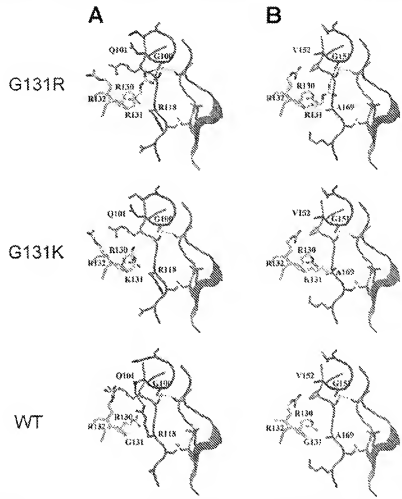

FIGURE 2: Structural impressions of the area around 131 for wild-type rhTRAIL and Gly-131 variants as determined by FoldX: (A) TRAIL-DR5 and (B) TRAIL-DR4.

showing a very small decrease in binding to soluble DcR2-Ig when compared with wild-type rhTRAIL (Figure 4D).

Taken together, these results indicate an increased affinity toward both death receptors DR4-Ig and DR5-Ig, with the highest increase observed for the lowest affinity death receptor DR4, confirming the prediction trend between DR4 and DR5 given by FoldX.

Biological Activity: Apoptotic Potential of rhTRAIL Variants in Cancer Cells. To examine the apoptotic potential of the G131 variants, a broad range of cell lines in which the TRAIL-death signal is transmitted by DR4, DR5, or both was tested. The sensitivity toward Gly-131 variants was assessed by comparing cell death induced by wild-type rhTRAIL and Gly-131 variants. Burkitt's lymphoma wild-type BJAB cells responsive to both DR4- and DR5-mediated cell death ($BJAB^{WT}$) and BJAB cells deficient in DR5 ($BJAB^{DR5\ DEF}$) (*33*) were tested first (Figure 5). In combination with 0.33 μg/mL cycloheximide, the variants G131R and G131K were able to induce an ~3-fold increase in cell death relative to wild-type rhTRAIL in wild-type BJAB cells (Figure 5A, Table 2). $BJAB^{DR5\ DEF}$ cells displayed markedly lower sensitivity to wild-type rhTRAIL, with a reduction in maximum cell death from 91% for wild-type BJAB to only 25% maximum cell death for the $BJAB^{DR5\ DEF}$ cell line (Figure 5B, Table 2). The Gly-131 variants retained a higher efficiency on the $BJAB^{DR5\ DEF}$ cell lines with a substantially augmented cell death induction (60% maximum cell death) when compared to wild-type rhTRAIL. In the absence of cycloheximide the Gly-131 variants were able to efficiently augment cell death in $BJAB^{WT}$ cell lines, reaching a maximum cell death induction of 56% against a maximum cell death induction of 36% for rhTRAIL WT (Figure 5C). No significant *in vitro* killing could be monitored using the same conditions for $BJAB^{DR5\ DEF}$ cells.

Study in colon carcinoma cell lines Colo205 and SW948 also showed that the mutants were able to induce significantly higher levels of cell death than wild-type rhTRAIL (Figure 6A,B). In Colo205 cells both DR4 and DR5 are functional, although in Colo205 cells DR5 is the predominant mediator of the TRAIL death signal (*19*). In contrast, in SW948 cells DR4 is the major mediator of TRAIL-induced apoptosis (*34*). As seen in Figure 6A,B, the Gly-131 variants could enhance cell death in both DR4- and DR5-sensitive colon carcinoma cell lines. The EC_{50} values and maximum cell death achieved by the variants versus wild-type rhTRAIL are listed in Table 2. Analysis of caspase (DEVDase) activity in SW948 cells showed a higher caspase activity induced by the Gly-131 variants (100 ng/mL) compared to wild-type rhTRAIL.

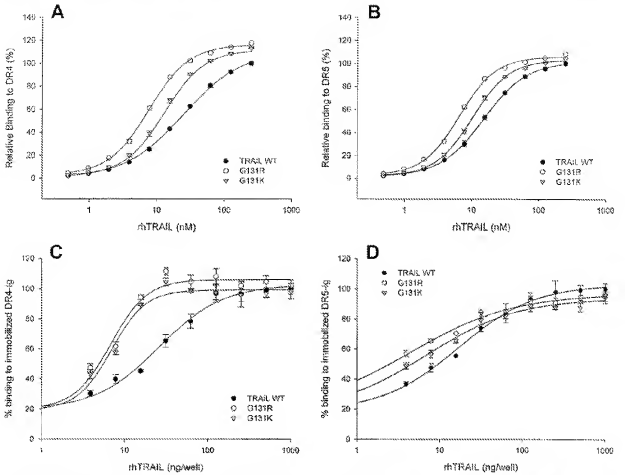

FIGURE 3: Receptor binding of wild-type rhTRAIL and Gly-131 variants as determined by SPR and ELISA. Receptor binding of wild-type rhTRAIL, G131R, and G131K to DR4-Ig as determined by SPR (A) or to DR5-Ig (B). To obtain pre-steady-state data that represent proper high-affinity complex formation, and assuming the initial fast off-rate to represent lower complexes, the response at each concentration was recorded 30 s after the end of the injections. Receptor binding was calculated relative to the response of wild-type rhTRAIL at 250 nM. (C) Receptor binding of wild-type rhTRAIL, G131R, and G131K to DR4-Ig as determined by ELISA or to DR5-Ig (D).

Table 1: Apparent DR4 and DR5 Binding Affinities of Wild-Type rhTRAIL, G131R, and G131K As Determined Using a Pre-Steady-State Approach by SPR and ELISA[a]

	SPR		ELISA	
protein	app K_D (nM), DR4	app K_D (nM), DR5	app K_D (nM), DR4	app K_D (nM), DR5
rhTRAIL WT	24.9 (±1.2)	17.8 (±1.8)	3.8 (±0.3)	2.5 (±0.2)
G131R	8.7 (±1.0)	7.9 (±1.3)	1.2 (±0.5)	0.9 (±0.4)
G131K	13.0 (±1.5)	12.3 (±1.8)	1.4 (±0.3)	1.2 (±0.3)

[a] Apparent K_D's were calculated using a four-parameter curve fitting tool.

confirming the stronger agonistic potential of the mutants (Figure 6C). In addition, HCT15 colon carcinoma, HepG2 hepatocellular carcinoma, and BxPC pancreatic carcinoma cells were examined (Figure 6D). On colon carcinoma HCT15 cells the Gly-131 were more effective only at low concentrations (5 and 10 ng/mL), whereas a similar apoptotic potential was observed at higher concentrations (Figure 6) (Supporting Information Figure S6). HepG2 cell type was the only cell type that did not display higher levels of apoptosis in comparison to rhTRAIL WT, whereas a significantly higher proapoptotic potential in BxPC cell lines was observed in comparison to wild-type rhTRAIL in almost all concentrations tested (Figure 6D).

ML-1 and EM-2 are acute myeloid leukemia and chronic myeloid leukemia cell lines, respectively, both cell lines solely DR4-responsive (*19*) (Figure 7A,B). The Gly-131 variants displayed a significantly higher proapoptotic potential in both leukemia cell lines in comparison to wild-type rhTRAIL. Supporting these results, in ML-1 cells G131R and G131K (100 ng/mL) induced a stronger processing of caspase-3 to its active p19/17 large subunits than wild-type rhTRAIL (100 ng/mL) (Supporting Information Figure S4). Processing of caspase-3 induced by G131R and G131K correlated with a higher percentage of cells with externalized phosphatidylserine compared to wild-type rhTRAIL (Supporting Information Figure S4). Pretreatment with the pan-caspase inhibitor of z-VAD.fmk (10 μM) almost completely prevented phosphatidylserine exposure and formation of the p19/17 large subunits, confirming the induction of a caspase-dependent apoptotic pathway.

Moreover, the variants were tested for activity on normal cells, namely, human nontransformed fibroblasts (hFB) from two different donors and human umbilical endothelial

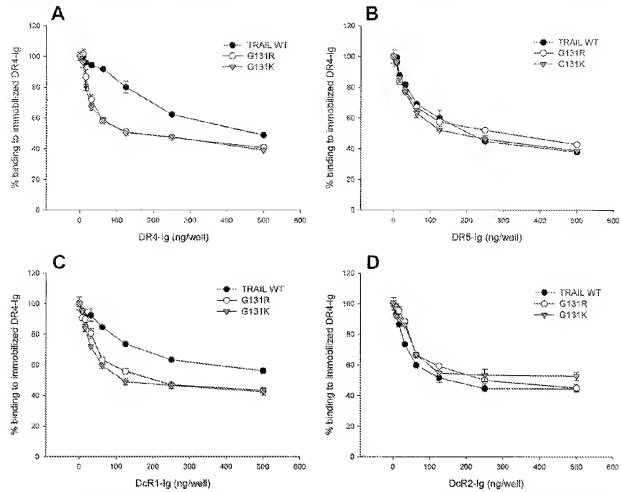

FIGURE 4: Competitive ELISA by TRAIL receptors of wild-type TRAIL and Gly-131 variants binding to immobilized DR4-Ig receptor using (A) soluble DR4-Ig as competitor, (B) soluble DR5-Ig as competitor, (C) soluble DcR1-Ig as competitor, or (D) soluble DcR2-Ig as competitor. Ten nanograms per well of wild-type rhTRAIL or Gly-131 variants was preincubated with 0–500 ng per well of DR4, DR5-Ig, DcR1-Ig, or DcR2-Ig for 1 h. Preincubated solutions were added to microuter plates coated with DR4-Ig. Binding of the selective variants at various concentrations of soluble receptor toward the immobilized DR4-Ig was calculated relative to the value measured on the presence of 0 ng per well of soluble receptor.

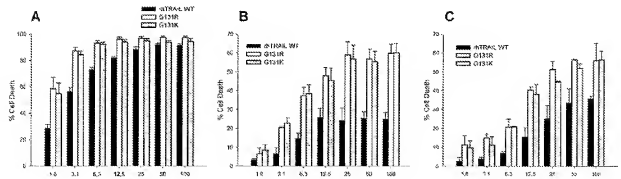

FIGURE 5: Cytotoxic potential (% cell death) of wild-type rhTRAIL or Gly-131 variants in BJAB cells responsive to both DR4- and DR5-mediated cell death ($BJAB^{WT}$) relative to cycloheximide control (0.33 μg/mL) (A), BJAB cells deficient for DR5 ($BJAB^{DR5\ DR5}$) relative to cycloheximide control (0.33 μg/mL) (B), and BJAB WT without cycloheximide (C). Cells were treated with wild-type rhTRAIL and Gly-131 variants or buffer control for 24 h. The percentage of cell death was calculated relative to the control wells containing no ligand. The data are the mean ± SEM of two independent experiments in triplicate.

Table 2: EC_{50} Values for BJAB WT, BJAB DR5 Deficient, Colo205, and SW948 cells[a]

	BJAB^{WT}		BJAB$^{DR5\,DEF}$		Colo205		SW948	
protein	EC_{50} (ng/mL)	max effect % cell death	EC_{50} (ng/mL)	max effect % cell death	EC_{50} (ng/mL)	max effect % cell death	EC_{50} (ng/mL)	max effect % cell death
rhTRAIL	2.8 ± 0.8	91 ± 2	5.48 ± 4	25 ± 3	9.8 ± 2.1	89.5 ± 5	11.9 ± 2.8	45 ± 2
G131R	1.0 ± 0.6	97 ± 3	4.7 ± 1.3	60 ± 4	6.1 ± 2.5	90.9 ± 4	3.15 ± 1.1	61 ± 4
G131K	1.1 ± 0.8	94 ± 3	4.4 ± 1.0	60 ± 5	7.5 ± 3.1	92.0 ± 4	7.0 ± 1.5	57 ± 3

[a] BJAB WT and BJAB DR5 deficient cells were treated in combination with 0.33 μg/mL cycloheximide. EC_{50} values were calculated using a four-parameter curve fitting tool.

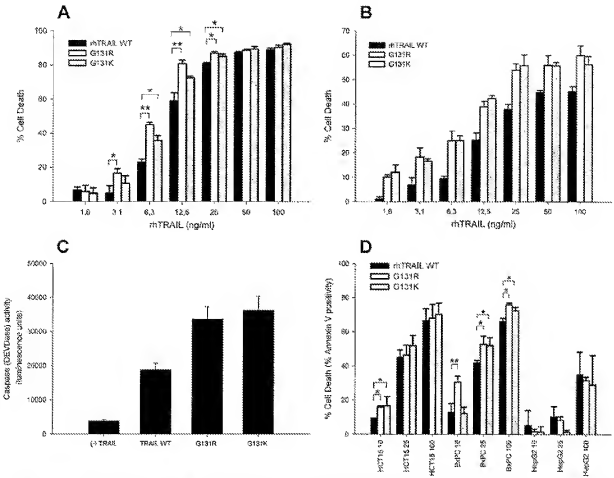

FIGURE 6: Sensitivity enhancement of cancer cell lines to TRAIL-induced apoptosis by Gly-131 variants on several cancer cell lines. Shown is the cytotoxic potential (% cell death) of wild-type rhTRAIL or Gly-131 variants in Colo205 colon carcinoma DR5 mediated cell line (A) and SW948 colon carcinoma DR4 mediated cell line (B). Cells were treated with wild-type rhTRAIL and Gly-131 variants or buffer control for 24 h. The percentage of cell death was calculated relative to the control wells containing no ligand. (C) Caspase (DEVDase) activity by wild-type rhTRAIL and variants G131R and G131K (100 ng/mL) after 20 h of treatment as measured by luminescence on SW948 cell lines. Apoptosis-inducing activity (annexin V staining) of wild-type rhTRAIL or Gly-131 variants in HCT15 colon carcinoma, BxPC pancreatic carcinoma, and HepG2 hepatocellular carcinoma (10, 25, and 100 ng/mL) (D). The results are mean values ± SEM ($n = 3$). Asterisks denote statistically significant differences (*, $P < 0.05$; **, $P < 0.001$) between the indicated pairs.

(HUVEC) cells. There was no significant difference in the response of the two donor hFB cell cultures. Neither of the Gly-131 variants nor rhTRAIL WT displayed significant activity on the cell lines studied, indicating that the increase in apoptotic activity had no effect on normal cells (Figure 7C,D).

Interestingly, a time-dependent incubation of ML-1 cells with the Gly-131 variants resulted in a faster caspase-8 activation, underlining their increased apoptotic activity (Supporting Information Figure S5).

Taken together, these results demonstrate that, by affinity enhancement primarily toward the death receptor 4, our variants could significantly potentiate the apoptotic property of TRAIL in a wide range of tumor cell lines.

DISCUSSION

TRAIL interacts with five receptors of the TNF-R family; however, only receptors DR4 and DR5 are able to induce apoptosis. From these two death receptors DR5 is the highest

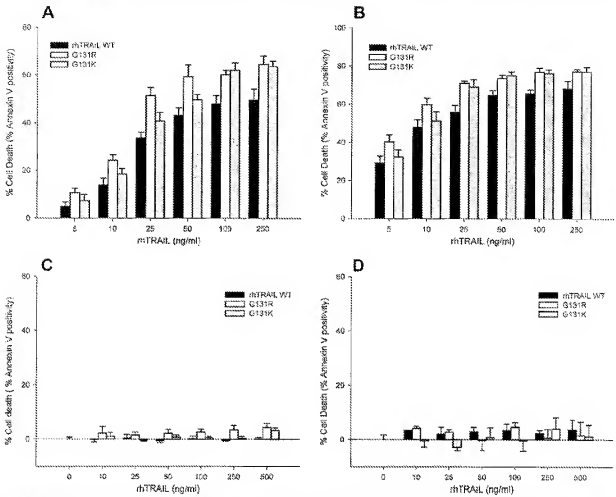

FIGURE 7: Apoptosis-inducing activity (annexin V staining) of wild-type rhTRAIL or Gly-131 variants in ML-1 chronic myeloid leukemia DR4 mediated cell line (A), EM-2 chronic myeloid leukemia DR4 mediated cell line (B), human umbilical vein endothelial cells (HUVEC) (C), and human primary, nontransformed fibroblasts (hFB) from two different donors (D). Cells were treated with the indicated concentrations of rhTRAIL WT, G131K, or G131R for 24 h after which induction of cell death was quantified with annexin V staining. The graph shows average percentage death induced ± SEM

affinity receptor (*18*, *19*, *25*) and the primary receptor leading to apoptosis. The difference in affinity for DR4 and DR5 may be a mechanism by which some cancer cells are more sensitive toward DR5-TRAIL-induced apoptosis.

As certain tumor cell lines appear to be only sensitive to DR4-mediated apoptosis, in particular certain leukemia and lymphoma tumors, and many other tumor cells are responsive to both DR4- and DR5-mediated apoptosis, we decided to design agonistic TRAIL variants by primarily increasing the affinity toward DR4 without drastically altering the affinity for DR5 and therefore increasing the general apoptotic potential of rhTRAIL.

Several DR4- and DR5-selective TRAIL variants have been developed in recent years using various methodologies; by using computational design (*19*, *25*), by employing directed evolution (*16*), or by a rational approach (*21*). The DR5-selective TRAIL variants have an increased affinity toward DR5 and significantly increased biological activity in appropriate DR5-sensitive cell lines when compared to wild-type rhTRAIL. In contrast, all previously developed DR4-selective TRAIL variants show a significantly reduced biological activity when compared to wild-type rhTRAIL. While the DR4-selective variant obtained by directed evolution showed an ~2-fold decrease in affinity for DR4 as measured by SPR (*16*), it was shown to be largely inactive in DR4-responsive Ramos cells (*21*). Changing one of the six amino acid mutations of this variant back to wild type restored biological activity although still being lower than wild-type rhTRAIL (*21*). In comparison, the DR4-selective variant generated by our group using computational protein design retained its affinity for the DR4 receptor with only small reduction of its proapoptotic potential (*25*). Nevertheless, at lower protein concentrations, all of the previously designed DR4-selective TRAIL variants were less active than wild-type rhTRAIL.

Therefore, in order to generate a TRAIL variant that is able to induce apoptosis more efficiently through DR4, we decided to focus on mutations that primarily improve the affinity toward DR4 and less on receptor specificity. The protein design algorithm FoldX identified in an *in silico* screen TRAIL G131R and G131K substitutions as promising ones in achieving this goal. Position 131 of TRAIL has not

been identified before as being important for receptor binding by the alanine scanning or phage display experiments (*16*, *32*).

Receptor binding experiments using SPR, ELISA, and competitive ELISA confirmed the design predictions, showing the highest gain in affinity for DR4 and a more modest affinity enhancement for DR5. It also confirmed that from the two variants constructed the G131R variant displayed the higher affinity for DR4 and DR5. The observed increase in affinity by mutations G131R and G131K for DcR1 and DcR2 is in accordance with the similar structural environment around position 131 as observed in TRAIL-DR4, TRAIL-DcR1, and TRAIL-DcR2 complexes. The absence of an Arg at the position equivalent to position 118 in DR5 explains why G131R and G131K have a higher affinity for DR4 and both of the decoy receptors than for DR5.

The G131R and G131K variants showed enhanced apoptosis-inducing activity in cell line assays. In both DR4- and DR5-responsive tumor cells, G131R and G131K variants showed a higher proapoptotic activity when compared to wild-type rhTRAIL. However, this effect was more pronounced in cells mainly responsive to DR4-mediated cell death. The increased maximum apoptotic activity of the variants in these cell lines suggests a clinical interest for these variants. Interestingly, although the G131R and G131K mutations also increased the affinity of TRAIL for DcR1 and DcR2 with the same magnitude as for DR4, this appears not to be important for the proapoptotic activity on the panel of cell lines tested. Given the reported differences in the affinity between decoy receptors and death-inducing TRAIL receptors (TRAIL has higher affinity toward the death-inducing receptors), at low concentrations TRAIL or the G131 variants probably preferentially bind to the death-inducing receptors and only at higher ligand concentrations do the decoy receptors get occupied. Due to this apparent, nonlinear correlation between decoy and death receptor expression and affinity, we hypothesize that the proapoptotic activity of TRAIL can be improved by simply improving its affinity for the death-inducing receptors (DR4, DR5) even if the affinity for decoy receptors also improves. Taken together, our designed variants show an enhanced apoptosis-inducing activity mediated through DR5 and, even more potently, through DR4.

In conclusion, these results show that it is possible to introduce new variations in rhTRAIL that significantly enhance its antitumor properties by increasing the affinity toward its death-inducing receptors.

ACKNOWLEDGMENT

We thank Dr. Andrew Thorburn (University of Colorado Health Sciences Center, Aurora, CO) for kindly providing the BJAB cell lines and Dr. Steven de Jong (University Medical Center, Groningen, The Netherlands) for providing the SW948 cell line and Francois Stricher (CRG, Barcelona) for helpful discussions regarding TRAIL design.

SUPPORTING INFORMATION AVAILABLE

Six figures which describe the gel filtration profile of variants constructed by mutagenesis, SPR sensorgrams for the death receptors, decoy receptor pre-steady-state curves, caspase-3 and caspase-8 activation in ML-1 cells, and apoptotic activity of variants on HCT15 and BxPc cells. This material is available free of charge via the Internet at http://pubs.acs.org.

REFERENCES

1. Ashkenazi, A. (2008) Targeting the extrinsic apoptosis pathway in cancer. *Cytokine Growth Factor Rev. 19*, 325–331.
2. Ashkenazi, A., Pai, R. C., Fong, S., Leung, S., Lawrence, D. A., Marsters, S. A., Blackie, C., Chang, L., McMurtrey, A. E., Hebert, A., DeForge, L., Koumenis, I. L., Lewis, D., Harris, L., Bussiere, J., Koeppen, H., Shahrokh, Z., and Schwall, R. H. (1999) Safety and antitumor activity of recombinant soluble Apo2 ligand. *J. Clin. Invest. 104*, 155–162.
3. Lawrence, D., Shahrokh, Z., Marsters, S., Achilles, K., Shih, D., Mounho, B., Hillan, K., Totpal, K., DeForge, L., Schow, P., Hooley, J., Sherwood, S., Pai, R., Leung, S., Khan, I., Gliniak, B., Bussiere, J., Smith, C. A., Strom, S. S., Kelley, S., Fox, J. A., Thomas, D., and Ashkenazi, A. (2001) Differential hepatocyte toxicity of recombinant Apo2L/TRAIL versions. *Nat. Med. 7*, 383–385.
4. LeBlanc, H. N., and Ashkenazi, A. (2003) Apo2L/TRAIL and its death and decoy receptors. *Cell Death Differ. 10*, 66–75.
5. Chaudhary, P. M., Eby, M., Jasmin, A., Bookwalter, A., Murray, J., and Hood, L. (1997) Death receptor 5, a new member of the TNFR family, and DR4 induce FADD-dependent apoptosis and activate the NF-kappaB pathway. *Immunity 7*, 821–830.
6. Kuang, A. A., Diehl, G. E., Zhang, J., and Winoto, A. (2000) FADD is required for DR4- and DR5-mediated apoptosis: lack of trail-induced apoptosis in FADD-deficient mouse embryonic fibroblasts. *J. Biol. Chem. 275*, 25065–25068.
7. Schneider, P., Thome, M., Burns, K., Bodmer, J. L., Hofmann, K., Kataoka, T., Holler, N., and Tschopp, J. (1997) TRAIL receptors 1 (DR4) and 2 (DR5) signal FADD-dependent apoptosis and activate NF-kappaB. *Immunity 7*, 831–836.
8. Bodmer, J. L., Holler, N., Reynard, S., Vinciguerra, P., Schneider, P., Juo, P., Blenis, J., and Tschopp, J. (2000) TRAIL receptor-2 signals apoptosis through FADD and caspase-8. *Nat. Cell Biol. 2*, 241–243.
9. Kischkel, F. C., Lawrence, D. A., Chuntharapai, A., Schow, P., Kim, K. J., and Ashkenazi, A. (2000) Apo2L/TRAIL-dependent recruitment of endogenous FADD and caspase-8 to death receptors 4 and 5. *Immunity 12*, 611–620.
10. Sprick, M. R., Weigand, M. A., Rieser, E., Rauch, C. T., Juo, P., Blenis, J., Krammer, P. H., and Walczak, H. (2000) FADD/MORT1 and caspase-8 are recruited to TRAIL receptors 1 and 2 and are essential for apoptosis mediated by TRAIL receptor 2. *Immunity 12*, 599–609.
11. Kimberley, F. C., and Screaton, G. R. (2004) Following a TRAIL: update on a ligand and its five receptors. *Cell Res. 14*, 359–372.
12. Chaney, L., Mruk, K., Archer, K., Woetfel, M., Mongkolsapaya, J., Screaton, G., Lenardo, M. J., and Chan, F. K. (2005) Pre-ligand assembly domain-mediated ligand-independent association between TRAIL receptor 4 (TR4) and TR2 regulates TRAIL-induced apoptosis. *Proc. Natl. Acad. Sci. U.S.A. 102*, 18099–18104.
13. Merino, D., Lalaoui, N., Morizot, A., Schneider, P., Solary, E., and Micheau, O. (2006) Differential inhibition of TRAIL-mediated DR5-DISC formation by decoy receptors 1 and 2. *Mol. Cell Biol. 26*, 7046–7055.
14. Ichikawa, K., Liu, W., Zhao, L., Wang, Z., Liu, D., Ohtsuka, T., Zhang, H., Mountz, J. D., Koopman, W. J., Kimberly, R. P., and Zhou, T. (2001) Tumoricidal activity of a novel anti-human DR5 monoclonal antibody without hepatocyte cytotoxicity. *Nat. Med. 7*, 954–960.
15. Ashkenazi, A., and Ashkenazi, A. (2003) Apo2L/TRAIL: apoptosis signaling, biology, and potential for cancer therapy. *Cytokine Growth Factor Rev. 14*, 337–348.
16. Kelley, R. F., Totpal, K., Lindstrom, S. H., Mathieu, M., Billeci, K., Deforge, L., Pai, R., Hymowitz, S. G., and Ashkenazi, A. (2005) Receptor-selective mutants of apoptosis-inducing ligand 2/tumor necrosis factor-related apoptosis-inducing ligand reveal a greater contribution of death receptor (DR) 5 than DR4 to apoptosis signaling. *J. Biol. Chem. 280*, 2205–2212.
17. Szegezdi, E., Cahill, S., Meyer, M., O'Dwyer, M., and Samali, A. (2006) TRAIL sensitisation by arsenic trioxide is caspase-8 dependent and involves modulation of death receptor components and Akt. *Br. J. Cancer 94*, 398–406.
18. Trunch, A., Sharma, S., Silverman, C., Khandekar, S., Reddy, M. P., Deen, K. C., McLaughlin, M. M., Srinivasula, S. M., Livi,

G. P., Marshall, L. A., Almenri, E. S., Williams, W. V., and Doyle, M. L. (2003) Temperature-sensitive differential affinity of TRAIL for its receptors. DR5 is the highest affinity receptor. *J. Biol. Chem. 275*, 23319–23325.

19. van der Sloot, A. M., Tur, V., Szegezdi, E., Mullally, M. M., Cool, R. H., Samali, A., Serrano, L., and Quax, W. J. (2006) Designed tumor necrosis factor-related apoptosis-inducing ligand variants initiating apoptosis exclusively via the DR5 receptor. *Proc. Natl. Acad. Sci. U.S.A. 103*, 8634–8639.
20. MacFarlane, M., Inoue, S., Kohlhaas, S. L., Majid, A., Harper, N., Kennedy, D. B., Dyer, M. J., and Cohen, G. M. (2005) Chronic lymphocytic leukemia cells exhibit apoptotic signaling via TRAIL-R1. *Cell Death Differ. 12*, 773–782.
21. MacFarlane, M., Kohlhaas, S. L., Sutcliffe, M. J., Dyer, M. J., and Cohen, G. M. (2005) TRAIL receptor-selective mutants signal to apoptosis via TRAIL-R1 in primary lymphoid malignancies. *Cancer Res. 65*, 11265–11270.
22. Kortemme, T., Joachimiak, L. A., Bullock, A. N., Schuler, A. D., Stoddard, B. L., and Baker, D. (2004) Computational redesign of protein-protein interaction specificity. *Nat. Struct. Mol. Biol. 11*, 371–379.
23. Reina, J., Lacroix, E., Hobson, S. D., Fernandez-Ballester, G., Rybin, V., Schwab, M. S., Serrano, L., and Gonzalez, C. (2002) Computer-aided design of a PDZ domain to recognize new target sequences. *Nat. Struct. Biol. 9*, 621–627.
24. Shifman, J. M., and Mayo, S. L. (2002) Modulating calmodulin binding specificity through computational protein design. *J. Mol. Biol. 323*, 417–423.
25. Tur, V., van der Sloot, A. M., Reis, C. R., Szegezdi, E., Cool, R. H., Samali, A., Serrano, L., and Quax, W. J. (2008) DR4 selective TRAIL variants obtained by structure based design. *J. Biol. Chem. 29*, 20560–20568.
26. Mongkolsapaya, J., Grimes, J. M., Chen, N., Xu, X. N., Stuart, D. I., Jones, E. Y., and Screaton, G. R. (1999) Structure of the TRAIL-DR5 complex reveals mechanisms conferring specificity in apoptotic initiation. *Nat. Struct. Biol. 6*, 1048–1053.
27. Guerois, R., Nielsen, J. E., and Serrano, L. (2002) Predicting changes in the stability of proteins and protein complexes: a study of more than 1000 mutations. *J. Mol. Biol. 320*, 369–387.
28. Schymkowitz, J. W., Rousseau, F., Martins, I. C., Ferkinghoff-Borg, J., Stricher, F., and Serrano, L. (2005) Prediction of water and metal binding sites and their affinities by using the Fold-X force field. *Proc. Natl. Acad. Sci. U.S.A. 102*, 10147–10152.
29. Hymowitz, S. G., O'Connell, M. P., Ultsch, M. H., Hurst, A., Totpal, K., Ashkenazi, A., de Vos, A. M., and Kelley, R. F. (2000) A unique zinc-binding site revealed by a high-resolution X-ray structure of homotrimeric Apo2L/TRAIL. *Biochemistry 39*, 633–640.
30. van der Sloot, A. M., Mullally, M. M., Fernandez-Ballester, G., Serrano, L., and Quax, W. J. (2004) Stabilization of TRAIL, an all-beta-sheet multimeric protein, using computational redesign. *Protein Eng. Des. Sel. 17*, 673–680.
31. Cha, S. S., Sung, B. J., Kim, Y. A., Song, Y. L., Kim, H. J., Kim, S., Lee, M. S., and Oh, B. H. (2000) Crystal structure of TRAIL-DR5 complex identifies a critical role of the unique frame insertion in conferring recognition specificity. *J. Biol. Chem. 275*, 31171–31177.
32. Hymowitz, S. G., Christinger, H. W., Fuh, G., Ultsch, M., O'Connell, M., Kelley, R. F., Ashkenazi, A., and de Vos, A. M. (1999) Triggering cell death: the crystal structure of Apo2L/TRAIL in a complex with death receptor 5. *Mol. Cell 4*, 563–571.
33. Thomas, L. R., Johnson, R. L., Reed, J. C., and Thorburn, A. (2004) The C-terminal tails of tumor necrosis factor-related apoptosis-inducing ligand (TRAIL) and Fas receptors have opposing functions in Fas-associated death domain (FADD) recruitment and can regulate agonist-specific mechanisms of receptor activation. *J. Biol. Chem. 279*, 52479–52486.
34. van Geelen, C. M., de Vries, E. G., Le, T. K., van Weeghel, R. P., and de Jong, S. (2003) Differential modulation of the TRAIL receptors and the CD95 receptor in colon carcinoma cell lines. *Br. J. Cancer 89*, 363–373.

BI801927X